UNIVERSITÄT ZU LÜBECK

From the Institute for Systemic Inflammation Research

of the University of Lübeck

Director: Prof. Dr. med. Jörg Köhl

Comprehensive analysis of parameters modulating food allergy in a murine model

Dissertation

for Fulfilment of

Requirements

for the Doctoral Degree

of the University of Lübeck

from the Department of Natural Sciences

Submitted by

Christina N. Rau

From Wolfenbüttel, Germany

Lübeck, June 2020

First referee: Prof. Dr. rer. nat. Rudolf Manz

Second referee: Prof. Dr. rer. nat Ulrich Günther

Date of oral examination: 14.09.20

Approved for printing: Lübeck, 30.09.20

STATEMENT OF AUTHENTICATION

I hereby declare that I have written the present thesis independently, without assistance from external parties and without use of other resources than those indicated. The ideas taken directly or indirectly from external sources (including electronic sources) are duly acknowledged in the text. The material, either in full or in part, has not been previously submitted for grading at this or any other academic institution.

Lübeck, 2021

Christina N. Rau

ACKNOWLEDGEMENT

It took me a long time to write this thesis once the laboratory work was completed. A few months that I intended for it to take became over a year. But the beautiful little distractions in the process were worth the wait. However, no human can do everything on his or her own. I am glad to be able to say thank you to the wonderful people that were there along side of me during one chapter which has now come to an end for another chapter to begin.

I would like to express my sincere gratitude to Rudolf Manz for the opportunity to work on this interesting research topic; what it was planned to be and what it became. You have been a mentor in science for many years now. Thank you for numerous out of the box thinking discussions that often led to new ideas, sharing your immense knowledge and understanding of immunology and for being a kind boss who always tries to be there for his group. Working for you early in my university years sparked my interest in immunology and set my path for my future scientific journey.

Furthermore, I would like to thank Fred Finkelman for the opportunity to spend nine months in his lab. Even outside the time spent there, his scientific knowledge, intelligence and creativity kept pushing me.

Money seems to make the world go round and without the funding from the DFG funded IRTG1911 with its spokespersons Jörg Köhl and Dave Hildeman, my project would not exist. But the IRTG is much more than just funding. The possibility to exchange scientifically with other young scientists facing similar potential struggles has been valuable. The stay in the laboratory of Fred Finkelman in the Cincinnati significantly changed my life, thank you for the opportunity of this research exchange.

I would also like to thank Dr. Christian Sina for his mentorship and help.

Work would have been a lot less enjoyable without the awesome members of the AG Manz. Moreover, this thesis would have not been possible without all of your guys' help and support. I love the collegiality that exists in this group. Naturally, providing help for big experiments in such a way is out of the ordinary. I thank everyone for all help and endless hours spent in the animal house. I would like to thank Ann-Katrin Clauder, Larissa Almeida and Timo Lindemann for funny conversations and all your help inside and outside of the lab. A huge thank you to Kathleen Kurwahn for your help in the lab, in the animal house, for keeping the lab work run smoothly and organising birthday presents, cookie baking, barbecues and much more.

Throughout all ups and downs, I could always count on my love, my husband Jason. You manage to challenge my thinking every day in a way that I can grow as a human and also as a scientist. You and our beautiful son Vincent make me smile and laugh all the time. Thank you for being the most wonderful little family ♥

TABLE OF CONTENT

ABSTRACT

Food allergy, a common cause of anaphylaxis, is mediated by basophil and mast cell release of vasoactive mediators that induce shock and diarrhoea. Release of these mediators is triggered by allergen crosslinking of IgE that is associated with these cells' high-affinity IgE-receptor, FcεRI.

In this study, a novel adjuvant-free murine model of hen's egg allergy was utilised to investigate serological factors that influence the development and severity of food allergy. While egg white (EW)-specific IgE, IL-4 and to a lesser extend IL-6 and TNFα were clearly correlated with increased signs of anaphylaxis, EW-specific IgG1 only showed the partially protective effect that had been described in literature. Yet, levels of IgG1-levels in serum specific for ovalbumin, the most abundant protein in EW, were more than 100-fold higher than those of IgE, which had been able to block IgE-mediated anaphylaxis in a passive transfer model.

Next generation sequencing (NGS) analysis of the IgG1 and IgE-repertoire in bone marrow and mesenteric lymph nodes of allergic mice revealed differences in the complementarity-determining region (CDR3) of both antibodies, i.e. the parts of the antibodies that most determine their antigen-binding. These differences derived from different VDJ-gene rearrangement and varying somatic hyper mutations. In accordance with existing literature the data imply that the majority of clones have a strong bias towards IgG1. Unexpectedly, a minor but considerable number of clones show a bias towards IgE, with little or no detectable IgG1.

Differential antigen/epitope recognition by IgE and IgG1 antibodies as indicated by the NGS results offers a potential explanation for insufficient blocking of IgE-mediated anaphylaxis by IgG1.

ZUSAMMENFASSUNG

Nahrungsmittelallergie, eine verbreitete Ursache für Anaphylaxie, wird durch die Freisetzung von vasoaktiven Mediatoren durch Basophile und Mastzellen vermittelt, welche Schock und Durchfall induzieren. Die Freisetzung dieser Mediatoren wird durch die Kreuzvernetzung von Allergen und IgE ausgelöst, das an hochaffinen IgE-Rezeptoren dieser Zellen gebunden ist.

In dieser Studie wurde ein neues Adjuvans-freies Mausmodell der Allergie gegen Hühnerei genutzt, um serologische Faktoren zu untersuchen, die die Entwicklung und Schwere von Nahrungsmittelallergien bestimmen. Während Eiweiß-spezifisches IgE, IL-4 und in einem geringeren Ausmaß IL-6 und TNFα eindeutig mit verstärkter Anaphylaxie korrelierten, zeigten Eiweiß-spezifische IgG1-Level nur teilweise einen protektiven Effekt, welcher in der Literatur beschrieben ist. Dennoch sind Mengen von IgG1 spezifisch für Ovalbumin, dem am meisten vorhandenen Protein in Eiweiß, mehr als 100-fach höher als die von IgE. Dieses Verhältnis verhinderte IgE-vermittelte Anaphylaxie in einem passiven Transfermodell.

Eine "*Next generation sequencing*" Analyse des Repertoires von IgG1 and IgE in Knochenmark und mesenterischem Lymphknoten von allergischen Mäusen zeigte Unterschiede in der „*Complementary-determining region (CDR3)*" dem Teil der Antikörper, welcher zum größten Ausmaß die Antigenbindung bestimmt. Diese Unterschiede entstammten unterschiedlichen VDJ-Genzusammenstellungen und verschiedenen somatischen Hypermutationen. In Übereinstimmung mit existierender Literatur weisen die hier generierten Daten darauf hin, dass die Mehrheit der Klone eine starke Tendenz zu IgG1 auf. Überraschenderweise zeigt ein geringerer, aber beträchtlicher Anteil von Klonen eine Tendenz zu IgE mit wenig oder nicht detektierbarem IgG1.

Unterschiedliche Antige-/Epitoperkennung von IgE und IgG1 Antikörpern wie durch das NGS-Ergebnis gezeigt bieten eine potentielle Erklärung für unzureichende Blockade von IgE-vermittelter Anaphylaxie durch IgG1.

1 INTRODUCTION

1.1 Food allergy

The term “food allergy” describes an “adverse reaction of the immune system to food antigens – allergens”. Over the past 20 years, the prevalence of allergic reactions to food components in children (0-17 years old) has increased from 3.5 to 5 % in Australia as an example of an industrialised country (*1*). In 2016 in Germany the prevalence of food allergy was 4.7 %(*2*). More dramatically, hospital admissions due to food-induced anaphylaxis in children under the age of 4 have increased 5-fold from (3.5/100,000 in 1994 to 17/100,000 in 2005) in Australia (*1*).

Based on immunopathological mechanisms, atopic food allergies can be categorised into IgE-mediated, IgE-independent and diseases of mixed aetiology. IgE-mediated food allergy is the most common allergic reaction to major food allergens, including hen’s egg, cow’s milk, seafood, fish, wheat, soybean, tree nuts and peanuts. The manifold signs and symptoms of an IgE-mediated allergic reaction towards food components include pruritus after allergen contact with skin, inflammatory gastrointestinal and airway reactions; as well as cardiovascular impairment that can cause a life-threatening anaphylactic shock (*3*–*5*).

In IgE-mediated food allergy, IgE binds to a high affinity receptor (FcεRI) on mast cells and basophils. Encounter of the cognate allergen crosslinks allergen-specific IgE and IgE-associated FcεRIs. This crosslinking activates mast cells, causing them to degranulate in seconds to minutes with release of proteases (e.g.; mMCP (mast cell metallo-protease) 1 and 7 and preformed mediators such as histamine, and to secrete cytokines, such as IL-4 and tumour necrosis factor alpha (TNFα), over a period of a few hours. With its ability to cause vasodilation, increase vascular permeability and heart rate and decreased cardiac contractility, histamine is a key player in the development of anaphylaxis (*6*).

Thus far, no specific therapy has been approved for food allergy. The only recommendations include avoiding the respective food and symptomatic treatment once the allergic reaction has occurred. However, promising clinical trials have tested different variants of allergen-specific immunotherapy (AIT) (*7*). Slowly increasing small doses of allergen are administered orally, sublingually or epicutaneously over up to 2 years. While in many trials, a majority of patients have become desensitised, as shown by tolerance of a specified, increased allergen dose at the end of treatment, most desensitised individuals regain sensitivity, some only one week after completion of treatment (*8*, *9*).

1.2 Egg allergy

Allergy to chicken (*Gallus gallus*) egg is the second most prevalent food allergic disorder in infants and children (*10*). As for food allergies in general, the estimated prevalence of egg

allergy in Europe varies among several studies. This is mainly due to different methods of data collection with a particularly weak identification when self-report is the "diagnostic tool". Also, the definition of the allergic disease varies among studies. The most recent meta-analysis of studies on egg allergy estimates an overall prevalence of 1.6 % in children aged 2.5 years (*11*). The prevalence of egg allergy is higher in younger age groups and decreases with age (*12*, *13*). This suggests that egg allergy resolves during childhood (*14*, *15*). The time point of resolution of egg allergy is under debate (*14*, *16*, *17*). Decreasing levels of egg-specific IgE over time have been shown to be a prognostic indicator of the development of tolerance to egg as well as the age at which first symptoms occurred, and the severity of these symptoms (*15*, *17*, *18*).

Due to varying prevalence depending on the method used and the potential of misdiagnosis, obtaining detailed medical history and performing a physical examination should be the first steps (*19*, *20*). Further diagnostic procedures can include determination of IgE titres, skin-prick tests and skin patch tests. However, total and allergen-specific IgE titres frequently vary among allergic individuals. Neither these titres nor skin tests completely correlate with clinical reactions. Hence despite its invasiveness, oral food challenge (OFC) remains the gold standard of food allergy testing (*19*, *21*, *22*).

1.2.1 Allergens in egg white

There are four major allergens in domestic chicken (*Gallus domesticus*) egg white (EW): Gal d 1-4 (*23*). The much-studied model protein ovalbumin (OVA, Gal d 2) is the most abundant allergen (~55% of the total protein). The biological function of OVA is not fully understood, but is has been shown to have some antibacterial properties when proteolyticly digested (*24*). The most immunogenic protein in EW is the heat-stable trypsin inhibitor ovomucoid (OVM, Gal d 1) which constitutes about 11 % of EW proteins (*24*, *25*). The potency of OVM to mount an immune reaction is so strong, that in the attempt to create monoclonal antibodies against OVA, <1% contaminations of ovomucoid lead to the generation of mainly ovomucoid specific antibodies. Most IgE in egg-allergic patients is raised against OVM and skin prick test diameters are largest when performed with OVM (*26*). Ovomucoid consists of three tandem domains with partial homology. IgE is primarily specific for domain 2, whereas IgG binds to all 3 domains similarly. Some epitopes of ovomucoid are recognised by IgE and IgG4 and some are unique for IgE or IgG4 (*27*). Ovotransferrin (Gal d 3, ~12 %), another EW allergen, is an iron-binding protein that has antimicrobial activity (*28*). A fourth EW allergen, lysozyme (Gal d 4, ~3,4 %) is utilized in food products because of its ability to lyse gram positive bacteria; Gal d 4-containing products in which eggs might not be obviously expected create a risk for egg allergic patients (*29*).

Amino acid chains from different protein domains can form tertiary structures that generate conformational epitopes. These are in addition to the sequential epitopes formed from amino acid primary sequences. Conformational epitopes are more sensitive to digestion and denaturation than sequential epitopes. Conformation epitopes, unlike sequential epitopes, can

also be destroyed when eggs are cooked; this can impact the allergenicity of some EW proteins (*23*).

However, IgE binding to OVA and OVM is not impaired by heat denaturation, suggesting that IgE mostly binds to sequential rather than conformational epitopes in these proteins (*30*).

Persisting egg allergy has been shown to correlate with higher IgE antibody titres against sequential epitopes, while increased IgE antibody titres against conformational epitopes correlate with transient allergy. 4 major IgE binding ovomucoid epitopes have been identified that are not recognised by serum from patients who outgrew egg allergy later in life (*31*). Generally, children with persistent egg allergy have higher OVM-specific IgE titers than children with transient allergy. Considering epitope heat-stability, this finding is consistent with the correlations with sequential and conformational epitopes (*26*).

1.2.2 Allergens and allergy-relevant components in egg yolk

Even though most egg proteins are present in EW, two allergens have been found in egg yolk. Chicken serum heat-labile albumin a-livetin (Gal d 5) is the more important allergen. It serves as a metal ion transporter in the avian blood stream (*30*). Chicken serum albumin has been identified as an aero-allergen, involved in bird-egg syndrome, a disease where exposure to birds (feathers, droppings etc.) leads to sensitisation and gastrointestinal manifestations because of cross reactions of egg proteins with airborne allergens (*32*, *33*). The second major egg yolk allergen: glycoprotein 42 (YGP42; Gal d 6). YGP42 is a fragment of vitellogenin-1 (VTG-1), which is a major precursor protein in chicken development. Presumably, patients with egg allergy get sensitised against both EW and EYP, because patients diagnosed with egg white allergy also have IgE against egg yolk proteins (*34*). Partial inhibition of IgE-binding to crude egg yolk by recombinant YGP42 suggest an allergenic potential of the protein fragment.

In addition to promotion of allergy induction by egg proteins, egg yolk lipids play an important role in allergy development. Lipids, predominantly triglycerides, constitute over 30% of egg yolk's weight (*28*). Saturated medium chain triglycerides can upregulate the unfolded protein response (UPR) in epithelial cells (CACO2-cells, a human intestinal epithelial cell line) that induces an allergic pro Th2-millieu (for more detail see section 1.3.2) (*35*, *36*).

1.3 Allergic sensitisation

1.3.1 Oral tolerance

The intestinal system faces potentially deathly pathogens every day. In addition, both large amounts of harmless yet foreign food proteins are present in the intestine and billions of commensal bacteria colonize the gut (*37*). A well-tuned immune response has to be able to

differentiate between threat and harmless foreign antigens to avoid triggering an overwhelming immune response to the up to 100 g of protein that are consumed daily (*38*).

Oral ingestion of antigens normally leads to a tolerogenic immune reaction (*39*, *40*), i.e. the absence of an inflammatory reaction in response to a particular foreign antigen. Controlled transmission through the intestinal mucosa, for example by microfold (M) cells, and uptake of antigen by $CD103^+$ DCs and CX3C-chemokine receptor 1 $(CX3CR1)^+$ cells guarantees a minimum of free antigen in the apical surface of the intestinal epithelium (*41*). $CD103^+$ DCs migrate to mesenteric lymph nodes, where they induce the development of antigen-specific forkhead box P3 (FOXP3) positive and negative interleukin 10 (IL-10)-secreting regulatory T (Treg) cells by secreting transforming growth factor (TGF)-β and retinoic acid (*42*, *43*). This suppresses formation of type 2 cytokines (e.g. IL-4) and T cell dependent antibodies, including IgE.

A healthy microbiome also contributes to intestinal tolerance. Studies have shown that intestinal Treg numbers are reduced in antibiotic-treated and germ-free mice; this facilitates allergic sensitisation (*44*, *45*). Supplementing germ free mice with certain bacteria, i. e. *Clostridia* species and *Bacteroides fragilis*, or short-chain fatty acids (microbiota-derived products) induces Tregs and suppresses type 2 cytokines leading to reduced allergic sensitisation as well as protection from colitis (*46*–*48*).

Healthy individuals without any history of food allergy still have allergen-specific IgG4 antibodies whereas IgE cannot be detected in the majority of them. IgG4 can also play a role in natural tolerance (*49*).

1.3.2 Initiation of a type 2-response

Allergic individuals most probably become sensitised to allergens early in childhood. The cause for development of an atopic disease is still under debate. Despite normally mediating tolerance, even oral ingestion of allergens can induce sensitisation when the barrier function of the mucosa is impaired. Here, mouse models have allowed insight into the induction of food allergy by intestinal barrier disruption by the adjuvants cholera toxin (CT) and Staphylococcal enterotoxin B (SEB), which lead to secretion of antigen-specific IgE and systemic anaphylaxis upon allergen-challenge (*50*, *51*). Furthermore, research on mouse models suggests that cutaneous exposure (*52*–*54*) or inhalation are probable causes for sensitisation against food allergen (*55*).

A barrier disruption can effect the normal, controlled transmission of antigen through the mucosa. Large amounts of antigen can reach immune cells on the apical site of the epithelium. In addition to physical trauma, saturated fatty acids (particularly medium chain triglycerides), which are among the fats in major allergenic foods, such as chicken's egg and cow's milk, can upregulate the UPR in epithelial cells (CACO2-cells, a human epithelial cell line). This in turn promotes the transcription of pro-Th2-cytokines such as IL-25, IL-33 and thymic stromal lymphopoietin (TSLP) (*35*, *36*). Secretion of these cytokines by epithelial cells causes dendritic

cells (DCs) to prime naïve $CD4^+$ T cells to secrete IL-4, IL-5 and IL-13, while IL-10 is decreased compared to other stimuli (*56*) and has direct stimulatory effects on Th2 cells, eosinophils, mast cells, and basophils. A tolerogenic environment can thus be shifted to a Th2-biased one. Repeated or long-term exposure of such a susceptible milieu to the allergen can lead to the generation of allergen-specific $CD4^+$ Th2 cells (*57*) that induce allergen-specific B cells to switch to synthesis and secretion of IgE (*58*). More detail about class-switch to IgE can be found in section 1.5.3.

Genetic predisposition also plays a role in allergy development (*59*, *60*). Other factors such as stress (*61*), differences in the microbiome (*62*) have been described to impact food allergy.

1.4 Allergic response – the effector phase

1.4.1 IgE, FcεRI and the regulation of mast cell activation

With a concentration of only about 100 ng/mL, IgE is the least abundant antibody isotype in the serum of healthy individuals; in contrast, IgG has a serum concentration of approximately 10 mg/mL. Also, the half-lives of both antibody-subclasses in serum differ greatly (*63*). IgG1 stays in the circulation longer (half-life of 3-6 days in mice; 21 days in humans) while IgE has a half-life of 12 hours in mice (*64*). After secretion, IgE is also quickly removed from serum and bound in tissue to FcεRI, the high affinity IgE-receptor, where it remains due to the receptor's high affinity ($K_a \sim 10^{10}$ M^{-1}) (*65*). FcεRI is a heterotetramer, composed of one α chain, which carries the IgE binding site, and one β chain and 2 γ chains, which are involved in FcεRI signalling and promote membrane α chain expression.

Murine FcεRI is expressed on mast cells and basophils, while in humans mast cells, basophils, monocytes, Langerhans cells, eosinophils and dendritic cells can express the α chain of this molecule on their surface (*66–70*). Antigen binding to IgE bound to FcεRI induces crosslinking of multiple FcεRI molecules. This initiates a signalling cascade that ultimately results in release of mediators, e.g. anaphylaxis-mediating histamine, proteases, secretion of cytokines and chemokines (*71*). For more details see section 1.4.2

In mice, antigen-specific mast cell activation can also be mediated by IgG through the activating receptor FcγRIII (*72*, *73*). Activation of FcεRI has been suggested to determine the severity of anaphylaxis, and activation of FcγRIII to impact the mortality of that response (*72*). However, this alternative activation of anaphylaxis can also be mediated by neutrophils and macrophages, which contribute to anaphylaxis by releasing platelet-activating factor (PAF) rather than histamine (*74*, *75*). Human skin derived mast cells have been shown to constitutively express FcγRIIA instead of FcγRIII and can be triggered to release histamine upon stimulation with anti-FcγRIIA monoclonal antibodies (mAb) (*76*).

Mast cells also express additional innate receptors such as toll-like receptors (TLRs) and complement receptors, which can contribute to danger and pathogen sensing (*77*, *78*).

In addition to the activating Ig-receptors, mouse mast cells and some human mast cells, including those in the gastrointestinal tract (*79*) but not skin-derived human mast cells(*76*), express the inhibitory receptor FcγRIIb on their surface. Human and mouse basophils both express this receptor and their activation has been shown to be inhibited by FcγRIIb-signalling (*80*).

1.4.2 Mediators of the allergic response

Allergen-mediated crosslinking of IgE-associated FcεRIs activates mast cells and basophils. The cytosol of these effector cells contains membrane vesicles that store preformed mediators that are almost instantly released upon activation. Among these are histamine, PAF, serotonin, heparin and proteolytic enzymes such as mMCP1 and mMCP7. Moreover, activation induces the production of lipid mediators, including prostaglandins (PGD2) and leukotrienes (LTC4), and *de novo* synthesis of cytokine and chemokine which are secreted with a delay of a few hours (*6*, *70*, *81*).

The histamine receptors 1 (H1) and 2 (H2) are both activated by histamine; this causes smooth muscle cell contraction in the airways and the gastrointestinal tract. Activation of these receptors in blood vessels induces vasodilation and enhances vascular permeability. With these effects, histamine is primarily responsible for the development of anaphylaxis (*75*). Anaphylaxis is defined as "a serious allergic reaction that is rapid in onset and may cause death" (*82*). It occurs systemically and can affect multiple organs. Signs of anaphylaxis are dependent on the health status of the patient as well as comorbidities. These signs include acutely compromised respiratory function, reduced blood pressure and associated signs of end-organ dysfunction (e.g. hypotonia [collapse], syncope, incontinence) as well as persistent gastrointestinal symptoms (e.g. abdominal cramps, diarrhoea, and vomiting) (*82*).

Mast cell degranulation also releases pre-synthesised TNFα. TNFα can activate neutrophils and recruit effector cells. The cytokines IL-4 and IL-5 are *de novo* synthesised upon mast cell and basophil activation. IL-4 triggers and maintains the Th2 response with Th2 cell proliferation and class-switch to IgE (*83*). Moreover, IL-4 promotes mast cell accumulation in the gut (*84*) and has been shown to exacerbate anaphylaxis in some murine models (*85*). IL-5 is involved in chemotaxis, activation and survival of eosinophils (*82*).

1.5 B cell development, activation and class-switch to IgE and IgG1

1.5.1 Antibodies – structure and function of different isotypes

Antibodies are the secreted form of the B cell receptor (BCR) without its membrane domain. An overview including parts of the gene locus that encodes for the antibody is illustrated in Figure 1.

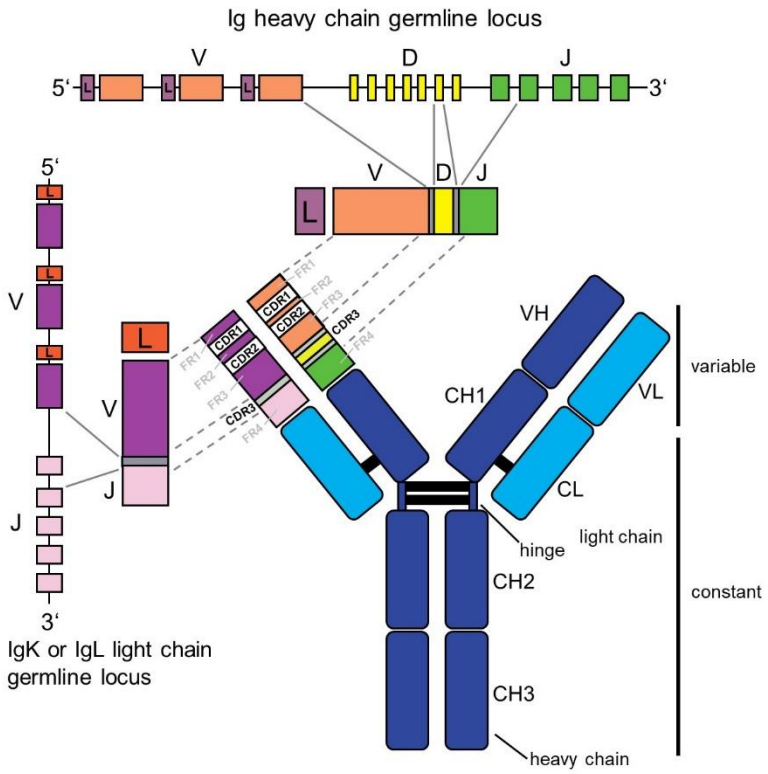

Figure 1: Antibody structure and encoding genes
The germline configuration of some of the multiple VDJ-genes of the Ig heavy chain is depicted on top. Similarly, the germline configuration of the light chain (VJ) genes is depicted on the left side. A linker (L) segment is located upstream of each V-gene. Joining of one of each gene segments (solid grey lines) results in gene loci that are unique to individual B cells. These rearranged loci are depicted below (IgH) or right of (IgL) the germline sequence. These rearranged loci get transcribed and translated into the variable region of the antibody molecule which is depicted as well. The variable region contains the complementarity regions (CDRs), which are the parts of the antibody V regions that interact with an antigen epitope. In addition to the variable region, which is depicted in more detail, the antibody also has a constant region. Ig heavy and light chains are linked by a disulphide bond., while two heavy chains are linked by several disulphide bonds. Figure modified from: Boyd and Joshi, 2014.

IgG and IgE antibodies are both composed of two heavy polypeptide chains that are connected by disulphide bonds and are each associated with a light chain through a disulphide bond. Heavy and light chain consist of a variable region that is highly diverse and that binds to epitopes on antigens and a constant region that differs between different Ig isotypes (IgA, IgM, IgD, IgG1-4 in human, IgG1,2a,2b and 3 in mice and IgE). A part of the constant region, the Fc fragment mediates effector functions by binding to receptors on target cells (*87*, *88*). A hinge region, where the disulphide bonds connecting the heavy chains are located, separates the Fc fragment from the Fab fragments that consist of the Ig light chain and the variable and a part of the constant region of the Ig heavy chain.

Antibodies are able to recognise an immense variety of antigens. The total amount of individual and unique antibodies, each derived from a particular B cell, is called the B cell or antibody repertoire.

To ensure the diversity of the B cell repertoire, numerous different individual variable (V)-, diversity (D)- and joining (J)-gene segments encode for the variable region of the heavy chain

and D- and J-genes for the light chain (*89–91*). Early in B cell development, one of each gene segment is randomly selected and joined by recombination-activating genes (RAG) recombinase to form the variable region. Unused gene segments are excised from the genome (*92*). The light chains can either be encoded by a κ- or a λ-gene locus. The numbers of V(D)J-genes for heavy and light chains of immunoglobulins (Ig) are noted in Table 1.

Table 1: Counts of V-, (D-) and J-gene segments encoding for the variable region of heavy and light chain of BCR/antibodies

Species	Locus	V-genes*	D-genes	J-genes*
Homo sapiens	IgH (heavy chain)	80 (39)	27	9 (6)
	Igκ (light chain)	75 (35)	-	5
	Igλ (light chain)	69 (30)	-	5
Mus musculus	IgH	190 (110)	12	4
	Igκ	140 (80)	-	5 (4)
	Igλ	4 (3)	-	5 (4)

*total genes including pseudo-genes; (functional genes are in Parentheses) (*93–101*)

This pool of V-, D- and J-gene segments only accounts for part of the germline-encoded diversity of the B cell repertoire. During the error-prone process of excision and re-joining of V(D)J-genes, there are either nucleotides lost or added by the enzyme terminal deoxynucleotidyl transferase (TdT). Furthermore, the D-gene segments can be spliced in 3 different reading frames, increasing diversity. Together with these modifications, the V(D)J-gene rearrangement and the combination of different heavy and light chains allow a theoretical variety of antibodies to recognise any antigen possible. The so called naïve pre-immune repertoire of humans is estimated to be greater than 10^{16} different immunoglobulins (*94*). Later, during the activation and maturation of B cells, point mutations are introduced that lead to an additional layer of diversity of the B cell repertoire (Figure 2).

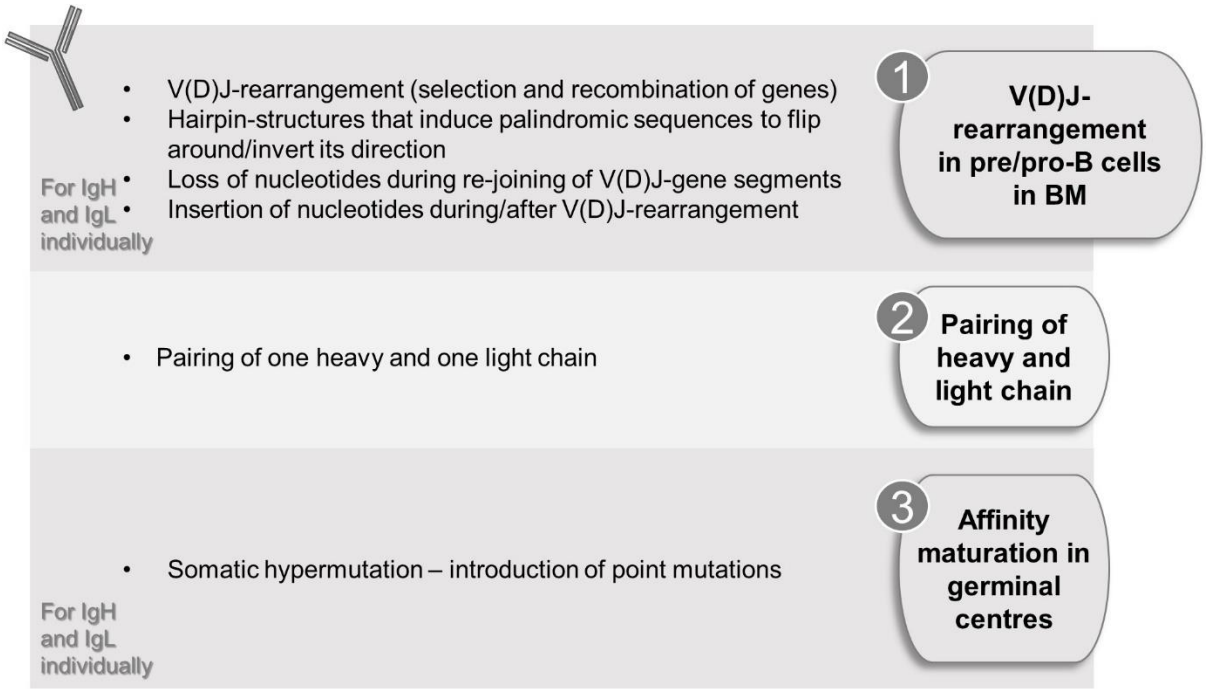

Figure 2: The diversity of the immunoglobulin repertoire
Different steps and processes contributing to the diversity of the immunoglobulin repertoire are described. **1.** (V(D)J-rearrangement in pre/pro-B cells in BM) and **2.** (Pairing of heavy and light chain) occur in naïve (pre/pro) B cells and is thus considered to be the naïve repertoire whereas **3.** (affinity maturation in germinal centres) is performed by mature antigen-experienced B cells. **1.** And **3.** occur for both the heavy and light chain.

The sequence of the variable region can functionally be differentiated into 3 hypervariable intervals termed complementarity-determining regions (CDRs) that are located between 4 more stable regions called framework regions (FRs) (*89*, *90*). In addition to being more variable, the CDRs stick out as loops of the V-region backbone, which consists of 2 β-sheets, and are predominantly responsible for epitope recognition. In multiple analysed X-ray spectra of antibody-antigen interaction, the loops of the CDRs insert into pockets that form the epitope on the antigen (*102*). Of the heavy chain CDRs, CDR3 is the most important for the diversity that allows binding to multiple antigens (*103*). It is also the loop to which all 3 gene segments V-, D- and J contribute.

Downstream of the variable gene locus of the heavy chain, 9 functional C_H-genes are located that are able to splice in 2 different ways that either result in a nonpolar membrane anchor terminus for the B cell Ig receptor (BCR) or a more polar terminus for secreted antibody (*104*). The different isotypes of antibodies contain different C_H-gene segments: Cμ (IgM), Cδ (IgD), Cγ (IgG), Cε (IgE) and Cα (IgA). During B cell development, B cells are able to change their Ig isotype by associating different heavy chain constant regions while the same variable region. This process in which parts of the IgH locus are excised and only a certain gene portion can be transcribed is called class-switch recombination (CSR) or just class-switch (for more details see section 1.5.3).

With the Fc part of its constant region, antibodies bind to cell membrane Fc receptors and execute a plethora of activating and inhibitory functions that differ for different Ig isotypes and Fc receptors.

1.5.2 Early B cell development

B cells are generated throughout life from pluripotent hematopoietic stem cells in the bone marrow. Through multipotent myeloid/lymphoid progenitors (MPPs) and common lymphoid progenitors (CLPs), pro-B and pre-B cells are formed (*105*). The first steps of creating the functioning BCR take place as early as during the formation of pro- and after that pre-B cells. First, the D and J-gene segments and following this the V and DJ-segments of the heavy chain are joined. The heavy chain variable region is rearranged and the μ heavy chain is expressed on the surface of the pre-B cell. This Igμ heavy chain pairs with a surrogate light chain to ensure successful BCR formation. This complex is called pre-BCR. Once, an Igμ is expressed on the surface, it signals to suppress the other allele to prevent the expression of two different BCRs on one B cell (*106*). This is followed by joining of κ or λ light chain VJ-genes, which replace the surrogate light chain to form a mature BCR. Immature B cells are now checked for autoreactivity. Strongly autoreactive B cells undergo apoptosis and only slightly or non-autoreactive B cells can leave the bone marrow as immature naïve B cells (*107*).

1.5.3 B cell activation and class-switch

After they left the bone marrow, immature B cells face another autoreactivity-based selection in the spleen before final differentiation into mature B cells (*107*). Next, mature naïve B cells recirculate through the blood stream and lymphatic system on the hunt for an antigen that is complimentary to their BCR. After ligation of a specific antigen and BCR, BCR-associated signalling molecules provide the first signal that ultimately results in B cell activation and proliferation (*108*). The antigen is internalised, processed to generate peptides in the endosome and peptides bound to major histocompatibility complex class II (MHCII) molecules are presented on the B cell surface. $CD4^+$ helper T cells with a T cell receptor (TCR) that is specific for the presented peptide/MHC class II complex interact with this complex these B cells through their TCR as well as through additional costimulatory molecules. This interaction facilitates complete activation and clonal expansion of B cells (*109*). This T cell-dependent B cell activation occurs in secondary lymphoid organs such as lymph nodes (LNs) and spleen. IgM is the initial antibody isotype that is secreted by these activated B cells and their progeny. Some cytokines can also induce an activated B cell to change the isotype of its BCR and secreted antibody (Table 2). This process is called immunoglobulin class switch. Of note, it affects the antibody isotype while preserving its specificity.

Table 2: Different cytokines induce switching to different antibody
The individual cytokines induce or inhibit the production of certain antibody classes. These data are drawn from experiments with mouse cells.

	Role of cytokine in regulating expression of mouse antibody classes						
Cytokines	IgM	IgG3	IgG1	IgG2b	IgG2a	IgE	IgA
IL-4	inhibits	inhibits	induces		inhibits	induces	
IL-5							Augments production
IFNγ	inhibits	induces	inhibits		induces	inhibits	
TGFβ	inhibits	inhibits		induces		inhibits	induces

Table modified from: Janeway's immunobiology (*110*)

In contrast to V(D)J-rearrangement, class-switch recombination alters the constant C-terminus of the antibody and occurs only in the IgH-gene of the antibody. Located upstream of the exons encoding for each C_H-gene segment are another exon, the I exon, and the first intron, called the switch (S) region, which contains large stretches of repetitive DNA sequences. The I region, which contains both I exon and S region, has to be activated in order for class-switch to begin (*111*). The enzyme responsible for initiation of CSR is activation-induced cytidine deaminase (AID). It deaminates deoxycytosine (dC) into deoxyuridine (dU) in the S regions. If the DNA repair machinery introduces a double strand break as a response to this deamination, an S region (i.e. Sμ) can be re-joined with a downstream S region resulting in a translocation of the V-region from being in front of Cμ to immediately 5' of another C_H. The C_H-gene segments in between are excised in the form of circular DNA-fragments and consequently are no longer available for transcription. After class-switch to a certain isotype, only isotypes whose genes are located downstream of the present one can be switched to and transcribed (*111*, *112*), unless class switching is accomplished by trans-recombination between the same alleles on sister chromosomes.

In allergic disorders, IgE and IgG1 in the mouse and IgE and IgG4 in humans are of particular interest. While IgE is thought to have evolved as a defence mechanism against ectoparasites and invading macroscopic parasites i.e. insects and helminths, respectively (*113*), it also mediates allergic symptoms. Murine IgG1 and human IgG4, on the other hand, are believed to be able to suppress symptoms.

Class-switch to these isotypes is induced by IL-4 (*114*, *115*). In addition to IL-4, also IL-13 can induce class-switch to IgE in humans and, to some extent, in mice (*116*). Both cytokines can signal through the type 2 IL-4R, which is composed of the IL-4Rα and IL-13Rα1 subunits (*117*, *118*), while only IL-4 can signal through the type 1 IL-4R, which is composed of IL-4Rα and the cytokine receptor common γ chain. Overlapping activities of both cytokines could be shown: IL-13 or IL-4 single-knockout mice exhibit a partially impaired Th2 response; double-mutant mice lacking both cytokines show a strongly reduced Th2 response (*83*). IFNγ on the other hand inhibits both IgE and IgG1 production (*119*, *120*). TGF-β has been shown to selectively inhibit IgE-transcription whereas IgG1-production can be unaffected. TGF-β's effect is mediated by the induction of the transcription factor Id2 which in turn inhibits the EA2 proteins that must bind

to IgE-promotors to activate its transcription (*121*). The transcription factor Bcl6, which is expressed in germinal centre B cells inhibits class-switch to IgE (*122*)

Two major pathways of class-switch to IgE have been described: Either directly from IgM to IgE or through an IgG1 intermediate (*111*). In the early 1990s, it was observed that γ1-sequences could be detected at the μ-ε-junction, the first evidence for a sequential class-switch(*123*, *124*). When stimulated with anti-CD40 mAb and IL-4, mature B cells will first express IgG1 and with a delay of several hours also IgE. In this culture system, also double-positive (IgE^+ & $IgG1^+$) B cell are detectable (*125*).

1.5.4 Germinal centre reaction and somatic hypermutation

While the primary or germline repertoire is formed already in the bone marrow during early B cell development, another level diversity of the BCR repertoire is introduced in germinal centres (GC, see Figure 3).

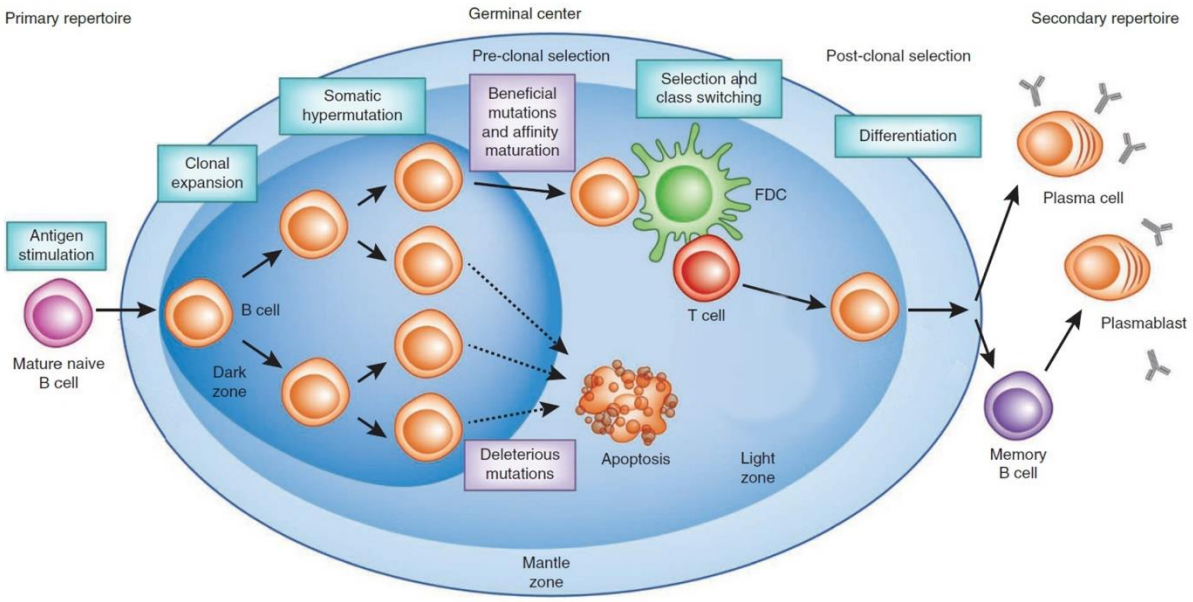

Figure 3: Key steps in the development of antigen-specific B cells.
Text boxes with black text indicate steps of normal B-cell differentiation and diversification of the antibody repertoire. Mature B cells migrate from the bone marrow to the periphery. When these cells are activated by cognate antigen in the presence of T-cell help, they may enter a germinal centre (GC). GC B cells proliferate resulting in clonal expansion. Subsequently, somatic hypermutation occurs catalysed by AID. B cells with mutations resulting in higher affinity for cognate antigen survive. Mutations leading to lower affinity will results in apoptosis of the respective B cell. Surviving, proliferated B cells can undergo (further) class-switch recombination and ultimately differentiate into memory B cells, antibody-secreting plasmablasts or plasma cells. Reencounter with the same cognate antigen induces memory B cells to either proliferate or differentiate into antibody-secreting cells. Figure modified from: Georgiou et al., 2014.

Germinal centres (GC) usually arise during the first 3 weeks after antigen exposure of a T dependent (TD) B cell response (*127–129*). They are specialised microenvironments in secondary lymphoid tissues where B cells are in contact with antigen, follicular dendritic and stoma cells. T follicular helper cells (T_{FH}) stimulate B cells through contact via the TCR, co-

stimulatory molecules and soluble mediators. The output of GCs are long-lived plasma cells or memory B cells with high affinity BCR/antibodies (*130*).

The affinity of the BCR can be increased when GC B cells undergo somatic hypermutation (SHM). Hereby, point mutations are introduced in the IgH and IgL V-region exons by AID, the same enzyme that is required for CSR. These mutations result in altered binding abilities of the BCR to the antigen. B cells whose BCR affinity is reduced by the mutations will undergo apoptosis, whereas a higher affinity BCR provides the B cell with survival and proliferation signals. This selection process is called affinity maturation (*131*, *132*).

1.6 Next Generation Sequencing /High Throughput Sequencing of the BCR/Ig-repertoire

Over the last decades, simultaneously sequencing of large amounts of DNA utilising next generation sequencing (NGS)/high throughput sequencing (HTS) has become affordable and reliable. Illumina, the most common sequencing platform, was used for my study. For sequencing on this platform, DNA or reversely transcribed RNA, complementary DNA (cDNA) of interest is tagged with adapters carrying a short unique sequence, the barcode that allows the pooling of many samples (multiplexing) yet recognising each sample. The other sequence is one that is complementary to oligonucleotides that are bound to the flow cell of the sequencer. The pooled DNA libraries are immobilised on the flow cell and amplified by bridging polymerase chain reaction (PCR) creating microscopically confined spots ("clusters") of similar template-sequences. Illumina utilises *sequencing by synthesis cyclic reversible termination (CRT)* approach (*133*): Nucleotides which are base-specifically fluorescently labelled are added and incorporated one by one. Each nucleotide contains a modified 3'-OH group which terminates the nascent DNA-chain once incorporated. After each addition of a new nucleotide (cycle), fluorescence is detected and information about the added nucleotide is saved. The 3'-blockage and fluorescent marker are removed, and the next nucleotide can be added. The previously added barcode is "read" by the same mechanism allowing identification of the sample to which the amplified sequence belongs. The sequenced result for one template (detected as one cluster) is called a read. The reads are then mapped to the genome of interest and further analyses can be performed (*134*).

1.6.1 BCR/Ig-repertoire analysis

The complex somatic gene rearrangements of immunoglobulins (Ig) yielding a highly diverse V-region (see 1.5.1 & Figure 2) are ideal targets for investigation using HTS. Early pioneering work using Sanger-sequencing (*135*) to approach investigation of the human and mouse Ig-repertoire was done by analysing up to hundreds of sequences one after the other (*136*, *137*). However, the sheer number of potential different Igs (10^{16}) (*94*) makes these experiments underpowered to

estimate the entire extent of the repertoire. A limiting factor of sequencing is the length of reads that oftentimes requires fragmentation of the DNA-sample. The juxtaposition of the V(D)J-gene segments due to the gene rearrangement, however, allows amplification of relatively short (<500 base pairs (bp)) sequences of genomic DNA (gDNA) or cDNA in B cells without loss of information. In contrast, in non-B cells the un-rearranged Ig-locus spans some kilobase pairs (kbp). Thus, it is not efficiently amplified at the gDNA-level and gets lost during PCR. Amplified Ig-cDNA will only be derived from B and plasma cells, because they are the only cells expressing this gene-locus. The properties of the Ig-gene locus itself therefore facilitates an effective bulk sequencing that was first performed in 2009 (*138*). Sorting techniques such as fluorescent activated cell sorting (FACS) are only required for particular scientific questions e.g. analysis of B cell subpopulations (*139*, *140*) or when the desire to enrich for target RNA or DNA is at hand. An enrichment is especially useful to increase NGS sensitivity when the analysed tissue only contains low numbers of B and plasma cells or the frequencies vary a lot per sample as in the lymphoma patient's tissue analysed by Pankikaran *et al.* where the frequency of lymphoma B cells varied from 0.1-10% (*141*).

In addition to sorting certain populations, single cell sorts are performed for Ig-repertoire analyses for a very important reason: While during any form of bulk Ig-sequencing, information about the complete immunoglobulin is lost, single cell sorting enables pairing of the heavy and light chain. This pairing improves an in-depth analysis of clonal relationships and is a requirement for cloning the Ig-cDNA followed by expression of the corresponding antibody. This recombinant, monoclonal antibody can then be subject to functional investigations such as epitope specificity and affinity (*142*, *143*).

1.6.2 Sample selection: gDNA or cDNA

When NGS-analyses of the Ig-repertoire are performed, the sample material has to be chosen. This depends on the research question at hand and can be either answered by sequencing gDNA or cDNA, which is reverse-transcribed RNA. Additionally, there are some technical reasons that might require one or the other. Because of its relative low stability, RNA-samples have to be quality controlled for degradation prior to analysis. gDNA exists as one copy per cell. Thus, the number of sequence reads is proportional to the number of cells of a certain clone. Since, different B cell stages express varying amounts of Ig-transcripts, large B cell population that expresses low amounts of Ig-transcripts can be "contaminated" by a few high expressing plasma cells. Yet, the relative expression levels of certain sequences in the repertoire can be estimated. The low copy number of gDNA though requires more PCR-cycles that can lead to amplification biases that are not as strong for higher abundant RNA/cDNA. The reverse transcription of RNA that has to be performed in order to obtain DNA that can be sequenced can introduce additional errors. Furthermore, at the gDNA level both productive and non-productive transcripts are sequenced whereas non-productive RNA transcripts are mostly degraded (nonsense-mediated

RNA decay). Thus, non-productive transcripts present only to a minor extent in the repertoire generated from cDNA (*144*, *145*).

1.6.3 Specific amplification of the variable region

There are different methods used to amplify the variable region of the Ig-gene. With the constant region bordering the variable region, the 3'-end of the VDJ-genes can easily be accessed using a primer that binds to this known sequence. Primers specific for the different constant IgH-chains even allow a selection of only certain isotypes to be amplified. At the 5'-part of the VDJ-genes, however, there are up to 80 V-genes that must be covered by primers in order for the VDJ-region to be amplified. One possible way to accomplish this is a 5'-rapid amplification of cDNA ends (5'-RACE). The 5'-RACE only makes use of a 3'-end primer (in the C-region) to reversely transcribe the mRNA into one strand of cDNA. In a next step, an oligonucleotide-adaptor is ligated to the 5'-end. Amplification of the cDNA can now occur with the C-region specific primer and one that is complementary to the previously ligated adaptor (*146*, *147*). 5'-RACE is less prone to primer bias and multiplexed PCR artefacts that result from primers within the VDJ-region and is better at amplifying highly mutated Ig-sequences where a primer would not be able to bind (*144*). However, the presence of RNA as the starting material as well as the ligation step are critical.

Alternatively, multiplexed primer mixtures directed against V, D, J, or constant regions allowing amplification of either cDNA or gDNA can be used and have been the dominant method used in literature to date (Boyd and Joshi, 2014). Potential obstacles with this method are PCR amplification bias due to different annealing efficacies of primers and the potential loss of highly mutated variable genes as a result of SHM preventing primers from annealing (*144*).

Primer mixes are usually specific for the V, D or J-gene families for cDNA- or gDNA-amplification and mainly target the framework regions, which are less mutated than CDRs (*148–150*). Primers targeting the leader sequence upstream of the V-gene segment have been used especially in studies investigating highly mutated Igs (*151*, *152*).

1.6.4 Data-analysis of sequenced Ig-repertoire

The raw data obtained from an Illumina sequencing run (binary base call (BCL) format) is converted into a fastq file, which contains the sequences of the clusters with a quality score per base and a unique identifier. Sequences are allocated to individual samples using the individual barcodes. Demultiplexing is the first step that the tool ClonoCalc, which was used in this study, provides (*153*). Some tools offer an immediate error correction as part of the pre-processing that uses the quality scores. The final scientific question determines the thoroughness with which low quality sequences/errors are corrected for. When only statistics about the CDR3-length distribution or V(D)J-segment usage are analysed, then sequencing errors are less of a

problem and highly homologous sequences are grouped together (*154*, *155*). However, further analyses of the Ig-repertoire mostly require higher sequence accuracy. In the tool MiXCR, based on the quality score of the bases during the V(D)J-germline alignment process, low quality sequences are either excluded from the analysis or if possible assigned to high quality reads (*156*).

The alignment of the Ig-locus faces more challenges than the one of other not as variable genes. Due to V(D)J-recombination including diversity-increasing "errors" and SHM V, D and J-gene segments can only be mapped partially. Yet, a correct V(D)J-alignment is pre-requisite for correct identification of SHM for each read, clonal group clustering, and to have a fair diversity approximation (*157*). Most algorithms choose the closest match among a number of potential germline gene segments from a database (counts of gene segments in the Ig-locus see Table 1) (*158*). In addition, the sequenced fragment of the constant region will be aligned and allows control for proper amplification of only the Ig-locus as well as identification of the isotype if multiple isotypes are present in the sample.

The field of Ig-repertoire analysis is rather young, and most labs utilise their own custom pipelines for bioinformatic analysis. Therefore, comparisons and meta-analysis are often difficult (*126*). Alongside with different analysis pipelines come slightly varying definitions of steps in the analysis potentially resulting in different interpretations.

Differences in definitions regarding clonal relationships and designation of clonotypes are particularly drastic: Some tools define clonotype as a unique antibody (based on the amino acid sequence). MiXCR and tools basing on this algorithm, that were used for this study are even more stringent and define a clonotype based on the unique nucleotide sequence of CDR1- and CDR3- or CDR3-sequence only (*153*, *156*). Others define a clonotype or clone as a certain germline sequence and will group all sequences with similar V(D)J-germline rearrangement under one clonotype, which can differ in sequences produced by SHM (*159*). Another approach to clonotype grouping that is mathematically rather than biologically defined is single linkage clustering (a statistical method for hierarchical clustering). This defines the distance between clones (e.g. groups) as the minimum distance between all pairs of points from the given group (*160*).

The analyses of the repertoire comprising the aligned and clonotyped reads can be manifold:

More simple statistical repertoire analyses (i.e. mean clonotype count, read count, V-gene usage count/percentages, CDR3-length distributions) can be clinically relevant, as illustrated by some studies that demonstrated V-genes usage biases in patients with autoantibodies (*161*, *162*). It has also been reported that longer CDR3-segments are poly- or autoreactive (*143*, *163*). The CDR3-region can be analysed more qualitatively with regards to chemical properties of the contained amino acids such as hydrophobicity, charge etc. (*143*, *164*). Ultimately, one of the main reasons to analyse the Ig-repertoire using HTS is a better insight into the diversity of the B cell repertoire than any low throughput approaches could provide. Even by itself, clonotype

count allows estimation of repertoire variety. The relative diversity of the repertoire, clonotypes per total reads, reveals selection pressure during the immune response on certain clones.

Diversity is commonly calculated using the generalized diversity index that was developed by Hill in 1973 and is more general that the mathematical formulation often used to estimate biological diversity in the field of ecology (*165*). Other indices derived from Hill's index have been developed for repertoire diversity quantification. The main point here is to estimate the total diversity based on a sample that might not totally represent the whole population (*166*, *167*).

Aligned sequences can be compared to the germline configuration and SHM can be detected, quantified and characterised with regards to their impact on the amino acid sequence (silent versus non-silent mutations).

2 MATERIAL

2.1 Mice

Balb/c mice were purchased from Charles River Laboratory (Sulzfeld, Germany) and kept under specific pathogen-free (SPF) conditions in individual ventilated cages (IVC) in the animal facility of the University of Lübeck/Gemeinsame Tierhaltung. Parts of the experiments were performed at the animal facility at the Cincinnati Children's Hospital Medical Center (CCHMC). There, Balb/c mice were purchased from Charles River Laboratories (Wilmington, Massachusetts, USA) or bred in house. Animals were fed acidified drinking water and standard chow *ad libitum* and held on a 12-h light cycle. Mice used for the experiments were between seven and eight weeks old at the start of the experiment and only female mice were used. All experiments were approved by the Ministerium für Energiewende, Landwirtschaft, Umwelt und ländliche Räume of the state Schleswig-Holstein with the permission number V 242-18318/2016 (29-3/16) or (for experiments performed at CCHMC) by the CCHMC IACUC. Only certified personnel performed experiments under sterile conditions in a laminar flow cabinet.

2.2 Antibodies

Table 3: List of antibodies used in this study

Antibody	Conjugation	Clone	Company	Reference number	Used for
Anti-IgG1	Biotin	Polyclonal goat	Southern Biotech	1070-08	ELISA
Anti-IgG2a	Biotin	Polyclonal goat	Southern Biotech	1080-08	
Anti-IgG2b	Biotin	Polyclonal goat	Southern Biotech	1090-08	
Anti-IgA	Biotin	C10-1	BD	556978	
Anti-IgE	unlabelled		BD	553419	
IgE-anti-OVA	unlabelled	2C6	Serotec	MCA2259	
IgG1-anti-OVA	unlabelled	OVA-14	Sigma	A6075	
IgG1-anti-TNP	unlabelled	H5	in house	-	

2.3 Kits

Table 4: List of commercially available kits used in this study

Kit	Company	Reference number	Application
BCA Protein Assay Kit	Pierce	23227	
MCPT-1 (mMCP-1) Mouse Uncoated ELISA Kit	Invitrogen	88-7503-88	
LEGENDplex™ Mouse Th1/Th2 Panel	BioLegend	740751	Cytokine measurements
RNeasy mini Kit	Qiagen	74104 or 74106	RNA extraction
RNA 6000 Pico kit	Agilent	5067-1513	RNA quality control
Qiagen-One-Step-RT-PCR Kit	Qiagen	210212	cDNA synthesis for NGS using barcoded primers
iR-Custom-X-Ps; small bulk primers; Mouse BCR heavy chain (MBHI-M) IgG1 and IgE specific	iRepertoire	-	NGS Library Preparation
Qiagen Multiplex PCR-Kit	Qiagen	206143	Amplification of NGS library
MinElute Gel Extraction Kit	Qiagen	28604	DNA extraction from agarose gel
PerfeCTa NGS Quantification Kit	Illumina	95455-500	Quantification of NGS library
MiSeq Reagents Kit v2 500Cycles	Illumina	MS-102-2003	NGS
PhiX Control v3	Illumina	FC-110-3001	NGS library control
QuantiNova™ Reverse Transcription Kit	Qiagen	205411	cDNA synthesis
QuantiNova™ SYBR® Green PCR Kit	Qiagen	208052, 208054, 208056	Quantitative PCR

2.4 Buffers and solutions

Table 5: List of buffers and solutions used in this study

Buffers/ Solution	Ingredients	Concentration	Company	Reference number
Dulbecco's Phosphate Buffered Saline (DPBS)			Life Technologies	14190-094
Anaesthetics (1X)	Ketanest S Rompun in DPBS	5 mg/ml 1.5 mg/ml	Pfizer Bayer Healthcare	847028001G 1320422
Isotonic NaCl solution	Sodium Cloride			
Tris-Saline (10x)	Trizma Base NaCl pH 7.2	15.13 g/L 43.8 g/L	Sigma Aldrich Sigma Aldrich	93362 529552
Washing buffer (WB)	1x Tris/Saline Tween 20	 0.05 %	 Sigma Aldrich	 P7949
Dilution buffer (DB)	Washing buffer SuperBlock™	 10 %	 Thermo Scientific	 37545
SuperSignal™ ELISA Femto Substrate	1x Tris/Saline Solution A Solution B	 5 % 5 %	 Thermo Scientific Thermo Scientific	 37075 37075
Bicarbonate buffer (1 M)	$NaHCO_3$ Na_2CO_3 pH 9.6	0.2 M 0.2 M	Sigma Aldrich Merck Millipore	S5761 106392
RNA*later* RNA Stabilization Reagent			Qiagen	76106

2.5 Primers

For NGS, the custom designed primers specific for murine IgG1 and IgE were synthesised by iRepertoire. Sequences that bind to the IgG1 and IgE-gene of the company bought primers listed below are a secret of the company. All primers contain Illumina barcodes:

5'-AATGATACGGCGACCACCGAGATCTACACTCTTTCCCTACACGACGCTCTTCCGATCT-NNN-Barcode

This sequence above is then followed by the gene-specific sequence. The amplicon that is generated is approximately 250 bp long. Used barcodes are listed together with additional information in Table 6.

Table 6: Mouse BCR heavy chain MBHI-M small bulk primers (5 reactions per kit): list of barcodes

Barcode number	sequence	sample run 1	sample run 2
cMBHI-01	GTGTCA	mLN_769	mLN_777
cMBHI-02	TCTGAC	BM_2	-
cMBHI-03	TGACTA	mLN_758	mLN_768
cMBHI-04	CGCTCT	BM_758	BM_4
cMBHI-05	AGATGA	mLN_4	BM_753
cMBHI-06	ACTCAT	BM_768	BM_758
cMBHI-08	AGACAC	BM_777	BM_769
cMBHI-09	ATGATA	mLN_2	mLN_1

2.6 Reagents

Table 7: List of other reagents used in this study

Name	Company	Reference number
Ovalbumin from chicken (OVA)	Sigma Aldrich	A5503
SuperBlock™ (TBS) Blocking Buffer Dry Blend	Thermo Scientific	37545
HRP-Streptavidin	Thermo Scientific	21126
SuperSignal™ ELISA Femto Substrate	Thermo Scientific	37075
Biotin N-hydroxysuccinimide ester(+)		H1759
DMSO	Sigma Aldrich	276855
Ketanest S	Pfizer	847028001G
Rompun	Bayer Healthcare	1320422
Sterillium® Virugard	Sterillium	9800122
Food colouring dye (Lebensmittelfarbe flüssig blau)	Städter	392311
Picrylsulfonic acid for TNP-BSA preparation	Sigma Aldrich	3182T
Bovine serum albumin (BSA)	Sigma Aldrich	A9418

2.7 Consumables

Table 8: List of consumables used in this study

Name	Company	Reference number
Cannulas for syringes (18G or 26G)	BD Medical Technology	303129 and 303800
ELISA plate sealer	R&D Systems	DY992
Syringe for injections (1 ml)	Braun	9166017V
Syringes (1 ml Luer-Lok)	BD Medical Technology	309628
gentleMACS M Tubes	Miltenyi	130-093-236, 130-096-335
Spectra/Por™ 1 6-8 kD MWCO Standard RC Dry Dialysis Tube	Spectrum labs	132665
Corning® 96-well Clear Flat Bottom Polystyrene High Bind Microplate	Corning	9018
Cell strainer (70 µm)	Greiner bio one	542070
Corning® 96-well White Flat Bottom Polystyrene High Bind Microplate	Corning	3922
Tegaderm™ 3M Film 6x7 cm	3 M	1624W
Polypropylene V-bottom plate	BioLegend	740379
MiniCollect® Z Serum Separator tubes	Greiner Bio-one	450472

2.8 Laboratory equipment

Laboratory materials of daily use such as pipettes, pipette tips, reaction tubes and cell culture material (plates, serological pipettes) were purchased from Sarstedt, Eppendorf or Th. Geyer.

Table 9: List of laboratory equipment used in this study

Name	Company	Reference number
Centrifuge 5810 R	Eppendorf	-
Centrifuge Microfuge 22R	Beckman Coulter	-
Compact M gel chamber	Biometra Biosciences	-
Image Quant 350 (UV transilluminator)	GE Healthcare	-
gentleMACS Dissociator	Miltenyi	130-093-235
Julabo SW-20C shaking water bath	Julabo	-
Laminar Flow Cabinet (LabGard Class II Biological Safety Cabinet NU-437)	NuAire/IBS Integra Biosciences	-
LSR II Flow cytometer	BD	-
Omega FLUOstar ELISA reader	BMG Labtech	-
pH meter	Mettler Toledo	-
ThermoMixer 5436	Eppendorf	-
Vortex Genie 2	Scientific Instruments	-
Labocult Incubator for ELISA plates	Servoprax	-
Microprobe Thermometer	Physitemp	BAT-12
Rectal Probe for Mice (Isolated)	Physitemp	RET-3-ISO
Reusable Feeding Needles (20G, cylindrical tip)	Fine Science Tools GmbH	18060-20
Bioanalyzer 2100	Agilent	G2939BA
MiSeq-System	Illumina	

2.9 Software

Table 10: List of software used in this study

Name	Version	Developer	Application
FLUOstar Omega	2.10	BMG Labtech	ELISA
MARS Data Analysis Software	2.30R2	BMG Labtech	ELISA data evaluation
GraphPad PRISM	5.03	Graphpad Software, Inc	Graphics and statistics
IQuant Capture 350	1.02	GE Healthcare	DNA detection with UV light
Microsoft Office	365 (2016)	Microsoft Corporation	Data and protocol management
LEGENDplex™ Data Analysis Software	8.0	BioLegend	Data analysis of LEGENDplex assay
R	3.3.1	The R Foundation for Statistical Computing	NGS data processing and analysis
R Studio	1.1.383	RStudio, Inc.	Work with R
FastQC	1.0.0	BaseSpace Labs	Quality control of NGS data
ClonoCalc		Fähnrich et al., 2017	
MiXCR		Bolotin et al., 2015	
R-packages used dplyr	 0.8.1		

3 METHODS

3.1 Egg preparation

3.1.1 Egg white (EW)

12-18 Eggs from a local grocery store were sterilised by wiping and spraying with Bacillol Virugard (the disinfectant was allowed to dry on the eggs) and subsequently irradiated for 10 mintues (min) with UV light. Egg white and egg yolk were separated into autoclaved beakers. (See paragraph 3.1.2 for additional information on egg yolk plasma preparation).

The egg white (EW) was transferred into dialysis tubing (Molecular weight cut off (MWCO) 6-8 kilo Dalton (kDa)) which had been pre-soaked in bi-distilled water (A. bidest.) and was dialysed against 4 L A. bidest. for 72 h at 4 °C. A. bidest. was exchanged every 12 h. The dialysed EW was then centrifuged for 10 min at 5.000x g, 4 °C. The supernatant was collected and then either concentrated with an Amicon stirred cell (filter membrane MWCO 10.000 Da) or lyophilised. The concentration of EW was measured with PierceTM BCA Protein Assay Kit (see paragraph 3.1.3). Concentrated or lyophilised EW was stored at -20 °C.

3.1.2 Egg yolk plasma (EYP)

Egg yolk was diluted 1:2 in sterile isotonic (0.9 %) saline solution. The egg yolk solution was centrifuged for 10 min at 13.000X g, 4 °C, yielding a solid and a liquid fraction. The liquid fraction – the egg yolk plasma (EYP) – was collected and stored at -20 °C.

3.1.3 BCA (Bicinchoninic acid) assay

The protein concentration of EW was determined with the Pierce BCA Protein Assay Kit. The BSA standard was diluted in DPBS according to the manufacturer's guide. The egg white sample was diluted 10-, 100- and 1000-fold in DPBS. Working reagent solution was made by mixing 50 parts of reagent A and 1 part of reagent B. 20 µL of each sample or standard dilution was mixed with 200 µL of working solution in clear 96-well microplate flat bottom high binding (Corning 9018) plates. Plates were sealed and subsequently incubated in an incubator for ELISA plates for 30 min at 37 °C. The optical density (OD) was measured with an ELISA reader at 562 nm. A standard curve was calculated with Excel, which was then used to determine the EW concentration.

3.2 Experimental food allergy

Balb/c mice were sensitised to EW and EYP either *intra-tracheally* (*i.t.*) or *epicutaneously* (skin patches) according to paragraph 3.2.1 and 3.2.2) and orally challenged subsequently. When *i.t.* sensitisation was performed, mice were orally challenged 3x per week, after skin-sensitisation 2x per week (according to paragraph 3.2.2).

3.2.1 Intra-tracheal sensitisation to EW plus EYP

1.25 mg EW was mixed with 1 mL EYP to yield an EW plus EYP-solution with a concentration of 1.25 mg/mL. The solution was filtered through a 70 µm cell strainer to retain large particles. Balb/c mice were anesthetised by intra peritoneal (*i.p.*) injection of 200 µL anaesthetics (5 mg/mL Ketanest S, 1.5 mg/mL Rompun in DPBS). Mice were fixed on a plastic board and then *intra-tracheally* (*i.t.*) inoculated with 40 µL of the EW plus EYP-solution (equal to 50 µg EW).

After every anaesthesia (also in the following, where it will be not mentioned again), mice were watched for 60-90 min and put under a warming light, if they were not recovering promptly. The procedure was repeated three times per week for two weeks.

3.2.2 Epicutaneous (skin) sensitisation to EW plus EYP

Prior to the first skin-sensitisation, Balb/c mice were anesthetised by *i.p.* injection of 200 µL anaesthetics and dorsal hair from the shoulders to the beginning of the tail was removed by shaving. The mice were given 24 h to recover from the anaesthesia. For skin-sensitisation, 1 mg EW was mixed with 1 mL EYP to yield an EW plus EYP-solution with a concentration of 1 mg/mL. A piece of sterile gauze (*circa* (*ca.*) 2x2 cm) was placed on the back of the mouse and slathered with 100 µL of the EW plus EYP-solution (equal to 100 µg EW). The soaked gauze was sealed air-tightly with a 6x7 cm Tegaderm™ Film cut in half. Premature detachment of the Tegaderm™ was prevented by fixing it in place with a plaster and a piece of soft cloth tape. The procedure of applying the skin-patches was performed three times within 3 weeks. One day before the re-patching was performed, the skin-patches from the previous week were removed. The last patch was removed after 6 days one day before first challenge.

3.2.3 Oral gavage challenge with EW plus EYP

Lyophilised egg white was dissolved in saline to a concentration of 1 g/mL. One part of the EW-solution was mixed with two parts of EYP. To assess occurrence of diarrhoea more easily, the solution was further mixed with 2-5 µL of a food colouring dye per 300 µL EW plus EYP-solution. To remove non-dissolved EW-precipitates, the mixture was centrifuged for 5 min at 300 x g, room temperature (RT) and kept at RT. Mice were fasted 4 h. Prior to the challenge, the

baseline rectal temperature of the mice was measured after the mice were given some time to become active. To measure rectal temperature, conscious mice were fixed and a temperature probe was inserted rectally until the temperature stayed constant. Subsequently, conscious mice received 300 µL of the EW plus EYP-solution (equal to 100 mg EW) by oral gavage (o.g.) with a re-usable feeding needle that was flushed and autoclaved after every use. Rectal temperature and diarrhoea development were assessed every 15 min for 1 h after each o.g. challenge. The procedure was repeated three times per week (for *i.t.* sensitisation) or two times per week (for skin-sensitisation).

3.2.4 Gut permeability assay

3.2.4.1 Preparation of biotinylated TNP-BSA

6 mg of picryl sulfonic acid (TNP) was dissolved in 300 µl DMSO. The TNP/DMSO solution was added to 30 mg BSA dissolved in 15 mL DPBS solution and incubated at RT O/N protected from light. The solution was transferred into dialysis tubing (MWCO 6-8 kDa) which had been pre-soaked in A. bidest. and was dialysed against 500 mL A. bidest. for >72 h at 4 °C (until the dialysate had lost its yellow colour. Biotin N-hydroxysuccinimide ester(+) (further referred to as biotin) was dissolved in DMSO. 1/10 volume of 1M Bicarbonate buffer (pH 9.6) was added to the TNP-BSA. At a molar ratio of 1:10 (protein:biotin), biotin was added dropwise to the protein solution; the mixture was vortexed after each addition of biotin and incubated for 1 h at RT with periodic shaking. The biotinylated TNP-BSA was transferred into dialysis tubing (MWCO 6-8 kDa) that had been pre-soaked in A. bidest. and dialysed against 500 mL DPBS for 72 h with buffer changes every 12 h. The product was stored at -20°C protected from light.

3.2.4.2 Oral gavage with biotinylated TNP-BSA

In order to measure mouse gut integrity, an antigen irrelevant to our EW and EYP model is given to the mice. Here, 10 mg (300 µL) of biotinylated TNP-BSA was given by oral gavage to mice that had first been fasted for 4 h. To measure the amount of biotinylated TNP-BSA that has entered the blood stream through the gut mucosa, mice were bled from the facial vein or tail vein 15 min after challenge. Blood was collected in serum tubes and allowed to clot for ca. 30 min at RT. The serum tubes were centrifuged for 10 min at 2000 x g at RT, after which serum biotin-TNP-BSA levels were determined by ELISA (see 3.3.4).

3.2.5 Sample collection

To obtain serum, mice were bled from the facial vein or tail vein and blood was collected in MiniCollect® Z Serum Separator tubes (Greiner One). Blood was allowed to clot for 30 min at RT (if no cytokines were measured in the particular sample) or at 4°C (if cytokines were measured. Subsequently, serum tubes were centrifuged for 10 min at 2000 x g at RT or 4°C

(indication mentioned above) and the serum was aliquoted to prevent multiple freezing and thawing cycles for cytokine measurements and stored at -80°C. Organs were harvested after mice were killed by cervical dislocation.

3.3 Enzyme-linked immunosorbent assay (ELISA)

3.3.1 EW/OVA-specific IgG1, IgA, IgG2a and IgG2b

White Costar® 96-well plates were coated with 50 µL EW or OVA at a concentration of 10 µg/mL in 1X Tris/saline overnight (O/N) at 4 °C. To block unspecific binding, plates were washed 5x with washing buffer (WB) and subsequently incubated with 100 µL dilution buffer (DB) for 60 min at RT.

Standard- (pooled serum samples for EW-specific antibodies and mouse-anti-OVA-IgG1 for anti-OVA-IgG1) and sample-dilutions in DB were prepared according to Table 11. The standard dilution was further 2-fold serially diluted in DB. As a negative control, serum from a naïve mouse was used and diluted similar to the samples.

Table 11: Standard and sample dilutions of EW/OVA-specific IgG1, IgA, IgG2a and IgG2b ELISAs

ELISA-specificity	**Standard**	**Standard dilution**	**Sample dilutions**	
			Serum of sensitised mice	Serum of challenged mice
EW-IgG1	Pooled EW/EYP sera	1:5000 ≙ 0.02 U	1:100, 1:1000 and 1:10000	1:2000, 20000 and 1:100000
EW-IgA	Pooled EW/EYP sera	1:200 ≙ 0.5 U	1:50, 1:100 and 1:500	1:100, 1:500 and 1:1000
EW-IgG2a	Pooled EW/EYP sera	1:1000 ≙ 0.01 U	1:500, 1:1000 and 1:50000	1:1000, 1:10000 and 1:100000
EW-IgG2b	Pooled EW/EYP sera	1:1000 ≙ 0.01 U	1:500, 1:1000 and 1:50000	1:1000, 1:10000 and 1:100000
OVA-IgG1	Mouse-anti-OVA-IgG1	500 ng/mL	1:100, 1:1000 and 1:10000	1:2000, 20000 and 1:100000

30 µL of each standard and sample dilution was added to the plates, with DB serving as blank. Plates were incubated for 60 min at RT. Then, plates were washed 5x and 30 µL biotinylated anti-mouse-IgG1, -IgA, -IgG2a or -IgG2b antibody (Ab) dependent on the ELISA specificity diluted in DB to a concentration of 200 ng/mL was added to each well. After incubation for 30 min at RT, plates were washed 5x and 30 µL streptavidin-horseradish peroxidase (HRP) diluted in DB to a concentration of 50 ng/mL were added to each well. Plates were incubated for 20-25 min at RT and afterwards washed 6x. 200 µL of 1X Tris/saline were added to each well

and kept on the plate for 3 min. Meanwhile, Super Signal ELISA Substrate was prepared with 18 mL 1X Tris/saline and 1 mL of each Super Signal Substrate component. When more was needed, the components were up-scaled accordingly. Tris/saline was removed from the plates and 150 µL Super Signal ELISA Substrate was added to each well. Relative luminescence units (RLU) were measured immediately with a Luminometer (ELISA reader).

3.3.2 EW/OVA-specific IgE

3.3.2.1 Biotinylation of EW/OVA

For detection of EW- and OVA-specific IgE, the proteins were coupled to biotin. Biotin was dissolved in DMSO. EW or OVA was dissolved in DPBS and 1/10 of 1M bicarbonate buffer (pH 9.6) was added. At a molar ratio of 1:10 (protein:biotin), biotin was added dropwise to the protein solution, the mixture was mixed by vortexing after each addition of biotin. The average molecular weight of EW was determined according to Table 12. The mixture was incubated for 1 h at RT while repeatedly being shaken.

Table 12: Average MW of EW based on MW of its components

component	MW (in Da)	percent of EW	percent of EW protein
OVA	43000	55%	67.6%
Ovomucoid	28000	11%	13.5%
Ovotransferrin	70000	12%	14.7%
Lysozyme	14000	3.4%	4.2%
Average MW EW	43742.01		

The biotinylated protein was transferred into dialysis tubing (MWCO 6-8 kDa) which had been pre-soaked in A. bidest. and dialysed against 500 mL DPBS for 72 h with buffer changes every 12 h.

3.3.2.2 Procedure of the assay

White Costar® 96-well plates were coated with 50 µL anti-mouse IgE monoclonal Ab (mAb) at a concentration of 5 µg/mL in 1X Tris/saline for overnight (O/N) at 4 °C. Blocking and sample preparation (for dilution for IgE ELISAs refer to table 13) as well as incubation with the streptavidin-HRP and further detection and measurements were performed similarly to the ELISAs for EW/OVA-specific antibodies of isotypes described in 3.3.1.

Table 13: Standard and sample dilutions of EW/OVA-specific IgE ELISAs

ELISA-specificity	Standard	Standard dilution	Sample dilutions	
			Serum of sensitised mice	Serum of challenged mice
EW-IgE	Pooled EW/EYP sera	1:20 ≙ 5 U	1:4, 1:10 and 1:50	1:10, 1:50 and 1:100
OVA-IgE	Mouse-anti-OVA-IgE	500 ng/mL	1:4, 1:10 and 1:50	1:10, 1:50 and 1:100

Differing from the previously described protocol, after incubation of the serum in this case the washed plates were incubated with 30 µL of 200 ng/mL biotinylated OVA or EW.

3.3.3 mMCP1

Mucosal mast cell protease-1 (mMCP-1) in mouse serum was detected with MCPT-1 (mMCP-1) Mouse Uncoated ELISA Kit (Invitrogen, 88-7503-88). Briefly, white Costar® 96-well plates were coated with 50 µL capture Ab diluted 1:250 in 1X Tris/Saline O/N at 4 °C. Coated plates were washed 5x with WB and wells were blocked for 60 min at RT with 100 µL DB. MMCP-1-standard was serially diluted in 2-fold dilution steps in DB starting at 50 ng/mL. Samples from naïve mice were diluted 1:10 and 1:100 in DB. Samples from challenged mice were diluted 1:100, 1:1000 and 1:10.000. 30 µL of each standard and sample dilution were added to the plates and incubated for 60 min at RT. Then, plates were washed 5x with WB. 30 µL detection Ab diluted 1:250 in DB was added to each well. After incubation for 30 min at RT, plates were washed 5x and 30 µL streptavidin-HRP diluted in DB to a concentration of 50 ng/mL was added to each well. Plates were incubated for 20-25 min at RT and afterwards washed 6x. 200 µL of 1X Tris/saline was added to each well and kept on the plate for 3 min. Meanwhile, Super Signal ELISA Substrate was prepared with 18 mL 1X Tris/saline and 1 mL of each Super Signal Substrate component. When more was needed, the components were up-scaled accordingly. Tris/saline was removed from the plates and 150 µL Super Signal ELISA Substrate was added to each well. Relative Luminescence Units (RLU) was measured immediately with a Luminometer (ELISA reader).

3.3.4 Biotinylated TNP-BSA

Serum samples collected after oral biotinylated TNP-BSA challenge (see 3.2.4.2) were used in this ELISA. White Costar® 96-well plates were coated with 50 µL anti-TNP IgG1 diluted to a concentration of 5 µg/mL in 1X Tris/Saline O/N at 4 °C. Coated plates were washed 5x with WB and wells were blocked for 60 min at RT with 100 µL DB. Biotinylated TNP-BSA serving as a standard was serially diluted in 2-fold dilution steps in DB starting at 150 ng/mL. Samples were

diluted 1:10, 1:20 and 1:100 in DB. Then, plates were washed 5x with WB and 30 µL Streptavidin-HRP diluted in DB to a concentration of 50 ng/mL was added to each well. Plates were incubated for 20-25 min at RT and afterwards washed 6x. 200 µL of 1X Tris/saline was added to each well and kept on the plate for 3 min. Meanwhile, Super Signal ELISA Substrate was prepared with 18 mL 1X Tris/saline and 1 mL of each Super Signal Substrate components. When more was needed, the components were up-scaled accordingly. Tris/saline was removed from the plates and 150 µL Super Signal ELISA Substrate was added to each well. Relative Luminescence Units (RLU) was measured immediately with a Luminometer (ELISA reader).

3.4 Bead-based immune assay for cytokine detection (LEGENDplex®)

Detection of the cytokines IFNγ, IL-2, IL-4, IL-5, IL-6, IL-10, IL-13 and TNFα in serum was performed using the LEGENDplex™ Mouse Th1/Th2 Panel (Biolegend, 740751) according to the manufacturer's guide in a polypropylene (PP) V-bottom plate. Briefly, after bringing all reagents to RT, the 8 different 13x beads containing capturing antibodies for the cytokines were sonicated for 1 min, mixed and diluted in assay buffer to yield a 1x mixture. Samples were diluted 2-fold, the standard was diluted by 3-fold serial dilution with the assay buffer serving as blank. In a PP V-bottom plate 6.25 µL assay buffer (for sample wells) or Matrix B (for standard wells) were added followed by 6.25 µL of sample or the standard. Mixed beads were vortexed and 6.25 µL was added to all wells. The plate was sealed, light-protected and incubated O/N at 4 °C on a rotator shaking at 800 rounds per minute (RPM). Then, plates were centrifuged at 250 x g for 5 min at RT and the supernatant was carefully removed with a pipette. 100 µL of the kit's wash buffer was added, plates were centrifuged at 250 x g for 5 min at RT and the supernatant was carefully removed with a pipette. 6.25 µL of detection antibody was added to all wells. The plate was sealed, light-protected and incubated for 30 min at RT on a rotator shaking at 800 RPM. Without washing 6.25 µL streptavidin-PE was added to the plates. The plate was sealed, light-protected and incubated for 30 min at RT on a rotator shaking at 800 RPM. Washing was performed similarly to the washing described after the O/N incubation. Finally, the beads were re-suspended in 250 µL of the kit's washing buffer and analysed on a LSRII flow cytometer.

3.5 Next generation sequencing (NGS) analysis of the IgE and IgG1 repertoire

NGS IgE and IgG1 repertoire analysis was performed with bone marrow (BM) and mesenteric lymph nodes (mLN) from EW/EYP skin-sensitised and orally challenged mice that exhibited clear signs of food allergy. Tissue samples were collected, cut into small pieces (ca. 2x2 mm), transferred into tubes with RNA*later* and incubated at 4°C O/N to be stored at -20°C in RNA*later* solution (Qiagen).

3.5.1 RNA-isolation

Tissue stored in RNAlater was diluted by addition of an equal volume of ice cold PBS immediately before centrifugation to reduce the density of the solution. The solution was then centrifuged for 5 min at 450 x g, 4°C, after which the supernatant was discarded. For RNA-isolation of the tissue, that was stored in RNA*later,* the RNeasy mini Kit (Qiagen #74104) was used according to the manufacturer's guide with some modifications.

The following tissue disruption was only performed for mLN-samples; for BM-samples consisting of cells stored in RNA*later*, cells were disrupted by rigorous pipetting. 600 µL RLT buffer (lysis buffer) per 30 mg of tissue was added into a gentle Macs M Tube and the tissue was transferred into the tube as well. The tissue was disrupted using a gentleMACS Dissociator running the pre-installed program "RNA_01". The cell lysate (similarly for all samples including BM) was collected at the bottom of the tube by centrifugation for 1 min at 2000 x g, 4°C. To get rid of any cell debris, the homogenised lysate was transferred to a reaction tube and centrifuged for 3 min at full speed. An equal volume of 70% ethanol was added to the cleared lysate and mixed. The mixture was added to an RNeasy spin column placed in a 2 ml collection tube and centrifuged for 15 seconds (s) at 10000 RPM. The flow-through was discarded. 700 µl of Buffer RW1 was added to the RNeasy spin column and centrifuged as described before. 500 µL of Buffer RPE was added to the column and centrifuged as described before. Another 500 µL of Buffer RPE was added to the column and centrifuged for 2 min at 10000 RPM. The membrane of the column was dried by centrifugation for 1 min at 10000 RPM collecting any flow-through in a new 2 mL collection tube. To elute the isolated RNA, the spin column was placed in a 1.5 mL collection tube, 40 µL RNAse-free water was added directly onto the membrane and centrifuged for 1 min at 10000 RPM. An aliquot of 5 µL was stored separately for quality control, which was performed using an Agilent Bioanalyzer 2100 and an RNA 6000 Pico kit (Agilent). Based on the integrity of ribosomal RNA RNA-integrity numbers (RIN) were determined (RIN=10 meaning intact RNA, RIN=0 completely degraded RNA). Only RNA-samples with RIN of 6 or higher were used for NGS-analyses.

3.5.2 Reverse transcription (PCR 1)

Reverse transcription of the RNA-samples was performed using the Qiagen-One-Step-RT-PCR Kit (Qiagen #210212) according to Table 14. The custom designed primers specific for murine IgG1 and IgE were synthesised by iRepertoire.

Table 14: Reaction components of reverse transcription for NGS-analysis

Component	Volume/reaction	Final concentration
RNA (500 ng)	4 µL	-
5x QIAGEN OneStep RT-PCR Buffer	5 µL	1x
desoxy-nucleoside tri-phosphates (dNTPs) 10 mM each	1 µL	400 µM of each dNTP
Mouse BCR heavy chain MBHI-M specific for IgG1 and IgE	3 µL	0.5–1.0 µM
QIAGEN OneStep RT-PCR Enzyme Mix	1 µL	-
RNAse-free water	11 µL	
Total volume	25 µL	

The reaction was run on a Thermal Cycler C1000 (Bio-Rad Laboratories) using conditions as described in Table 15.

Table 15: Conditions for reverse transcription (PCR 1)

Step	Temperature	Time	Repeat/Cycles
Reverse transcription	50°C	40 min	
Initial PCR activation step	95°C	15 min	
Amplification	94°C	30 s	15x
	60°C	2 min	
	72°C	30 s	
	94°C	30 s	10x
	72°C	2 min	
Final extension	72°C	10 min	

3.5.3 cDNA library amplification (PCR 2)

The product of PCR 1 was the further amplified using generic primers provided in the iRepertoire Kit that bind Illumina-adaptors introduced by the primers used in PCR 1. For the subsequent amplification the Qiagen Multiplex PCR Kit (Qiagen #206143) was used according to Table 16

Table 16: Reaction components of PCR 2 for NGS-analysis

Component	Volume/reaction	Final concentration
Product of PCR 1	1 µL	-
2x QIAGEN Multiplex PCR Master Mix	12.5 µL	1x
Communal primers for Illumina (iRepertoire)	2.5 µL	0.2 µM
RNAse-free water	9 µL	
Total volume	25 µL	

The reaction was run on a Thermal Cycler C1000 (Bio-Rad Laboratories) using conditions as described in Table 17.

Table 17: Conditions for PCR 2

Step	Temperature	Time	Repeat/Cycles
Initial PCR activation step	95°C	15 min	
Amplification	94°C	30 s	40x
	55°C	30 s	
	72°C	30 s	
Final extension	72°C	5 min	

The product of PCR 2 was mixed with loading dye and transferred to a 2% agarose gel and run for 45 min at 110 V.

The bands corresponding to the appropriate bp length were cut out and collected for DNA-extraction.

3.5.4 Library purification and isolation (Gel extraction)

DNA-recovery from the agarose gel was performed using a MinElute Gel Extraction Kit (Qiagen 28604) according to the manufacturer's guide.

3.5.5 Library quantification

The extracted DNA was quantified using the PerfeCTa NGS Quantification Kit (Illumina #95455-500). First, samples were diluted 1:10000 with 1x dilution buffer (1:10 dilution of 10x dilution buffer provided in the kit), the standard was serially diluted. Reaction components were added according to

Table 18.

Table 18: Reaction components for PerfeCTa NGS Quantification

Component	Volume/reaction	Final concentration
Product of PCR 2 (1:10000 diluted)	4 µL	-
2x Perfecta Sybr Green SuperMix	10 µL	1x
Illumina Primer Mix (10 µM each)	0.6 µL	0.24 µM each
PCR-grade water	5.4 µL	
Total volume	2 µL	

3.5.6 Sequencing run

For preparation of the library for paired-end sequencing with the Illumina MiSeq system 5 µL aliquots of each sample at a concentration of 2 nM (diluted with Tris/HCl based on concentration determination as described above) were pooled and PhiX Control v3 was added to the library as an internal sequencing control. Approximately 1-1.5 million sequencing reads per sample of the BCR library were obtained

3.5.7 Data processing and analysis

First, the quality of the NGS data was determined using FastQC. The data was de-multiplexed into the individual samples with ClonoCalc (*153*). The determination of clonotypes (unique CDR3 nucleotide-sequences) was performed using MiXCR (*168*). The output data included a clone ID that was given by the program sorted by occurrence of this sequence starting at 1 for the most abundant clonotype, abundance of the clonotype (number of sequences, percentage of this clonotype of all sequences), aligned V-, D-, J- and C-gene (the C-gene alignment allows separation of sequences into IgE and IgG1), CDR3 nucleotide and amino acid sequence, the quality score and length of the CDR3-region. Additionally, to avoid artificial diversity due to PCR errors, all clonotype sequences that appeared only once were removed.

Overlapping sequences between IgE and IgG1 were determined using InteractiVenn (*169*).

For determination of clonotypes that share V-, D-and J- genes, the R programming language with package dplyr with command inner_join was used.

3.6 Statistics

Statistical analysis of data was calculated with GraphPad Prism software.

Data sets were tested for normality using the D'Agostino & Pearson omnibus normality test and the test was chosen accordingly and indicated in the respective figures. *$p<0.05$, **$p<0.01$, and ***$p<0.001$. Data were plotted as mean ± SEM.

For analyses of multiple groups compared at different time points the 2-Way ANOVA with Bonferroni post-test correction was used to test differences among the groups. For multi-group analyses, where one of the parameters tested was not normally distributed, without taking time into account, the Kruskal-Wallis test with Dunns multiple comparison test was used.

For the two-parameter correlations, the Spearman's coefficient (rho; r) was calculated.

4 RESULTS

4.1 Food allergy induction without artificial adjuvants in a new mouse model

Most established mouse models for food allergy use non-physiological adjuvant-based immunisation/sensitisation methods (*170*). In contrast, the murine EW/EYP food allergy model used here takes advantage of the adjuvant property of the saturated fats in egg yolk plasma (EYP) (*36*) which may represent a natural means of allergy sensitisation and allows the omission of artificial adjuvants (*171*).

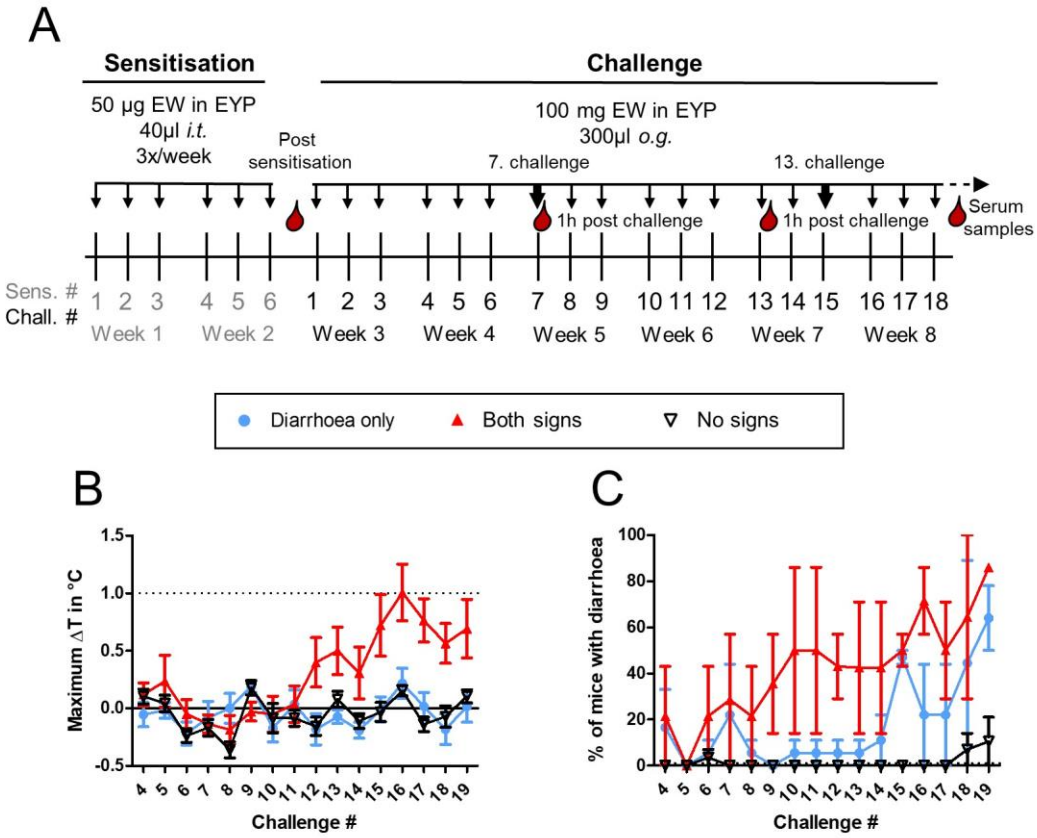

Figure 4: The development of food allergy signs varies among mice
Female Balb/c mice were sensitised to and challenged with EW/EYP according to section 3.2. Blood was taken after the sensitisation phase, before the first challenge or 1h after the respective challenge, as indicated. Immediately after each challenge, the rectal temperature was measured every 15 min for 1h and occurrence of diarrhoea was observed. Based on the development of these signs of food allergy, mice were categorised into different groups: mice that had at least 2 episodes of diarrhoea but never a temperature drop ≥ 1°C in response to a challenge (Diarrhoea only; n=11), mice that had at least one episode of diarrhoea and at least 2 episodes of a temperature drop (max. ΔT ≥ 1°C) in response to a challenge (Both signs; n=14) and mice, that neither developed diarrhoea more than once nor a temperature drop in response to a challenge (No signs; n=28). Mice that developed max. ΔT between 0.5°C and 1°C were excluded from the analysis to not be falsely categorised. In total, 53 mice were analysed. For handling reasons, the large number of mice were analysed at two separate times. Pooled data are shown. (**A**) Experimental scheme. (**B**) Max. ΔT at challenges 4 to 19 for the three groups "Diarrhoea only", " Both signs" and "No signs", as indicated. Data presented as mean ± SEM max. ΔT of all mice in each group. (**C**) Occurrence of diarrhoea, for the three groups, as indicated. Data presented as mean ± SEM of the percentage of mice in each group showing diarrhoea.

Mice were intra-tracheally sensitised to and orally challenged with egg white (EW) and EYP according to section 3.2 and Figure 4A. Later, diarrhoea, drop in the body temperature in response to allergen-rechallenge and serum parameters were analysed at various times.

Within the 8 weeks of observation, mice were challenged 19 times. During this period, the development of the disease greatly differed among individual mice (Figure 4B&C). Mice were grouped according to whether or not they developed signs of food allergy in the course of the experiment. About half of the mice never showed any sign of food allergy (at least 2x diarrhoea and/or temperature drop over 1°C). This group of mice is called "no sign". Among those mice that developed sign, these vary in onset and severity. While about a fifth (11/53) of the mice developed diarrhoea but no sign of systemic anaphylaxis (measured as temperature drop ("Diarrhoea only"), approximately a quarter of the mice (14/53) also developed a drop in the body temperature ("Both signs").

The temperature drop usually occurred at a later challenge than diarrhoea and increased in severity over time up to an average of about 0.5-1°C while the maximum was 6°C for an individual mouse. The percentage of mice with diarrhoea at the particular challenge reached 90-100% in the group showing both signs and 70-80% in the group of mice that only develop diarrhoea. It has to be noticed, that both signs varied even for one mouse between subsequent challenges; however, the occurrence of signs stabilized as disease progressed.

4.2 IgE levels strongly correlate with the development of signs

Serological factors were compared between the aforementioned groups that were formed based on differences in the signs of food allergy.

4.2.1 The development of food allergy signs is associated with elevated EW-specific antibody titres, especially IgE, and a decreased EW-IgG1/IgE-ratio

In food allergy, allergen-specific antibodies of various immunoglobulin subclasses are secreted; among them IgE drives the disease and IgG1 (IgG4 in humans) which is induced by a partially similar cytokine milieu as IgE (IgE is induced by IL-4 and IL-13; IgG1 is induced by IL-4, IgG4 is induced by IL-4 or IL-13 in the presence of IL-10) (*114*, *115*). Multiple proteins in EW contribute to its allergenicity (*23*), therefore antibodies against the whole EW-mixture were measured by ELISA. EW-specific IgE, IgG1, IgA, IgG2a and IgG2b are measured at different time points in the course of the experiment (after sensitisation/before the first challenge and 1 h after challenge 7 and 13; Figure 5).

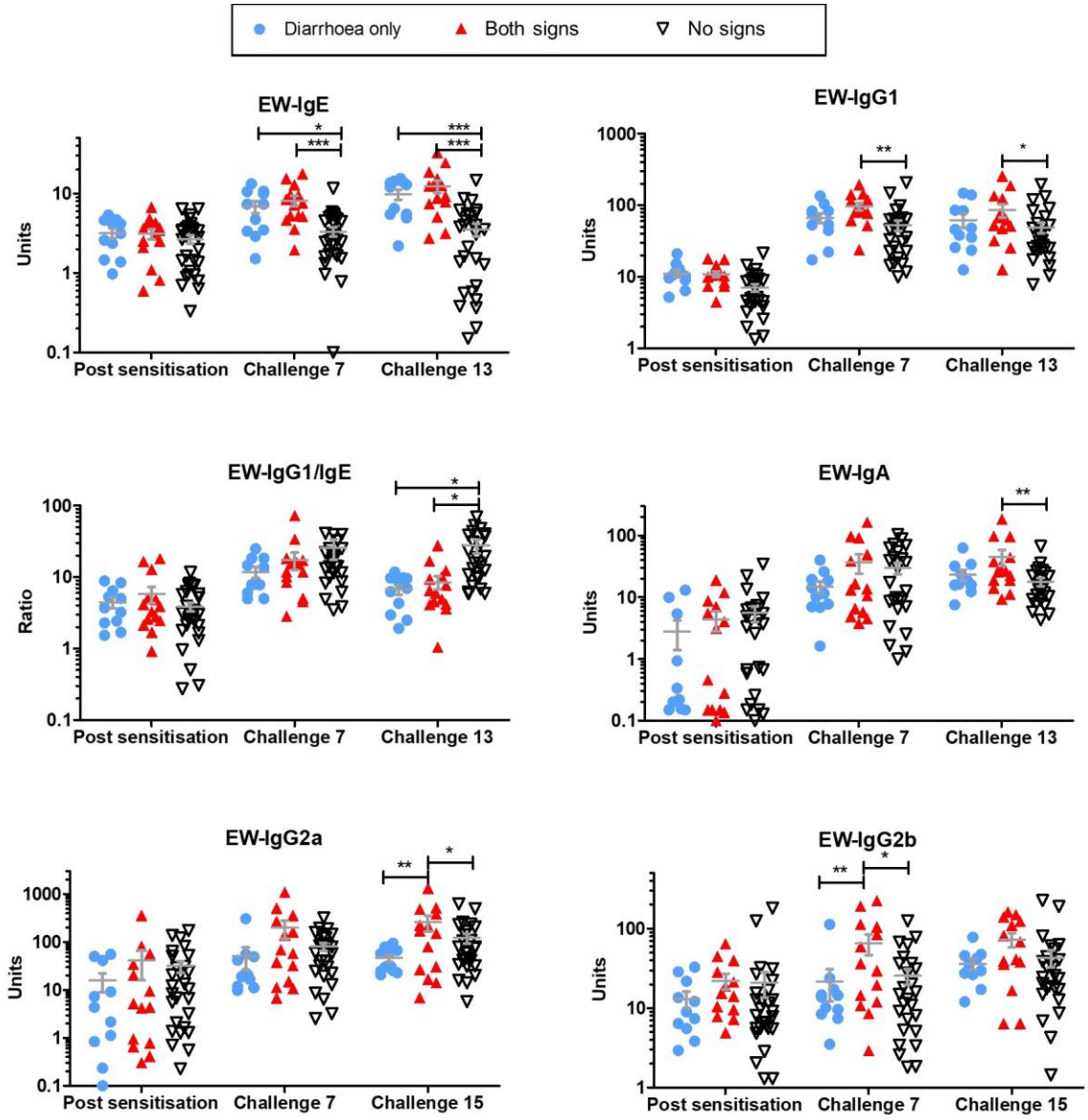

Figure 5: EW-specific antibody titres in mice with and without food allergy signs
Female Balb/c mice were sensitised to and challenged with egg white and egg yolk plasma according to section 3.2/Figure 4A. Based on the development of food allergy signs after each challenge, mice were categorised into different groups, as explained in detail in Figure 4A: Diarrhoea only (n=11), Both signs (n=14) and No signs (n=28).Serum was taken at indicated time points (after the sensitisation phase before the first challenge or 1h after the respective challenge) and relative EW-specific IgE, IgG1, IgA, IgG2a and IgG2b were measured by ELISA. Pooled sera of EW/EYP-allergic mice was used as a standard resembling 100 units of each antibody. Statistics: 2-Way ANOVA with Bonferroni post-test; not significant (no mark): $p > 0.05$ *: $p<0.05$, **$p< 0.01$, ***: $p<0.001$. Mean ± SEM is shown.

Before the start of the first challenge (post sensitisation), there were no detectable differences in any of the measured EW-specific antibodies (IgE, IgG1, IgA, IgG2a and IgG2b) between mice that showed signs and those that did not (Figure 5).

Levels of all EW-specific antibody subclasses rose overall from sensitisation over the 7th to the 13th challenge. However, a more severe increase could be seen for IgE, IgG1 and IgA. EW-IgE only rises in mice that developed signs while there is no increase in mice that never showed signs. This selective increase resulted in significantly higher EW-IgE levels in mice that

developed signs compared to those that did not. This difference was more pronounced for the group of mice that had both signs. Only mice that developed both signs showed increased EW-IgG1 levels compared to the mice that lacked signs at challenges 7 and 13, though there was a trend of higher IgG1 levels in the group with only diarrhoea at challenge 7. Despite higher EW-IgG1-levels in mice that have both signs, the ratio of EW-IgG1 to IgE at challenge 13 is lower in both groups that had signs than in those that lacked signs.

EW-specific IgA was higher in the group of mice that had both signs than the one without signs. Similar to IgA, IgG2a was increased in mice that had both signs compared to sign-free mice, but also in those that only developed diarrhoea. EW-specific IgG2b had a high SEM at all time points. It was significantly increased at challenge 7 in the mouse group with both signs compared to mice with no signs or diarrhoea only, at challenge 13 this difference is only a trend.

The most prominent difference between mice that develop signs and those that don't is in the level of EW-specific IgE. In average, signatic mice - diarrhoea alone or together with a temperature drop - showed higher allergen-specific IgE titres than mice that don't develop the disease. This finding supports the idea that our model resembles an IgE-mediated type of food allergy with a pathophysiology much related to the human disease. IgE-mediated food allergy is the most common cause of anaphylaxis in patients and is characterised by its fast onset and high severity of disease (*172*). This fast onset of signs could also be seen in the temperature drop that already starts to manifest within 15 minutes (data not shown).

Mice that showed both signs had elevated IgG1 levels compared to those that did not. On one hand, IgG1 in mice (and IgG4 in humans) has been associated with protection from food allergy (*173–176*), on the other hand it can be elevated in allergic individuals, because the IL-4-rich milieu induces class-switch to IgG1 (*114*, *115*).

Even though both EW-specific IgE and IgG1 were elevated in mice that showed signs, the group of mice with no signs exhibited a higher IgG1/IgE-ratio than mice with diarrhoea or anaphylaxis and diarrhoea.

4.2.2 Even mice that exhibit signs of food allergy have 100-fold higher OVA-specific IgG1 levels than IgE

Up to this point, we had analysed antibodies against the whole mixture of proteins present in EW. This is a good measure for the overall allergen-specific antibody response, but it is not possible to absolutely quantify the antibodies, because a known standard serum is lacking. The most abundant protein in EW is ovalbumin (OVA) which accounts for approximately 55% of all EW protein (*23*). However, monoclonal mouse IgG1anti-OVA (clone: OVA-14) and IgE anti-OVA (clone: 2C6) antibodies are available and were used as standards; allowing absolute quantification of serum levels of IgG1 and IgE anti-OVA at challenge 13 (Figure 6).

OVA-IgE was elevated in mice that showed both signs (max. temperature drop ≥ 1°C and diarrhoea), compared to sign-free mice. Mice that only had diarrhoea showed a trend of increased OVA-IgE levels that was not significant. There were no differences between the different disease groups with regards to OVA-IgG1. Mice that never developed any signs had a ratio of serum OVA-IgG1/IgE of approximately 1000. Mice that developed signs still reached an at least 100-fold excess of OVA-IgG1. This was remarkable, because it showed that such a great excess in allergen-specific serum IgG1 was not sufficient to suppress food allergy signs. In conclusion, IgG1-mediated protection seems to be limited.

OVA-specific IgE and IgG1 strongly correlated with EW-specific IgE and IgG1, respectively (Figure 6B). Relationships between EW-IgG1 and IgE were comparable to those of OVA-IgG1 and IgE and could thus be used as a surrogate for quantification of the ratio of overall allergen-specific IgG1 to IgE.

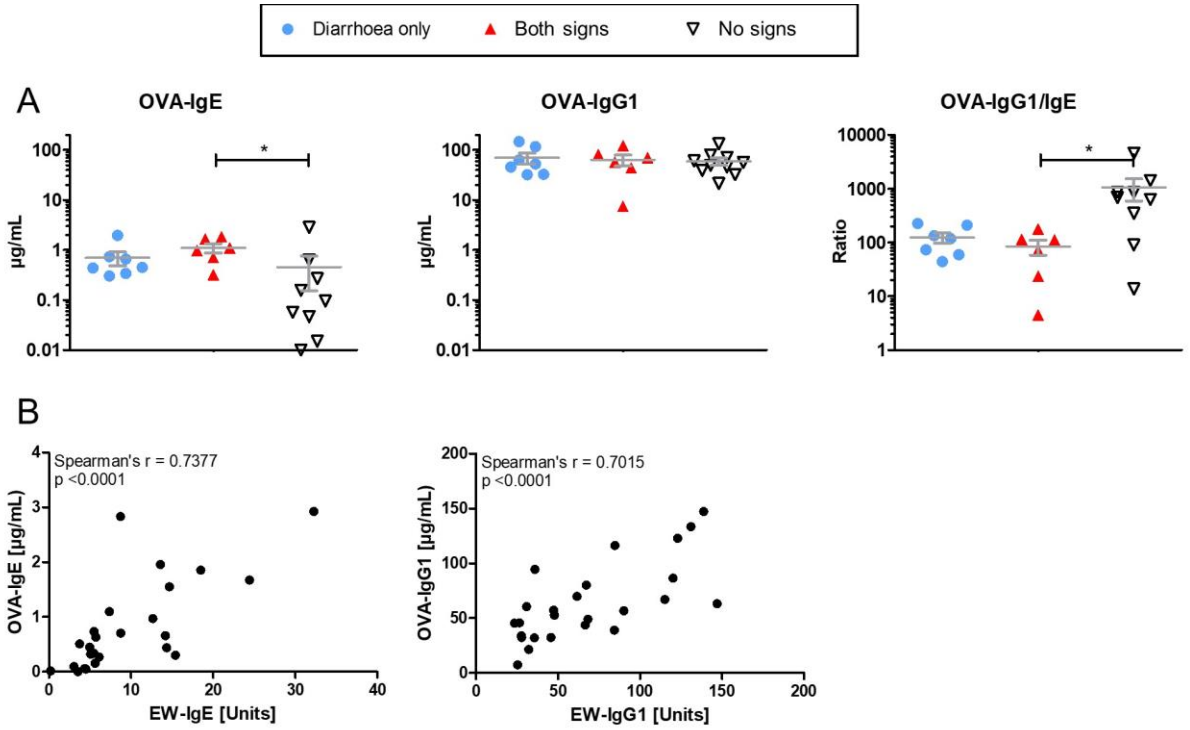

Figure 6: OVA-specific IgE, IgG1 and their ratios
Female Balb/c mice were sensitised to and challenged with egg white and egg yolk plasma according to section 3.2 /Figure 4A and grouped based on the occurrence of food allergy signs as described in Figure 4. Serum was taken at challenge 13 and OVA-specific IgE and IgG1 were measured by ELISA. Monoclonal mouse anti-OVA IgE and IgG1 served as standards for each antibody respectively. The ratio between OVA-IgE/IgG1 was calculated as well. (**A**) Groupwise comparison of EW-IgE, -IgG1 and EW-IgG1/IgE-ratio. Statistics: Kuskal-Wallis-Test with Dunn's multiple comparison test as post-test. * $p<0.05$, n=32, mean ±SEM are displayed. (**B**) OVA-specific IgE and IgG1 were correlated to the respective EW-specific antibodies. Statistics: n=32; $p < 0.5$ is significant.

4.2.3 A higher mMCP1 production after allergen-challenge is associated with the development of signs of food allergy.

When a food-allergen enters the body of a sensitised individual, the first cells to respond are basophils and mast cells. These cells are activated by allergen-mediated crosslinking of IgE bound to FcεRI present on their cell surface. Subsequent to this activation, pre-formed mediators stored in vesicles inside the mast cells are immediately released and drive the symptoms of acute allergic reactions. One of these mediators is the mast cell metallo-protease 1 (mMCP1), which is produced by a mast cell type found in the mucosa and which is associated with local symptoms such as diarrhoea (*177*).

mMCP1-levels were analysed at challenge 7 and 13. At both times, mMCP1-levels were significantly increased in mice that developed signs compared to those that did not (Figure 7). Highest levels were detected in the group of mice that developed a temperature drop over 1°C in addition to diarrhoea. This observation may indicate that mMCP1 is not only associated with diarrhoea, but also with anaphylaxis or that the same disease features that cause increased mMCP1 (e.g.; IgE and mast cells) also cause anaphylaxis.

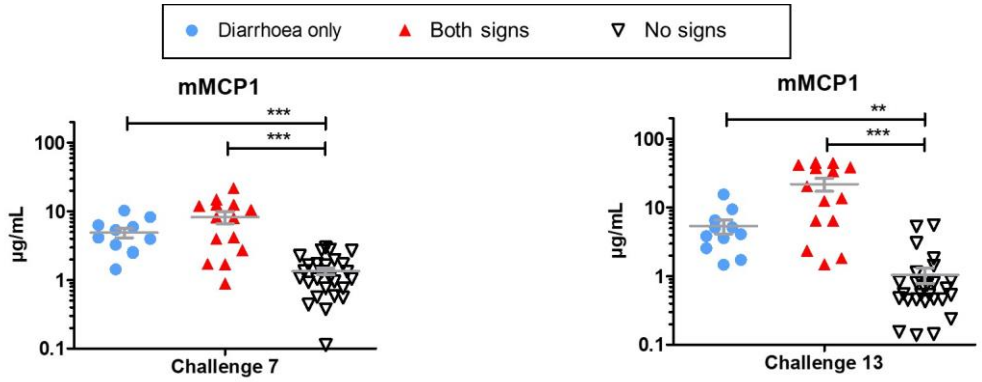

Figure 7: mMCP1 levels are increased in mice that show signs of food allergy
Female Balb/c mice were sensitised to and challenged with egg white and egg yolk plasma according to section 3.2 /Figure 4A. Based on the development of signs within 1h after each challenge over the time course of the experiment, mice were categorised into different groups, as mentioned in Fig. 1A: Diarrhoea only (n=11), Both signs (n=14) and No signs (n=28).
Sera were taken at indicated time points (1h after challenge 7 and challenge 13) and mMCP1 levels were measured by ELISA. Statistics: Kuskal-Wallis test with Dunn's post-test; not significant (no mark): p> 0.05, **p< 0.01, ***: p<0.001. Mean ± SEM is shown.

4.2.4 IL-4, IL-6 and TNFα are associated with the development of signs of food allergy

Cytokines shape the antibody response greatly. IL-4 induces class-switch to both IgE and IgG1 in mice and to IgG4 and IgE in humans (*115*), while IFNγ inhibits IgE and IgG1 production (*119*, *120*). In addition to the allergen-specific antibodies, also cytokines were analysed and compared between mice with and without food allergy signs.

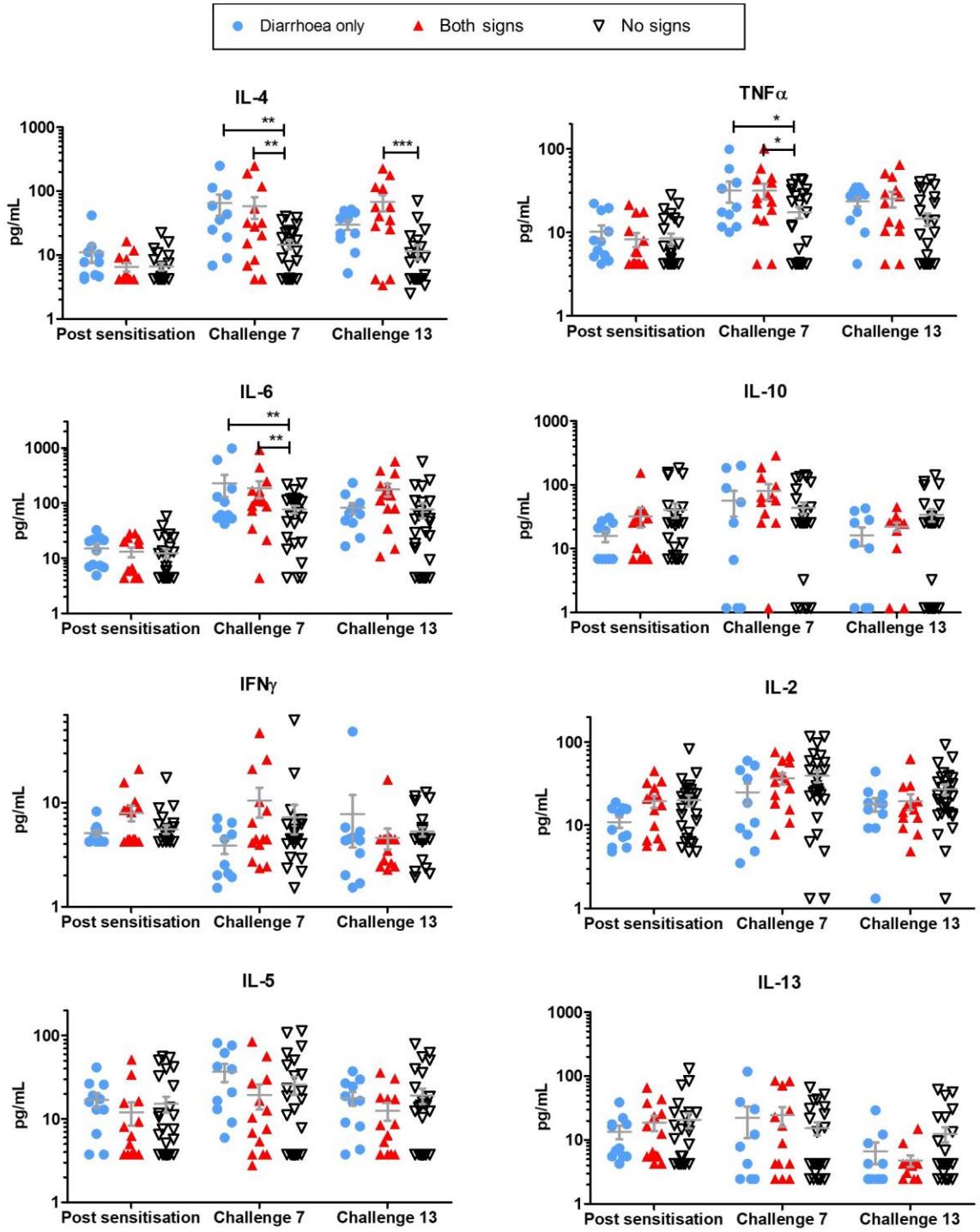

Figure 8: Quantitative differences in IL-4, TNFα and IL-6 between mice that have or lack signs of food allergy

Female Balb/c mice were sensitised to and challenged with egg white and egg yolk plasma according to section 3.2 / Figure 4A. Based on the development of signs of food allergy within 1h after each challenge over the time course of the experiment, mice were categorised into different groups, as mentioned in Fig. 1A: Diarrhoea only (n=11), Both signs (n=14) and No signs (n=28).Serum was taken at indicated time points (after the sensitisation phase before the first challenge or 1h after the respective challenge) and IL-4, TNFα, IL-6, IL-10, IFNγ, IL-2, IL-5 and IL-13 were measured by a fluorescently labelled bead-based immuno-assay. Statistics: 2-Way ANOVA with Bonferroni post-test; not significant (no mark): p> 0.05 *: p<0.05, **p< 0.01, ***: p<0.001. Mean ± SEM are indicated.

Before the first challenge, there were no detectable differences between the any of the groups of mice with regard to the measured cytokines (Figure 8). IL-4, TNFα and IL-6 were elevated in both groups with disease features after the 7th challenge. IL-4 was still increased at challenge 13, yet only as a trend for mice that only had diarrhoea. In contrast, the levels of the other cytokines were not different between the groups at challenge 13 anymore. There were no detectable differences between mice that had or lacked disease signs at any measured time-point for IL-10, IFNγ, IL-2, IL-5 and IL-13.

The strongly increased IL-4 levels in mice that develop both local and systemic features of food allergy are in accordance with the important role that this cytokine plays in Type 1 allergic responses such as food allergy, both in induction as well as maintenance (*178*). Like IL-4, IL-6 and TNFα can be secreted by mast cells and are consistent with increased inflammation.

4.2.5 Comprehensive correlation analysis between serum parameters and the severity of food allergy symptoms

In the previous analyses, mice were separated into three groups based on whether they developed symptoms of food allergy in the course of the experiment or not. Next, the impact of the measured serum parameters on the severity of the disease in individual mice at a certain time was analysed independent of such groups (Figure 9). The serum parameters were measured at a particular challenge (7 and 13) and were evaluated for their correlation with the severity of diarrhoea and maximum temperature drop, in the course of the 5 following challenges (7-11 and 13-17). The parameter diarrhoea was measured as a sum of occurrences (from 0 to 5) and the maximum temperature drop was averaged over this time.

At the timepoint of challenges 7-11, a negative correlation between the maximum average temperature drop and EW-specific IgA, IgG2a and IgG2b and a positive correlation with IL-4, TNFα, IL-6 and IL-5 were detectable (Figure 9A). However, temperature drops at these early challenges were low and did not differ a lot, making a correlation analysis weaker. The occurrence of diarrhoea was a clearer parameter at these time points (challenge phases). The allergy-mediating antibody EW-IgE correlated with the occurrence of diarrhoea, while the ratio of EW-IgG1/IgE negatively correlated. EW-IgG2a correlated negatively with diarrhoea at this timepoint as well. In contrast to the average max. temperature drop, the occurrence of diarrhoea correlated strongly with mMCP1. mMCP1 is one of the enzymes that are released upon activation by mucosal mast cells, which are believed to be responsible for the local intestinal symptom diarrhoea. The correlation with mMCP1 is thus not unexpected. Similar to the average max. temperature drop, the occurrence of diarrhoea correlated with the cytokines IL-4 and TNFα.

At later challenges, more mice developed the symptoms of food allergy. The max. average temperature drops at challenge 13-17 had increased markedly compared to the earlier timepoint. There were also more mice showing diarrhoea compared to the earlier timepoints.

At challenge 13-17 (Figure 9B), the average max. temperature drop only correlated with mMCP1 and IL-4, while there was a negative correlation with IL-5; however overall these correlations were relatively weak. At this later timepoint, the occurrence of diarrhoea correlated with EW-IgE, IgG1, IgA and IgG2b. Despite positive correlations of both IgG1 and IgE with the occurrence of diarrhoea, there was a negative correlation with IgG1/IgE ratio. The occurrence of diarrhoea at challenges 13-17 correlated more strongly with mMCP1 as well as the cytokines IL-4, TNFα and IL-6, while there was a weaker negative correlation with IFNγ.

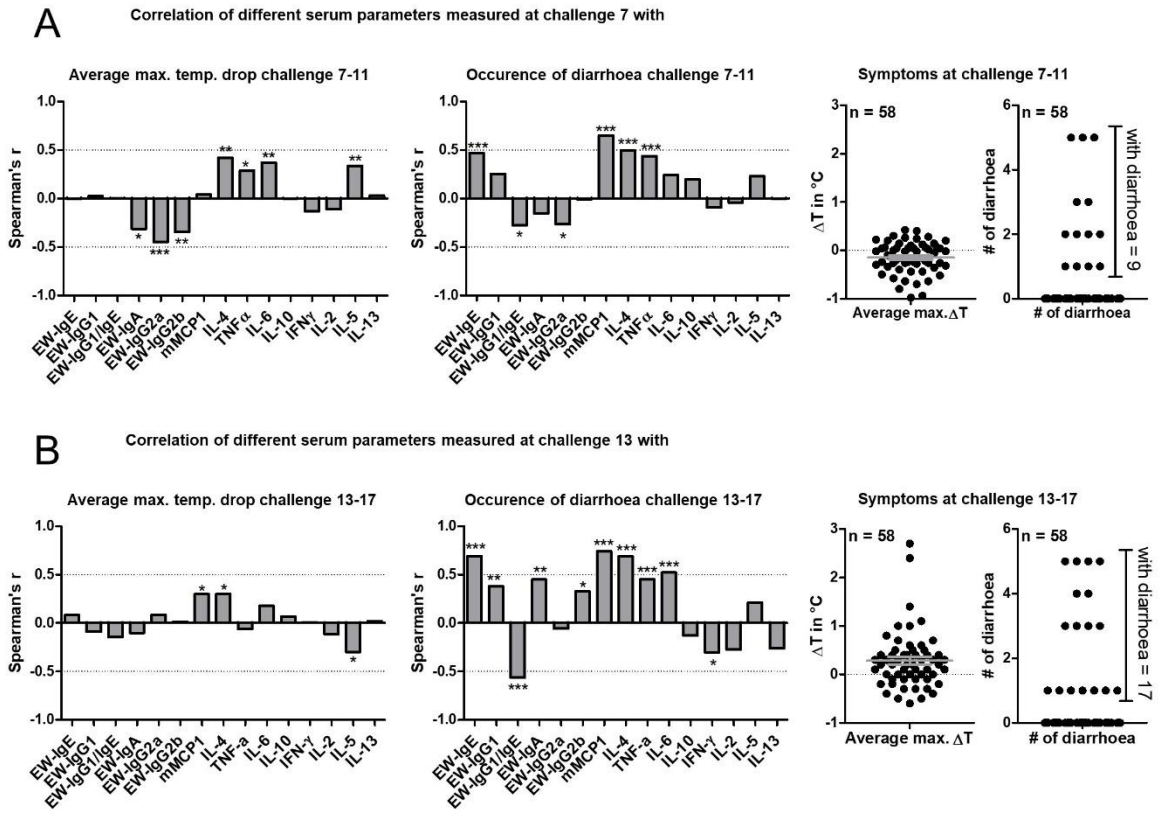

Figure 9: Correlation of serological parameters with severity of food allergy signs
Female Balb/c mice were sensitised to and challenged with egg white and egg yolk plasma according to section 3.2 /Figure 4A. Serum was taken 1h after challenge 7 and 13) and indicated EW-specific antibodies, mMCP1 and cytokines were measured with ELISA/fluorescently labelled bead-based immuno-assay (cytokines). (**A**) Serum parameters of samples taken after challenge 7 were correlated to the average maximum temperature drop and the number of challenges after which a mouse developed diarrhoea calculated over challenge 7-11. Spearman's r is shown for each parameter (not significant (no mark): p> 0.05, *: p<0.05, **: p< 0.01, ***: p<0.001). Average maximum temperature drops and number of occurrences of diarrhoea are shown in the right panel for challenge 7-11 (Mean ± SEM). (**B**) Similarly, serum parameters of samples taken after challenge 13 were correlated to the average maximum temperature drop and the number of challenges after which a mouse developed diarrhoea calculated for challenge 13-17. Spearman's r is shown for each parameter (not significant (no mark): p> 0.05, *: p<0.05, **: p< 0.01, ***: p<0.001). Average maximum temperature drops and number of occurrence of diarrhoea are again shown in the right panel (Mean ± SEM).

Throughout the different timepoints and signs, IL-4 correlated with both measured signs of food allergy. mMCP1 correlated very strongly with diarrhoea at both timepoints.

Of particular interest was the strong positive correlation of IgE with diarrhoea and the negative correlation of the IgG1/IgE ratio, especially at challenges 13-17 when IgG1 alone also positively correlates with the occurrence of diarrhoea.

Hence, despite the positive correlation of EW-IgG1 and the occurrence of diarrhoea, in relation to IgE, higher IgG1 levels were associated with less severe local signs of food allergy. However, overall IgE seems to have a bigger impact on the development of signs of food allergy.

Class-switch to both IgE and IgG1 is mediated by the cytokine IL-4 (*115*). Accordingly, expression of the two antibody subclasses correlated with each other in individual mice (Figure 10A). Levels of both, EW-IgE and -IgG1 also correlated with IL-4 at both challenges (Figure 10B). This finding is in accordance with the idea that IL-4 mediates class-switch to both antibody classes.

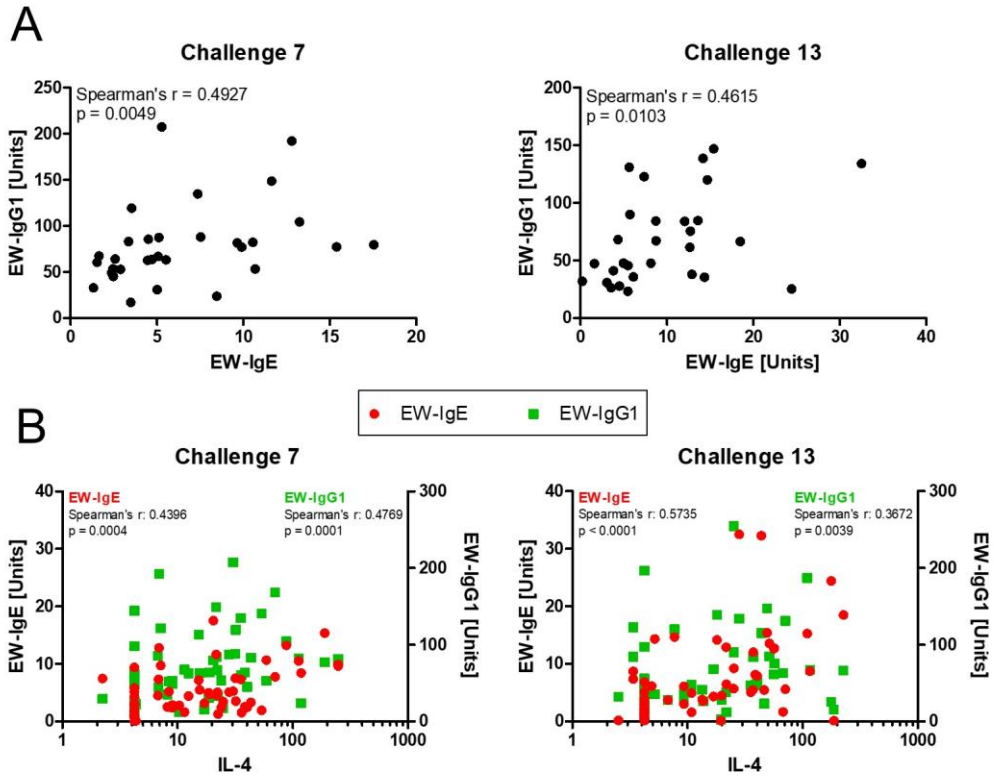

Figure 10: EW-IgE and IgG1 correlate with each other and with IL-4
Female Balb/c mice were sensitised to and challenged with egg white and egg yolk plasma according to section 3.2 / Figure 4A. Serum was taken at indicated time points (1h after challenges 7 and 13) and EW-specific IgE and IgG1 and IL-4 were measured with ELISA/fluorescently labelled bead-based immuno-assay (IL-4). (**A**) EW-IgG1 and IgE serum levels at challenge 7 and 13 are plotted and correlated. (**B**) EW-IgE (left y-axis, red circles ●) and EW-IgG1 (right y-axis, green squares ■) were also plotted against and correlated with IL-4. Statistics: Correlation calculating spearman's r; $p < 0.05$ is significant.

The correlations between IL-4 and both EW-IgE and IgG1 led me to deepen the insight into different parameters and their effect on the severity of food allergy parameters in the light of potential correlations between these parameters utilising multiparameter modelling. In total 6 serum parameters (EW-IgE, EW-IgG1/IgE ratio, IL-5, TNFα, IL-6 and IL-4) were selected based on the potential role they seemed to play for the severity of food allergy symptoms in the

bivariate Spearman correlation as described above (Figure 9). mMCP1 was not included in the analysis because it is secreted by mast cells in response to activation and mechanistically responsible for diarrhoea. Limited numbers of mice only allow the analysis of a limited number of parameters in parallel and mMCP1 was not analysed to allow analysis of a different parameter instead. Prior to the actual multiparameter modelling analysis, these parameters were examined for their correlation with one another at different timepoints of serum sampling (Figure 11).

At all timepoints, EW-IgE inversely correlated with the respective EW-IgG1/IgE ratios, which was simply a result of the mathematical correlation between the two parameters. The expression of the cytokines IL-5, TNFα, IL-6 and IL-4 correlated positively with EW-IgE. However, IL-4 levels showed the strongest correlation with IgE expression. The correlation between TNFα, IL-6, IL-5 and IL-4 with IgE increased over time.

Generally, there was a particularly strong correlation of all cytokines with one another after the sensitisation, which stayed strong at the other measured time points.

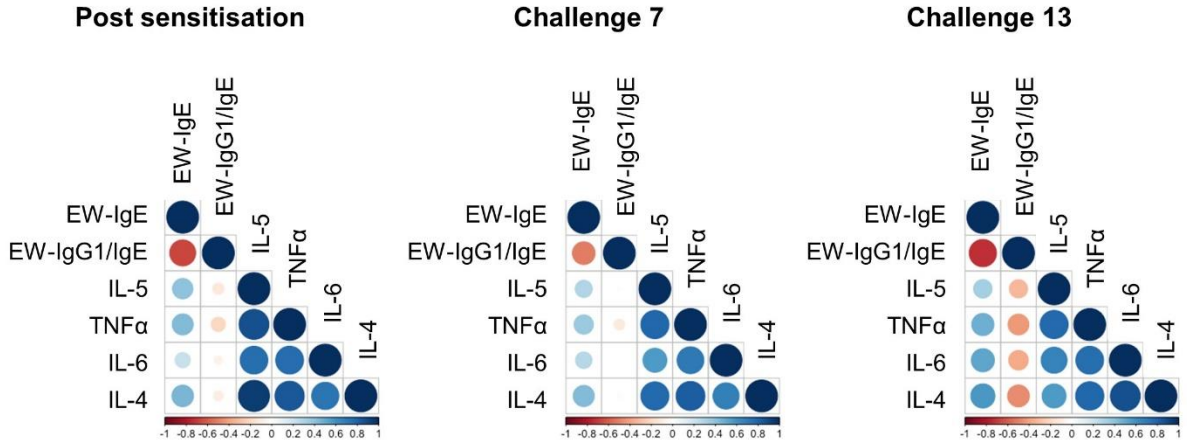

Figure 11: Correlation of selected serum parameters with one another
Female Balb/c mice were sensitised to and challenged with egg white and egg yolk plasma according to section 3.2 / Figure 4A. Serum was taken at indicated time points (post sensitisation, 1h after the challenge 7 and challenge 13) and EW-IgE, EW-IgG1/IgE ratio, IL-5, TNFα, IL-6 and IL-4 were correlated with each other. Spearman's r is depicted by the size and colour of the circles (Dark red = negative correlation (r=-1) to dark blue = positive correlation (r=1)). The bigger the circle, the stronger the correlation. EW-specific antibodies and cytokines were measured with ELISA/fluorescently labelled bead-based immuno-assay (cytokines). Statistics: Correlation calculating spearman's r

For technical reasons it was impossible to acquire data from this many mice at the same time. Primary analysis indicated that there is an impact of the experiment on various measured parameters (Data not shown). The multiparameter modelling of the selected serum parameters (EW-IgE, EW-IgG1/IgE ratio, IL-5, TNFα, IL-6 and IL-4) was thus performed taking into account that the total data was collected in two experiments. The maximum average temperature drop over 5 indicated challenges and occurrence diarrhoea were again treated as individual outcome parameters. The effect of serum parameters on the average max. temp. drop was modelled in a

linear regression model. The occurrence of diarrhoea within the 5 indicated challenges was transformed into a binary variable with the two different outcomes: 0 = no diarrhoea and 1 = diarrhoea occurred between 1 and 5 times. The modelling for the effect of the serum parameters on diarrhoea was done using a linear regression.

High EW-specific IgE-levels that were measured at challenge 7 (Table 19) correlated with both average max. temp. drop and diarrhoea, the effect on diarrhoea was relatively strong. This was also true in a prognostic manner, early high IgE (challenge 7) correlated with later average max. temperature drops and diarrhoea (challenges 13-17). Early high TNFα-levels correlated with late high temperature drops. While IL-4 measured at challenge 7 correlated with diarrhoea at challenges 13-17, IL-4 measured at challenge 13 (Table 20) correlated with both occurrence of diarrhoea and max. average temp. drop. At the later timepoint the EW-IgG1/IgE-ratio correlated with the severity of both disease parameters.

As previously observed the multiparameter analysis could confirm that overall, there was not one parameter that stuck out in impacting the severity of food allergy. EW-IgE correlated with disease parameters at an earlier timepoint while it seemed to be taken over by IgG1/IgE at the late time point. The multiparameter analysis could also confirm the strong role of IL-4 in impacting the severity of food allergy.

Table 19: Effect of various serum parameters measured at challenge 7 on diarrhoea or maximum average temperature drop
Multivariate model used and T-test performed to check for significance of model. Diarrhoea was seen as a binary variable (0/1), logistic regression modelling was performed for this outcome parameter. Modelling with average maximum temperature drop was performed using linear regression. ns: p<0.05; *: p<0.01; **: p<0.01; ***: p<0.001

Effect on diarrhoea at challenge 7-11				
	Estimate	**Std. Error**	**95% confidence interval**	**Pr(>|t|)**
(Intercept)	-5.6578780	1.7194660	-9.028 - -2.288	0.0010001 **(**)**
IgE	0.2955818	0.1039142	0.092 - 0.499	0.0044484 **(**)**
Experiment	1.5044846	0.8854769	-0.231 - 3.24	0.0893066
Effect on max. average temp. drop at challenge 13-17				
	Estimate	Std. Error	95% confidence interval	Pr(>|t|)
(Intercept)	0.6350633	0.1678474	0.306 - 0.964	0.0003783 **(***)**
IgE	0.0422674	0.0145951	0.013 - 0.070	0.0053816 **(**)**
TNFα	0.0066485	0.0028816	0.001 - 0.012	0.0247623 **(*)**
Experiment	-0.4809805	0.1170990	-0.71 - -0.25	0.0001316 **(**)**
Effect on diarrhoea at challenge 13-17				
	Estimate	**Std. Error**	**95% confidence interval**	**Pr(>|t|)**
(Intercept)	-3.6524406	2.4542370	-8.463 - 1.158	0.1366933
IgE	0.5359837	0.2140097	0.117 - 0.955	0.0122630 **(*)**
IL-5	-0.0585480	0.0335212	-0.124 - 0.007	0.0807070
IL-4	0.3030079	0.1075131	0.092 - 0.514	0.0048274 **(**)**
Experiment	-3.3993356	2.1974587	-7.707 - 0.908	0.1218778

Table 20: Effect of various serum parameters measured at challenge 13 on diarrhoea or maximum average temperature drop
Multivariate model used and t-test performed to check for significance of model. Diarrhoea was seen as a binary variable (0/1), logistic regression modelling was performed for this outcome parameter. Modelling with average maximum temperature drop was performed using linear regression. ns: p<0.05; *: p<0.01; **: p<0.01; ***: p<0.001

Effect on max. average temp. drop at challenge 13-17				
	Estimate	**Std. Error**	**95% confidence interval**	**Pr(>|t|)**
(Intercept)	0.6446508	0.1520545	0.347 - 0.943	0.0000863 **(***)**
EW-IgG1/IgE ratio	-0.0037195	0.0017070	-0.007 - -0.0004	0.0336346 **(*)**
IL-5	-0.0071734	0.0030153	-0.013 - -0.001	0.0208577 **(*)**
IL-4	0.0071732	0.0009658	0.005 - 0.009	<0.0001 **(***)**
Experiment	-0.2732557	0.1012334	-0.47 - -0.075	0.0092136 **(**)**
Effect on diarrhoea at challenge 13-17				
	Estimate	**Std. Error**	**95% confidence interval**	**Pr(>|t|)**
(Intercept)	-0.8111475	1.8832546	-4.502 - 2.880	0.6666750
EW-IgG1/IgE ratio	-0.1897028	0.0648273	-0.316 - -0.06	0.0034305 **(**)**
IL-4	0.0886748	0.0264584	0.036 - 0.140	0.0008038 **(***)**
Experiment	-0.2084715	1.0331475	-2.2 - 1.816	0.8400864

4.2.6 The severity of food allergy is independent of the gut permeability

In order to induce an anaphylactic reaction in sensitised individuals, the orally ingested allergen has to be taken up systemically (*179*). How well the allergen can be absorbed also depends on the permeability and integrity of the gut. A way to measure these parameters *in vivo* is the oral administration of an antigen that is entirely naïve to the organism and the subsequent drawing of a blood sample to analyse how much of the ingested allergen has reached the blood stream. In this study, TNP-BSA was used as an irrelevant antigen, which was biotinylated for easier detection by ELISA (Figure 12).

The serum levels of orally administered TNP-BSA-biotin did not correlate with either average maximum temperature drop or the occurrence of diarrhoea in the following challenges in this model of food allergy. The permeability of the gut at the time of the EW/EYP challenge apparently did not have an impact on the severity of the signs as much as the immunological parameters measured.

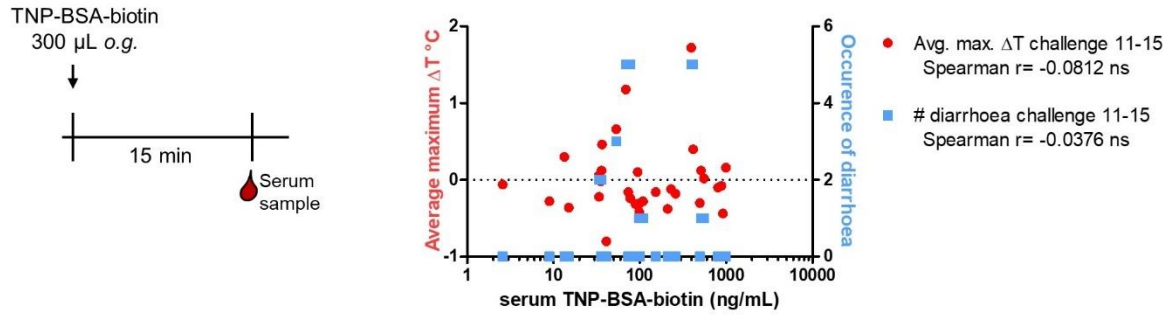

Figure 12: The severity of symptoms of food allergy do not correlate with gut permeability
Female Balb/c mice were sensitised to and challenged with egg white and egg yolk plasma according to section 3.2 /Figure 4A. Prior to the EW/EYP-challenge 10, biotinylated TNP-BSA was orally administered to the mice and a blood sample was taken after 15 min. The serum levels of biotinylated TNP-BSA were measured by ELISA and plotted against the average maximum temperature drop (left y-axis, red circles ●) and the occurrence of diarrhoea (right y-axis, blue squares ■). Statistics: Correlation calculating spearman's r; $p < 0.5$ is significant; ns = not significant; n=32.

4.3 The repertoires of IgE and IgG1 differ in the CDR3 region

Murine IgG1 (and correspondingly IgG4 in humans) is believed to protect against allergic diseases by binding to the inhibitory receptor FcγRIIb and/or competing with IgE for binding to allergen (*180*). However, IgG1 had little or no protective effect in the EW/EYP food allergy model (Figure 5, Figure 9, Figure 6). One possible explanation for little or no protection is that IgE and IgG1 may bind to different allergen epitopes, preventing a potential blocking effect of IgG1. Alternatively, or in addition, IgE and IgG1 antibodies could exhibit different affinities. In both cases, different binding of IgE and IgG1 to allergen should be reflected by different gene sequences coding for the Ig binding site, particularly the CDR3 part of the Ig heavy chain V region. This could result from either differences between IgE and IgG1 in VDJ segment usage during early B cell development, or distinct mutations introduced into the CDR3-regions by hypermutation occurring after activation of mature B cells within the germinal centre. In order to investigate this hypothesis, the repertoires of IgE and IgG1 in bone marrow and the mesenteric lymph node, which drains the intestine, were analysed by NGS (Figure 13).

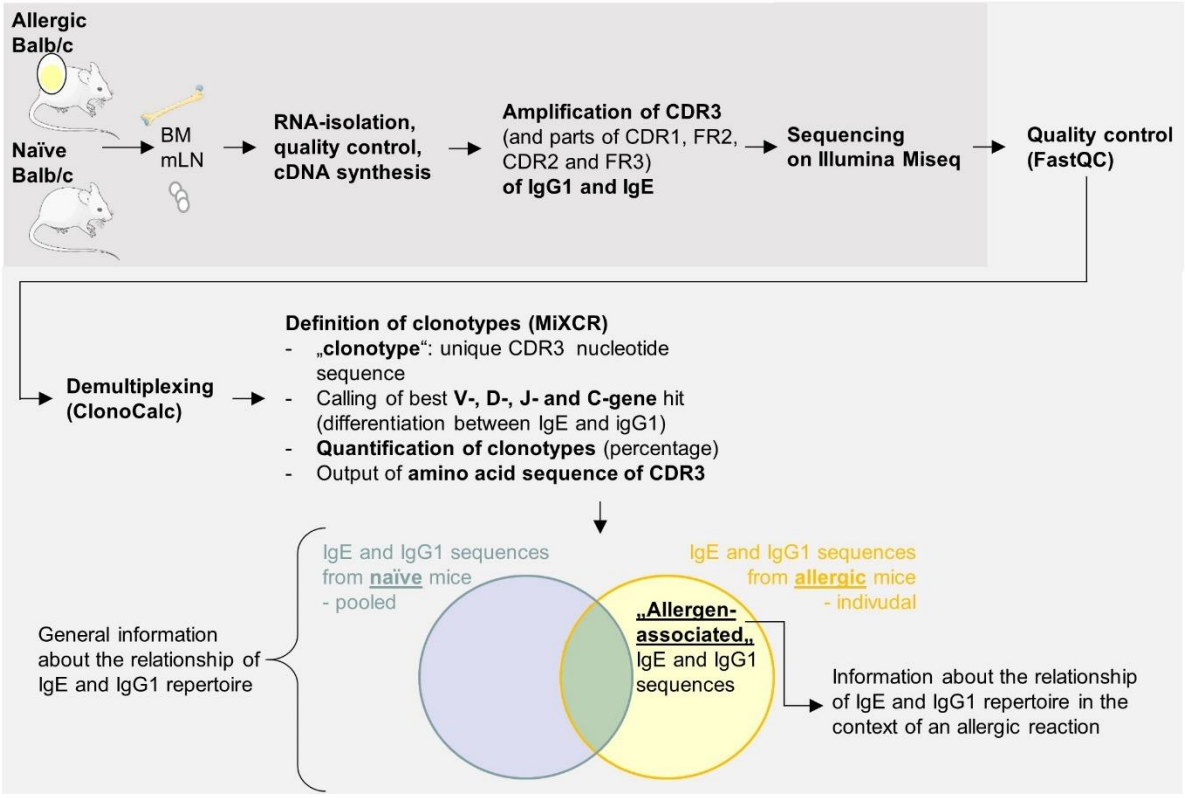

Figure 13: Workflow of the repertoire analysis of IgG1 and IgE from allergic and naïve mice
Female Balb/c mice were sensitised to and challenged with egg white and egg yolk plasma according to section 3.2.2. Bone marrow and mesenteric lymph node were taken from 5 mice that had persistent symptoms of food allergy (temperature drop ≥ 1°C and diarrhoea in response to challenges; "**allergic mice**") and 3 similarly housed mice that have never been in contact with EW/EYP ("**naïve**" or "**control**"). RNA was isolated and cDNA synthesised according to section 3.5 using primers specific for conserved regions in the V-gene on one side and for the constant region of IgE and IgG1 respectively allowing an amplification of the CDR3 region as well as parts of CDR1, FR2, CDR2 and FR3. The NGS data quality was determined using FastQC (Supplementary figure 1) and de-multiplexed into the individual samples with ClonoCalc (Fähnrich et al., 2017). The determination of clonotypes (unique CDR3 nucleotide-sequences) was performed using MiXCR (Bolotin et al., 2015).

In order to be able to study the repertoire of IgE and IgG1 in the context of food allergy, RNA-samples of mice with symptomatic food allergy (EW/EYP) and naïve mice were analysed. By using RNA instead of DNA, the focus of the analysis was on plasma cells, which produce approximately 1000-fold higher amounts of antibody per cell than B. Plasma cells are terminally differentiated B cells that develop during an immune response.

Overall, there were higher numbers of clonotypes/clones (unique CDR3 nt-sequences, see Figure 13) of both IgE and IgG1 in mLN than in BM (Supplementary figure 2). CDR3-amino acid sequences occurring in the pooled samples of naïve mice were expected not to be allergen-specific. These amino acid sequences were subtracted from the sequences occurring in the allergic mice, leading to a remaining pool of allergen-associated clones. Highly frequent clonotypes differed between allergic and naïve individuals in terms of their V-gene usage (Supplementary figure 3). This demonstrated the validity of differentiating between allergic and naïve CDR3 nt-sequences and analysing the allergen-associated sequences, as described below.

4.3.1 The IgE- and IgG1-repertoires show differences regarding quantity and diversity in BM and mLN

The quantities and diversity of the IgE and IgG1 repertoire are depicted in Figure 14.

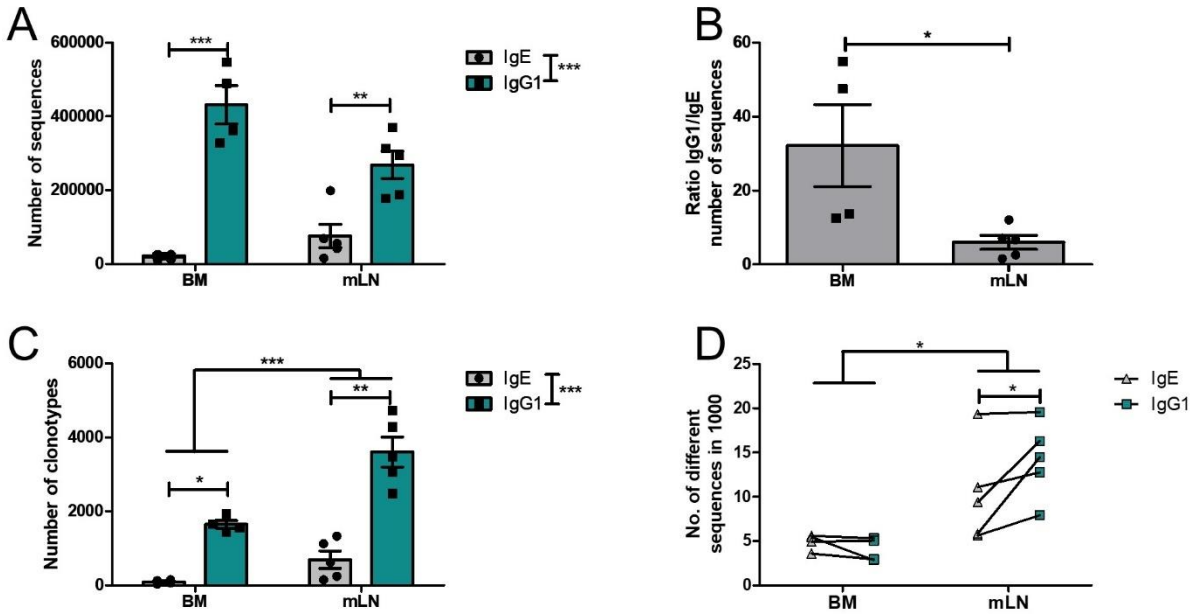

Figure 14: Differences in quantity and diversity of the repertoire between BM and mLN, IgE and IgG1
Allergen-associated CDR3 nucleotide sequences of allergic mice (definition see Figure 13) with a read count >1 were analysed. (**A**) Total number of all sequences of the respective isotype in BM and mLN (**B**) The ratio of sequence numbers of IgG1 and IgE in BM and mLN. (**C**) The number of clonotypes of IgE and IgG1 are shown for BM and mLN. (**D**) Relative clonal diversities are calculated as the number of clonotypes (in other words unique CDR3 nt-sequences) per 1000 sequences and are displayed for IgE and IgG1 in BM and mLN. Statistics: 2-way ANOVA (row-matched) with Bonferroni post-test *: $p<0.05$, **: $p<0.01$, ***: $p<0.001$, n=4-5, mean ±SEM are displayed.

Not only does the number of clonotypes quantify the respective repertoire, it also provides information about the absolute diversity. The more clonotypes that are detectable, the more different epitopes can potentially be recognised by the antibodies that are encoded by the analysed sequences. The relative diversity of the number of clonotypes or unique nt-sequences that occur in 1000 detected sequences indicates if there are a lot of low abundant clonotypes or few highly enriched ones and thus can be used as a measure for a selective pressure for certain sequences (*181*).

Considering the higher IgG1 antibody levels that were present in the serum compared to IgE (Figure 6), it was not surprising that also the numbers of IgG1-sequences were significantly higher than those of IgE-sequences in both organs (Figure 14A). Theoretically, higher quantities of sequences of either isotype can mean greater numbers of cells that produce the respective mRNA and/or a greater production of mRNA by the cells that produce the isotype. However, because IgE^+ and IgG^+ plasma cells produce similar quantities of antibody (*182*), the observed different quantities of IgE- and IgG1-sequences most likely reflect different numbers of cells producing the different isotypes.

The ratio of IgG1- to IgE-sequences was significantly higher in the BM compared to the local gut draining mLN (Figure 14B). Generally, the overall lower numbers in IgE-sequences also led to a lower number of clonotypes compared to IgG1 (Figure 14C). Even though the absolute numbers of IgG1-sequences seemed to be slightly lower in mLN than in BM, the number of IgG1-clonotypes (clones, unique CDR3 nt-sequences) was 3- to 6-fold higher in mLN. Higher numbers of IgG1 clonotypes indicate greater diversity of the IgG1-repertoire.

The relationships of numbers of sequences per isotype in BM and mLN, the ratio between them, and the numbers of clonotypes were comparable when all sequences and when only the allergen-associated sequences were considered (Supplementary figure 4).

Overall, the aforementioned correlations between total numbers of sequences and numbers of clonotypes resulted in a higher relative diversity (number of unique CDR3 nt-sequences per 1000 sequences) of the allergen-associated repertoire in the mLN compared to the BM (Figure 14D). Compared to a study in which the IgE and IgG1 repertoires were compared during systemic infection (*183*), the relative clonal diversity was lower in the EW/EYP food allergy model. The mLN is the draining lymph node of the gut, the organ that was repeatedly inoculated with EW and EYP. The chronic inflammation that goes hand in hand with the repeated challenges and allergic reaction can increase the diversity of sequences in the mLN compared to the bone marrow. Only a fraction of the memory B cells and plasma cells that were formed in the mLN in the process of the allergic reaction will migrate to the bone marrow and establish there as part of the memory compartment (*184*, *185*). While in BM, IgE and IgG1 had similar relative diversities, the IgG1-repertoire showed a slightly higher relative diversity than the IgE-repertoire. The difference between IgE and IgG1 repertoires with regards to relative clonal diversity was detected in analysis of allergen-associated sequences, but not in analysis all

sequences (Supplementary figure 4). Organ-specific differences in relative clonal diversity existed regardless of allergen-association.

4.3.2 IgE- and IgG1-repertoires differ in their CDR3 regions

The quantitative differences in the clonal diversity of IgE and IgG1 CDR3 regions provide little information about their specific qualitative differences. In the following, potential overlaps in the amino-acid sequences of the CDR3-region of IgG1 and IgE were analysed (Figure 15).

In the mesenteric lymph node, only about 50 of the approximately 650 allergen-associated IgE amino acid CDR3 sequences were also found in the IgG1 repertoire (which consisted of ca. 3600 unique CDR3 AA-sequences; Figure 15A). Although absolute numbers of unique CDR3 AA-sequences were lower in bone marrow (unique IgE: 90, overlapping: 9, unique IgG1: 2100), in both organs only about 8% of unique IgE CDR3 AA-sequences actually overlapped with those found in the IgG1 repertoire (Figure 15B). This left 90% of the unique IgE CDR3 AA-sequences with the potential for different epitope binding than IgG1. In addition to all allergen-associated unique CDR3 AA-sequences, the 50 most abundant IgE sequences were compared to IgG1 (Figure 15C and D); this demonstrated similar percentages of IgE that overlapped with IgG1. Furthermore, non-allergen-associated sequences showed a low overlap of IgE CDR3 amino acid sequences with IgG1, as apparent from an analysis that did not exclude sequences that were detected in naive mice (Supplementary figure 5).

In direct comparison, allergen-associated IgE AA-sequences showed even less overlap with IgG1 than did total sequences (Supplementary figure 5). This difference was particularly pronounced in BM. Interestingly, the analysis of only the 50 most abundant IgE clonotypes did not reveal lower overlapping IgE and IgG1-sequences among allergen associated than total sequences. This means that less abundant IgE-clones that were not detected in the allergen-associated sequences accounted for this difference. Thus, the more highly abundant unique IgE CDR3 AA-sequences were also found in the allergen-associated sequences.

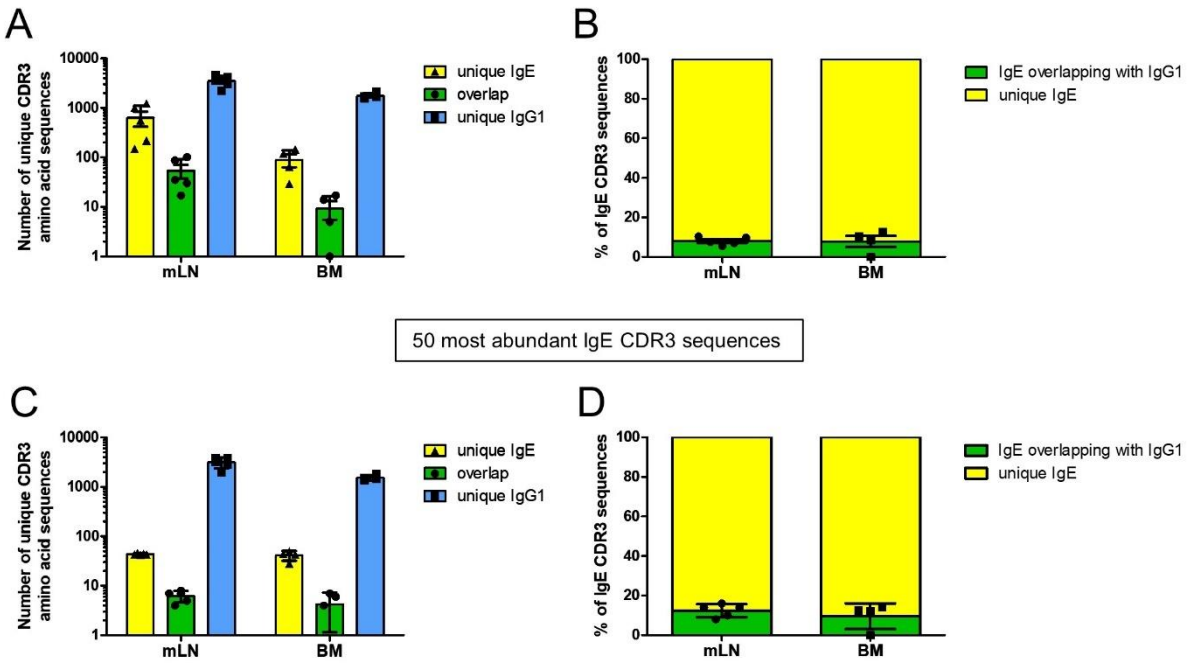

Figure 15: The great majority of IgE CDR3 amino acid sequences do not occur in IgG1
Overlaps of allergen-associated CDR3 amino acid sequences of IgG1 and IgE from allergic mice with a read count >1 were calculated using InteractiVenn (*169*). (**A**) The number of sequences being either uniquely present in IgE (yellow triangle), present in both IgE and IgG1 =overlap (green circle) or uniquely present in IgG1 (blue square). (**B**) Percentages of IgE sequences being either unique (yellow) or also present in the IgG1 repertoire (green). (**C**) Number of sequences uniquely present in IgE (yellow triangle), present in both IgE and IgG1 =overlap (green circle) or uniquely present in IgG1 (blue square), among the 50 most abundant allergen-associated IgE CDR3 amino acid sequences. (**D**) Percentages of IgE sequences being either unique (yellow) or also present in the IgG1 repertoire (green), among the 50 most abundant allergen-associated IgE CDR3 amino acid sequences

The large differences between the IgG1 and IgE-repertoire are surprising. Data obtained in studies that examined the IgE and IgG1 repertoire in helminth infected and OVA+Alum *i.p.* immunized mice were interpreted as showing great overlap between the IgE and IgG1 repertoires (*183*).

4.3.3 No differences in the usage of specific V-, D- or J-genes between IgE and IgG1

So far, my results indicate that most IgE AA-sequences are not represented in the repertoire of IgG1 CDR3 sequences. Next, I addressed the question of whether these differences are based on alternative VDJ-segment usage. To this end, the usage of particular V-, D- and J-gene families was analysed for IgE and IgG1 in bone marrow and mesenteric lymph node.

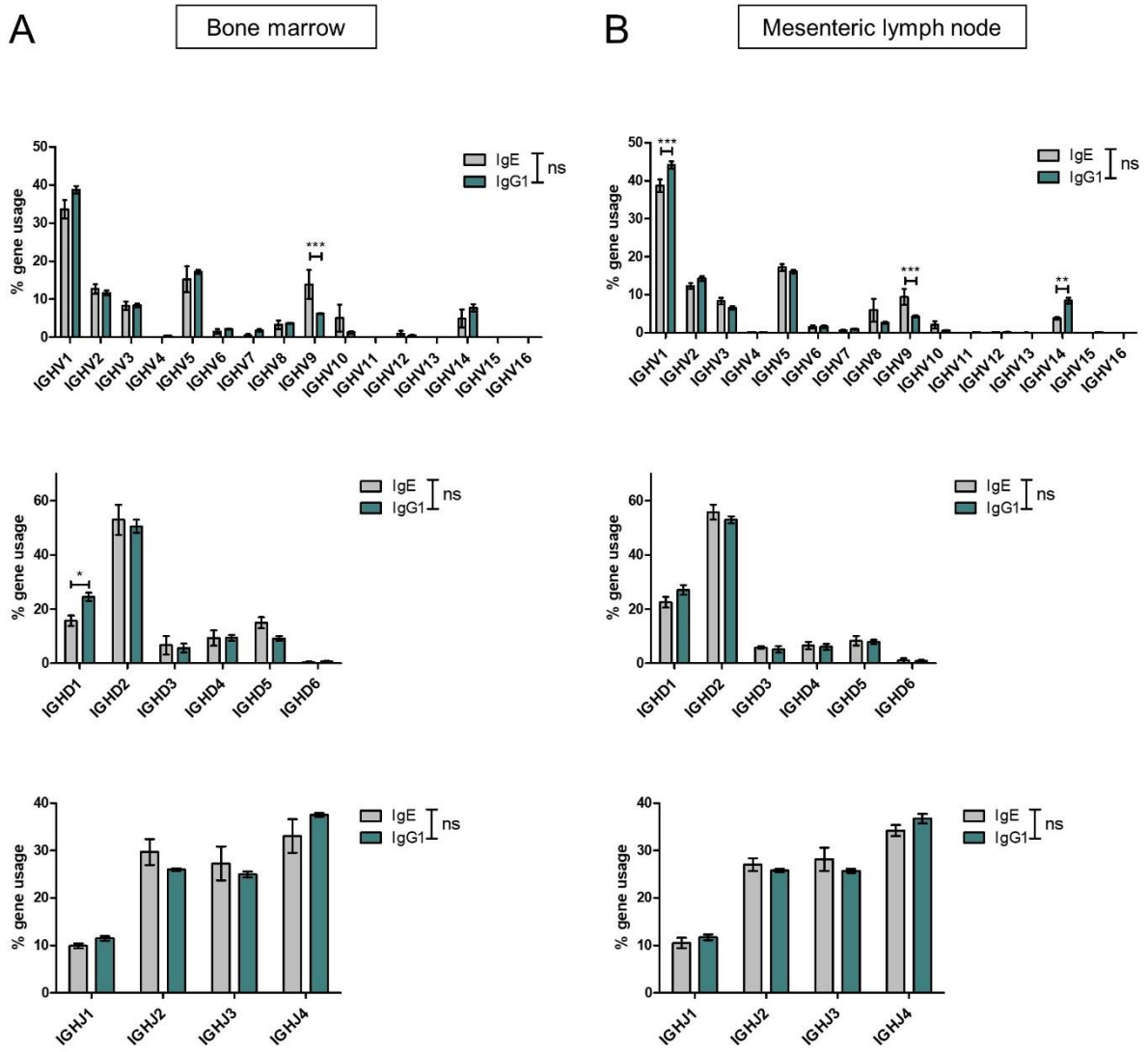

Figure 16: No overall differences of usage of V-, D- and J-gene families between IgE and IgG1
Usage of different V-, D- and J-gene families among allergen-associated (see Figure 13) IgE and IgG1-sequences from allergic mice with a read count >1 were analysed using MiXCR (Bolotin et al., 2015). % usage of a certain V-, D- and J--gene family was calculated for allergen-associated IgE and IgG1-sequences in (**A**) bone marrow and (**B**)mesenteric lymph node. Statistics: 2-Way ANOVA with Bonferroni post-test; not significant (no mark/ns): p> 0.05, *: p<0.05, **: p< 0.01, ***: p<0.001. Mean ± SEM are indicated; n=4 and 5.

Overall, there was no difference in usage of specific V-, D- and J-gene families between IgE and IgG1 in BM or in mLN (Figure 16). Both isotypes shared the same preference for the IGHV1, 2, 3, 5, 8, 9, 10 and 14 families with lower percentages of use for IGHV6, 7 and 10. This was true for both BM and mLN with IGHV1 being the most abundant V-gene family used (ca. 40%) followed by IGHV5 (ca. 20%). A higher preference for IGHV9 by IgE could be observed in both mLN and BM. IgG1 showed a higher usage of gene families IGHV1 and 14 only in the mLN, with a tendency also visible in BM. The most abundant D-gene family was IGHD2 (ca. 45%) followed by IGHD1 (ca. 20%) in both BM and mLN. There was a slightly higher usage of IGHD1 by IgE compared to IgG1 in BM. The abundance of IGHJ2, 3 and 4 was approximately similar (ca. 30%)

in BM and mLN while IGHJ1 had a lower usage (ca. 10%) with no differences between IgG1 and IgE being true for both BM and mLN.

This finding is comparable with the aforecited IgE and IgG1 repertoire study in murine helminth-infection and OVA-immunisation models (*183*).

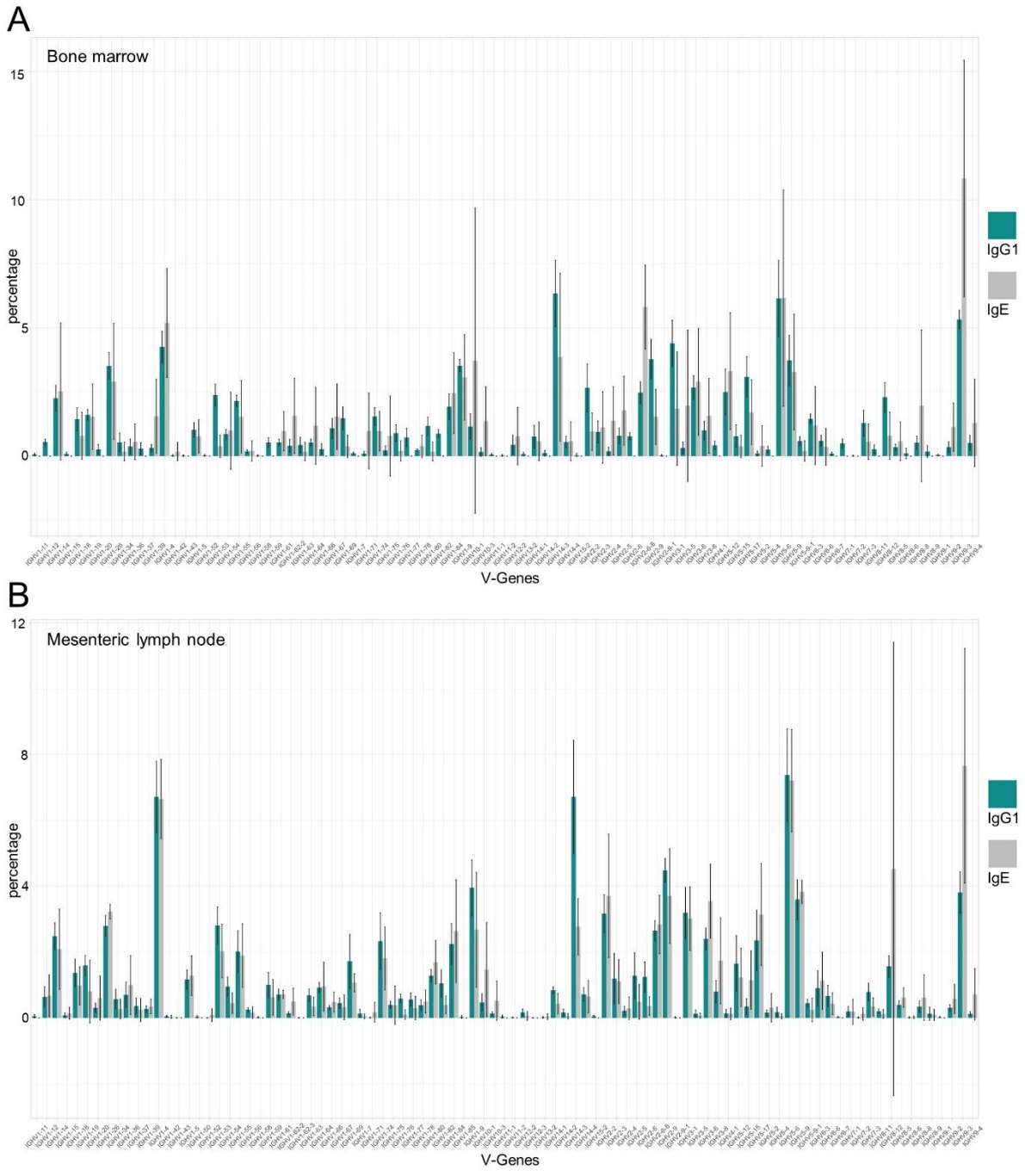

Figure 17: No differences in usage of individual V-genes between IgE and IgG1
Usage of different V-genes among allergen-associated IgE and IgG1-sequences from allergic mice with a read count >1 were analysed using MiXCR (Bolotin et al., 2015). % usage of a specific V-gene was calculated for allergen-associated IgE and IgG1-sequences (**A**) in bone marrow and (**B**) mesenteric lymph node. Mean ± SEM are indicated; n=4 and 5.

Among the 15 IGHV-gene subgroups or families, there are 97 functional IGHV genes described in mice (*186*). The abundance of individual V-genes was analysed for the IgE and IgG1-repertoire in both BM and mLN (Figure 17). No particular V-genes were used exclusively or preferentially by IgE or IgG1 in bone marrow or mLN.

4.3.4 Most but not all VDJ-sequences appear within the IgE and the IgG1 compartment

We additionally compared the usage of recombined V-D-J-sequences between IgE and IgG1. Clones that exhibited the same V-, D- and J-genes were considered overlapping, while any deviation in one of the genes, was called "unique VDJ-usage" (Figure 18).

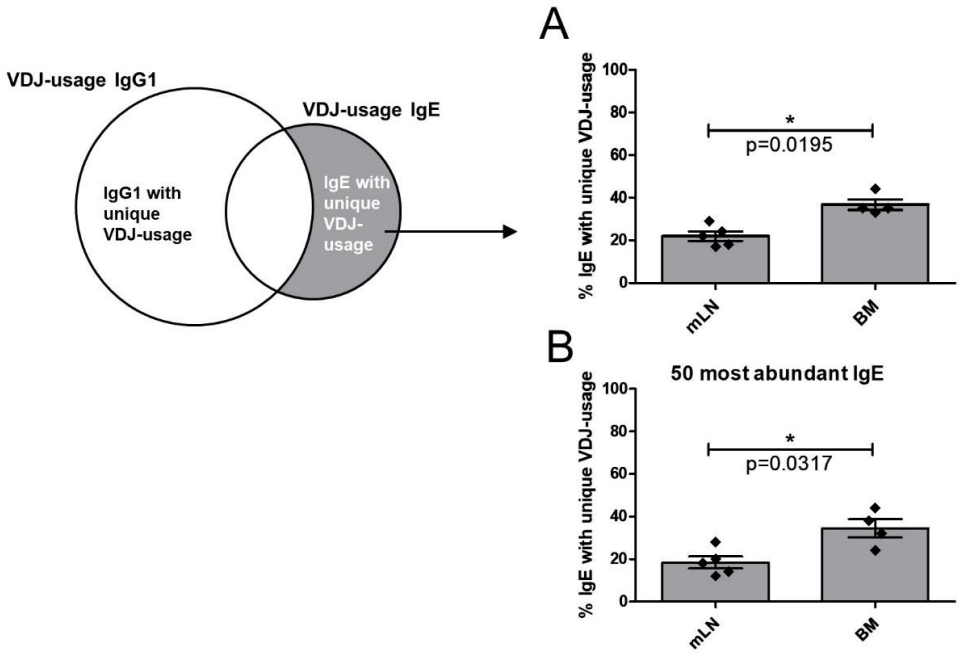

Figure 18: Some IgE uses unique VDJs
Usage of different V-genes among allergen-associated IgE and IgG1-sequences from allergic mice with a read count >1 was analysed using MiXCR (Bolotin et al., 2015). Sequences with a VDJ that were represented in IgE or IgG1, but not both isotypes were considered "unique VDJ-usage". The percentage of IgE VDJ-selection/usage that could not be found in the IgG1 repertoire is displayed for all (**A**) allergen-associated clones and for (**B**) only the 50 most abundant IgE-clones. Statistics: Mann-Whitney-Test; *: $p<0.05$; Means ± SEM are indicated; n=4 and 5.

20% of allergen-associated IgE clones in mLN and 40% in BM had a VDJ that was not found in the IgG1 repertoire (Figure 18A). In the BM there were significantly more IgE-clones with a unique VDJ than in the mLN. The numbers and coherence could also be found when looking only at the 50 most abundant allergen-associated IgE-clones (Figure 18B). Almost half of the IgE clones in the BM, and approximately 20% in mLN derived from a B cell clones that was not present among the IgG1-clones. VDJ-recombination occurs during the development of B cell precursors into immature B cells within the bone marrow (*187*). Hence, some of the differences in the CDR3-sequences of IgE and IgG1 could be explained by direct isotype switching of specific B cell clones to IgE without an intermediate IgG1 stage.

5 DISCUSSION

5.1 Overview

The aim of the study was to identify factors that impact the development and severity of food allergy to egg in a novel murine model. Oral antigen challenge induced mice to rapidly develop signs of food allergy including hypothermia and diarrhoea. These signs were associated with high levels of allergen-specific IgE. Although we expected clinical food allergy features to be limited by the much higher serum concentrations of allergen-specific IgG1, this was not the case; IgG1 levels correlated positively rather than negatively with the severity of clinical disease, along with serum levels of IL-4, TNFα and IL-6 one hour after oral egg challenge. However, a positive correlation of IgG1 levels with allergic disease may well have reflected the induction of both IgG1 and IgE responses by IL-4. The failure of the high IgG1 levels to suppress IgE-mediated disease raised questions about why suppression failed to occur.

NGS-analysis of the CDR3-regions of mesenteric lymph nodes and bone marrow RNA of mice exhibiting food allergy demonstrated that the limited ability of IgG1 to inhibit IgE-mediated food allergy could, in part, be explained by differences in the CDR3-amino acid sequences of IgE and IgG1 antibodies. Only a minority of CDR3-amino acid sequences of IgE antibodies could be found in IgG1 antibodies. In addition, approximately 10-20% of IgE sequences showed VDJ-rearrangements which were not found within the IgG1 compartment. This suggests that many IgE-secreting clones were generated by direct class-switch from Cμ to Cε, instead of almost solely through a sequential class-switch via IgG1, as suggested by many previous studies. Despite this, V, D, and J chain families were shared nearly equally by IgG1 and IgE.

Repertoire studies further revealed that IgG1 was considerably more abundant than IgE on a transcript level, in addition to the protein level. Also, repertoire diversity was noticeably greater for IgG1 than for IgE in both BM and mLN.

5.2 The experimental model resembles human food allergy

5.2.1 Skin and lung sensitisation with EW/EYP promote food allergy development

Most mouse models used to analyse food allergy immunology utilise model antigens, typically single proteins, and artificial adjuvants to induce an allergic response that mice do not develop spontaneously. The EW/EYP food allergy model with its *i.t.* or epicutaneous sensitisation provides a natural way to induce signs of the disease.

The most commonly used model antigen is OVA, the main component of EW. OVA has been particularly useful because of the availability of T cell receptor-transgenic mice e.g. OT-I (*188*) that allow the analysis of OVA-specific T cell populations in the course of the allergic reaction. In addition, there are other immunological tools to study the reaction to OVA such as well-defined peptides and monoclonal antibodies.

Induction of allergic reactions to OVA (and other individual food proteins) has generally required the use of adjuvants. Alum is used as an adjuvant for *i.p.* sensitisation. When followed by intra gastric challenges, this induces both systemic and local anaphylaxis manifested as hypothermia and diarrhoea, respectively (*176*). These disease features are comparable to the EW/EYP food allergy model. However, it has been shown that the route of sensitisation greatly modifies the epitopes that are recognised by IgE antibodies. Thus, such *i.p.* OVA/alum sensitisation of mice provokes antibodies to OVA epitopes different from those observed in allergic humans (*189*).

The default immune response to orally ingested proteins is oral tolerance (*39*), which can be broken by using cholera toxin (CT) as an oral adjuvant (*190*). CT actively disrupts the intestinal barrier, allowing food allergens to enter the lamina propria and contact immune cells. Furthermore, CT induces an epithelial cell pro-Th2 cytokine response (*190, manuscript in preparation*). A benefit of oral sensitisation is that gastrointestinal digestion of food allergens reduces them to the same components that provoke a clinical reaction to the same foods. However, neither alum as used for *i.p.* immunisation, nor CT for oral sensitisation are comparable to natural sensitisation.

Comparable to a report by Wavrin *et al.*, the EW/EYP food allergy mouse model used the whole food (EW+EYP) to induce a Th2-response resulting in allergen-specific IgE secretion. Wavrin *et al.'s* airway sensitisation, unlike skin sensitisation, failed to induce a greater increase in allergen-specific IgE compared to adjuvant-free oral challenges. In the *i.t.* sensitized EW/EYP food allergy model, IgE levels increased along with the number of oral challenges. In addition to development of allergen-specific antibodies, some mice developed clinical features of food allergy. The lack of requirement for an adjuvant in our EW/EYP food allergy model for induction of clinical signs may be explained by the saturated triglycerides in EY which account for 23% to 27-28% of its weight (*192*). Fatty acids released from these triglycerides by lipase digestion are potent detergents that might induce mucosal damage, causing an increase in epithelial permeability that allows increased antigen entry (*193*). In the intestine, fatty acids might

increase systemic absorption of food protein, facilitating an allergic response to the absorbed food (*179*). Although this might be generally important for FA development, gut permeability at the time of oral antigen challenge did not correlate with disease severity in our study. As another mechanism, saturated fatty acids upregulate the unfolded protein response (UPR) in epithelial cells. This promotes transcription of the pro-Th2-cytokines IL-25, IL-33 and TSLP (*35*, *36*), which are essential for the induction and maintenance of food allergy. These cytokines cause dendritic cells (DCs) to prime naïve CD4+ T cells to secrete IL-4, IL-5 and IL-13, but less IL-10 (*56*). Furthermore, they act directly on T cells to promote Th2 differentiation and stimulate basophils, eosinophils and mast cells (*190, manuscript in preparation*).

The *i.t.* and epicutaneous routes of sensitisation in the EW/EYP food allergy more closely resemble natural human allergen sensitisation. Airway sensitisation was proposed for the "bird-egg syndrome" (*194*). Another study associated household peanut consumption with development of peanut allergy in infants (*195*) and treatment of children with atopic dermatitis (AD) with peanut oil correlated with a higher risk of developing peanut allergy (*196*). Furthermore, skin or lung exposure to whole milk led to an induction of a Th2-response and milk allergen-specific IgE-production, while selective exposure to purified major milk allergen, bovine β-lactoglobulin (BLG), did not (*197*).

For analyses of the BCR repertoire, mice were skin-sensitised. This route of immunisation also led to development of allergen-specific antibodies (IgE in particular, data not shown) and clinical food allergy.

In conclusion, the EW/EYP model offers clinically relevant sensitisation by providing a natural route of exposure to allergen and avoids the use of a clinically irrelevant adjuvant. This makes it useful for analysing the complexities of FA and deciphering the mechanisms that promote the human disease.

5.2.2 The EW/EYP food allergy model most likely represents IgE-mediated disease

Overall, serum levels of EW-specific IgE consistently differed the most between mice that developed or failed to develop diarrhoea and/or hypothermia. In addition, the frequency with which oral egg challenge induced diarrhoea correlated with EW-specific IgE levels. These findings and the rapidity of the pathological responses to oral egg challenge support the type I hypersensitivity nature of our EW/EYP FA model.

An IgE-mediated type I hypersensitivity reaction is the most common cause of anaphylaxis in humans and is characterised by its rapid onset (*172*). This fast onset of signs of food allergy can also be seen in the temperature drop that becomes apparent within 15 minutes (data not shown). IgE is used as a diagnostic biomarker for FA (*198*). Allergen-specific IgE levels are elevated in children that develop a positive reaction to oral challenge with the allergenic food (e.g.; milk, egg, peanut) compared to those who fail to react. However, the correlation with IgE level was weaker for some allergens, including wheat and soy (*199*). In addition, allergen-

specific IgE is not a perfect diagnostic marker for symptomatic food allergy. Analogous to some mice in the EW/EYP food allergy model, some food allergy patients lack detectable food allergen-specific IgE levels and some humans have elevated IgE without ever developing an adverse reaction to food (*199*).

In addition to an IgE-mediated aetiology, food allergy can have a mixed pathogenesis in which both IgE-dependent and -independent pathways play a role. One additional mechanism involves a delayed (6-48h post exposure) response that is associated with atopic dermatitis caused by Th2-cells (*200*, *201*). This is unlikely to be the mechanism responsible for diarrhoea or hypothermia in the EW/EYP food allergy model, because these can develop in less than 15 minutes.

5.2.3 In addition to IgE, IgG1, IL-4, IL-6 and TNFα correlate with severity and development of food allergy signs

To further characterise the EW/EYP model, antibodies, cytokines and effector cell mediators were analysed. As in the murine EW/EYP model, multiple factors, including allergen-specific IgG levels correlate with the development and severity of human food allergy, as shown for childhood allergy to egg, milk, soy, and fish (*202*). Mice that developed both diarrhoea and hypothermia to oral egg challenge had elevated IgG1 levels. Although IgG1 in mice and IgG4 in humans has been associated with protection from food allergy (*173–176*), it can be elevated in allergic individuals, because IL-4 promotes class-switch to both isotypes (*114*, *115*).

A factor that consistently correlated with the disease features was mMCP1. It was elevated in mice that developed diarrhoea and/or hypothermia and correlated with disease severity. mMCP1 is secreted by mucosal mast cells (*203*). Secretion of mMCP1 leads to increased epithelial permeability in the gut and thus may contribute to the development of diarrhoea and enhancement of a Th2-response (*204*, *205*). Systemic symptoms are more associated with histamine, which is predominantly secreted by connective tissue mast cells rather than mucosal mast cells (*206*). Consistent with this, mMCP1 has been shown to correlate with diarrhoea, but not with hypothermia, in one recent study (*177*). In contrast, in the EW/EYP model, mMCP1 strongly correlated with both hypothermia and diarrhoea. The former results may need to be interpreted carefully because different mouse models were used to analyse mast cell contributions to diarrhoea and hypothermia, whereas the BALB/c EW/EYP food allergy model allows analysis of both signs of disease. It is also possible that mice with severe connective tissue mast cell-dependent hypothermia also activate mucosal mast cells and consequently develop higher mMCP1 levels. To better elucidate the role of connective tissue mast cells in this model, histamine levels and connective tissue mast cell-specific mMCP7 levels could be measured.

The discrete difference between mucosal and connective tissue mast cells that is seen in mice does not exist as such in humans. This makes comparison between human and mouse mast cell

markers difficult. However, human mast cell tryptase (MCT) is associated with increased severity of human anaphylaxis (*207*).

The search for further factors modulating signs of the IgE-mediated anaphylaxis in the EW/EYP food allergy model revealed correlations of the cytokines IL-4, IL-6 and TNFα with the disease.

IL-4 is one of the hallmark cytokines of a type 1 allergic response, because it is required for the class-switch to IgE (*114*, *115*). It is strongly increased in mice that show signs of food allergy and correlated with the severity of food allergy signs.

Mast cell tryptase, histamine, IL-6 and IL-10 were all elevated in human subjects with severe anaphylaxis when compared with patients with less severe disease (*207*). Except for IL-10, these parameters also correlated with more severe disease in the EW/EYP food allergy model.

It is noteworthy that it cannot be clearly differentiated whether increased cytokine levels are the cause for a more severe reaction to antigen challenge or secreted as a result of a stronger effector cell response. While IL-4 and IL-6 have to be *de novo* synthesised, preformed TNFα can also be secreted by mast cells from granules within minutes upon activation (*208*). Still, it has been shown in a murine anaphylaxis model that did not utilise an oral challenge, that IL-4 can be detected in serum within 1 hour of antigen challenge. The main sources of this IL-4 in the secondary reaction upon antigen challenge are basophils and memory T cells (*209*). The strong correlations of IL-4 with disease severity might indicate a role of basophils. Additionally, more IL-4 and IL-6 might be produced by cells other than the immediate effector cells. Thus, other cytokines that are solely *de novo* synthesised by these effector cells (mast cells and basophils). such as IL-5 and IL-13, cannot be found to be elevated 1h after the challenge.

Overall, serological parameters correlate well between human food allergy and the murine EW/EYP model, suggesting that this model is suitable for studying the mechanisms involved in the human disease.

5.3 Allergen-specific IgE has a major impact on disease severity while the protective capacity of IgG1 is limited

Serological differences between mice that develop symptoms compared to those that don't most strongly reflect EW-IgE. It was the single factor that most strongly and consistently correlated with development and severity of food allergy in the EW/EYP food allergy model.

IgG1 in mice and IgG4 in humans has been associated with protection from IgE-mediated anaphylaxis/food allergy (*173–176*). This protective role of allergen-specific IgG1 is limited in the EW/EYP food allergy model. For a quantitative comparison, OVA-specific antibodies were analysed. While there were higher OVA-IgG1/IgE ratios measurable in mice that did not develop any disease, the OVA-IgG1 levels of mice, that showed symptoms are still more than 100-fold

higher than OVA-IgE. These ratios were sufficient to block anaphylaxis in a passive IgE-transfer model (*176*).

One mode of protection is competition between IgG1 and IgE for allergen binding (*176*, *210*). To block this binding, a sufficient IgG1/IgE-ratio could be required in serum. However, the development of severe food allergy symptoms of mice despite high OVA-IgG1 titres implies that in this model IgG1 may not sufficiently suppress IgE-mediated anaphylaxis. Despite the excess of IgG1 to OVA, this level may have been insufficient to prevent absorbed antigen from binding to mast cell-associated IgE to trigger mast cell degranulation. This possibility would be particularly likely if little or no egg-specific IgG1 antibodies bound to the same egg proteins or to the same epitopes on egg proteins that are recognised by IgE antibodies.

Lower OVA- and OVM-specific IgE titres and a higher IgG4/IgE-ratio were associated with a strong response to OIT for egg allergy in a clinical trial by Wright et al (*174*). This is consistent with our observation that high IgG1/IgE correlates with less severe disease in our murine EW/EYP model. The stronger correlations of EW-IgE with a more severe disease however imply an even more important role simply of IgE in this model. In a comparable skin sensitisation model, food allergy could be suppressed by administration of anti-FcεRIa mAb highlighting the importance of IgE (*211*).

5.4 Differences in the IgG1 and IgE repertoire

Analysis of our serological and clinical data suggests that diarrhoea and hypothermia in the EW/EYP food allergy model are IgE-dependent; other studies with the same model have shown this more explicitly by suppressing disease features with an anti-FcεRIα mAb treatment in mice (*212*). IgE induces these disease features by binding to FcεRIA on mast cells and basophils and activating them to release mediators such as histamine, proteases and cytokines upon crosslinking by the cognate allergen (*213*). Murine IgG1 and human IgG4 have been shown to protect against diarrhoea and systemic anaphylaxis by binding to the inhibitory receptor FcγRIIb and by blocking IgE from binding to allergen (*180*).

The inability of IgG1 to convincingly block IgE-mediated anaphylaxis in this study could potentially be caused by differences between IgE and IgG1 binding to egg allergen epitopes. EW and EYP contain multiple proteins, each of which has multiple epitopes. Failure of sufficient quantities of IgG1 to bind to any allergen or allergen epitope recognized by IgE could prevent IgG1 from inhibiting IgE-mediated egg allergy.

Ig antigen binding sites are encoded by different gene segments. The Ig antigen binding site of each unique B cell clone is encoded by a unique nucleotide-sequence (clonotype). Amino acid sequences that are encoded by different clonotypes can still be similar or identical, because more than one codon can encode the same amino acid. However, unique amino-acid sequences give rise to unique Ig antigen-binding sites. The diversity of the B cell repertoire derives initially from the number of these different V-, D- and J-gene segments. This theoretically allows

recognition of any antigen. Additional layers of B cell repertoire diversity are introduced first by the way in which V, D, and J segments recombine and changes induced by TDT, and later by the somatic hypermutation that occurs in germinal centers.

IgG1 must bind the same or closely situated epitopes as IgE to block IgE-mediated anaphylaxis by shielding the antigen from IgE. In order to analyse similarities in the binding capacities of IgG1 and IgE, the repertoires of IgE and IgG1 were analysed from total RNA of BM and mLN of mice showing symptoms of food allergy.

5.4.1 Differences in the CDR3-regions of IgG1 and IgE may explain the limited blocking capacity of IgG1

Though my data do not exclude the possibility that allergen-specific IgG1 can block IgE mediated allergy, some mice with very high IgG1/IgE ratios still developed diarrhoea and hypothermia. Also, IgG1 clones were more diverse than IgE clones, which should give IgG1 the potential to recognise more distinct epitopes than IgE. However, the diversity of the repertoire does not give information about the specificity of the clones and whether IgE and IgG1 have similar or different fine specificities.

In both mLN and BM, only about 8% of allergen-associated IgE V region CDR3 AA sequences overlapped with those found in the IgG1 repertoire. This left 90% of IgE clonotypes with the potential to bind epitopes that were not bound by IgG1. The same finding held true when only the 50 most abundant clones were considered. The large majority of the IgE-clonotypes had an amino-acid sequence that differed from any of those detected in the IgG1-repertoire and could potentially bind different epitopes. This observation could explain how large amounts of IgG1 failed to completely block IgE-mediated food allergy symptoms.

Differences in the CDR3-sequences and their potentially different specificities can either result in binding different epitopes on the same protein or on different proteins of the EW/EYP-mixture. Studies mapping linear IgE and IgG4-bound epitopes in the serum of egg-allergy patients have shown that at least in the case of ovomucoid, the most allergenic protein of the EW-mixture, there are indeed epitopes that are recognised by IgE but not by IgG4 (*214*, *215*). A similar experiment could be performed on sera from mice that were sensitised in the EW/EYP food allergy model in order to check whether IgE and IgG1 bind to different proteins and/or epitopes.

Different CDR3-regions do not prove that IgE and IgG1 bind different epitopes; different amino acid sequences might still bind similarly. Here, a computational analysis of the physico-chemical properties of amino acids (hydrophobicity, polarity etc.) might shine more light on the matter. Ultimate proof could only be provided if both Ig heavy and light chain of the antibody were sequenced, cloned and used to produce antibodies that were then analysed in a epitope binding assay as was done by Croote *et al.* (*142*).

IgG1 (in mice; IgG4 in humans) is unique in that it binds inhibitory FcγRIIB with higher affinity than it binds to any of the stimulatory FcγRs. Thus, it is considered to be anti-inflammatory. But all Ig isotypes have the potential to prevent IgE-mediated anaphylaxis by blocking epitopes that could potentially be bound by IgE (*216*). It would be of interest to analyse the repertoires of other isotypes with regards to similarities with IgE. Here, only IgG1 has been analysed because of its close developmental relationship with IgE. One study of human peripheral blood mononuclear cells (PBMC) however showed that at least in humans, B cells that express IgG isotypes other than IgG4 also significantly contribute to the IgE-repertoire and do so to a much greater extent than IgM-expressing B cells, indicating that the majority of IgE is derived from an indirect class-switch, at least in the model that was studied (*149*).

5.4.2 Different clonal descent and differential somatic hypermutation contribute to differences in IgE and IgG1 CDR3-region repertoires

In our study, only 8% of allergen-associated IgE-CDR3 amino acid sequences were shared with the IgG1-repertoire regardless of whether mLN or BM, allergen-associated or total sequences, or only the 50 most abundant IgE or IgG1 sequences were analysed. This low overlap was not expected: On one hand, many IgE-clones develop from IgG1-(IgG4-) clones that share the same VDJ-recombination (*115*, *149*). On the other hand, IgE^+ B cells are believed not to undergo considerable SHM because they are rare in the gertube minal centres where these mutations are introduced (*217–219*). With this premise, a further change in the sequence of IgE would be unlikely. Also, Turqueti-Neves *et al.* observed in a comparable repertoire analysis comparing IgE and IgG1 repertoires in two murine models that there was great overlap between IgE and IgG1 repertoires (*183*). Their results might differ from ours because the mice in our EW/EYP food allergy models are hyper-immunised compared to those of Turqueti-Neves. Repeated immunisation might drive direct switching from IgM to IgE, IgE hypermutation in GCs, and generation of long-lived IgE-secreting plasma cells. This hypothesis needs to be tested.

Although I amplified samples with primers for both IgE and IgG1-heavy chains in the same tube in order to avoid biases that occur when samples are amplified in separate reaction tubes, Turqueti-Neves *et al.* analysed IgE and IgG1 in separate reactions. In addition, the ways in which we compared CDR3-sequences for IgE and IgG1 differed. Turqueti-Neves *et al.* compared the overlap between the 50 most frequent CDR3 sequences in the IgE-repertoire with the same CDR3 sequences in the IgG1- and IgM-repertoires without showing sequences that differ. They focused on showing that the IgE repertoire is more closely related to that of IgG1 than to IgM. Their results are in concert with the results of other human studies (*149*). In contrast, I found a considerable number of IgE-clones that did not share their VDJ-gene rearrangements with IgG1 clones, which indicates they either developed from non-IgG1-, potentially IgM-clones, or that any IgG1 clone from which they could have developed had been lost.

An IgE^+ B cell can develop either from an IgM^+ B cell through direct class-switch or indirectly from an $IgG1^+$ B cell, with at least 30% of the IgE-clones having developed through the IgG1-

intermediate stage (*115*). In an analysis of circular DNA-fragments generated during class-switching, Liu *et al.* claimed that such an analysis might overestimate the number of clones that had switched from IgM to IgE because some circular DNA is rapidly degraded and because it is unclear whether the number of switch-circles represents the number of switched B cells (*149*).

Analysis of IgM⁺ B cells or transcripts may miss some of the B cell VDJs that were initially generated because some of the IgM+ clones might have lost due to death or class switching by the time of analysis.(*220*).

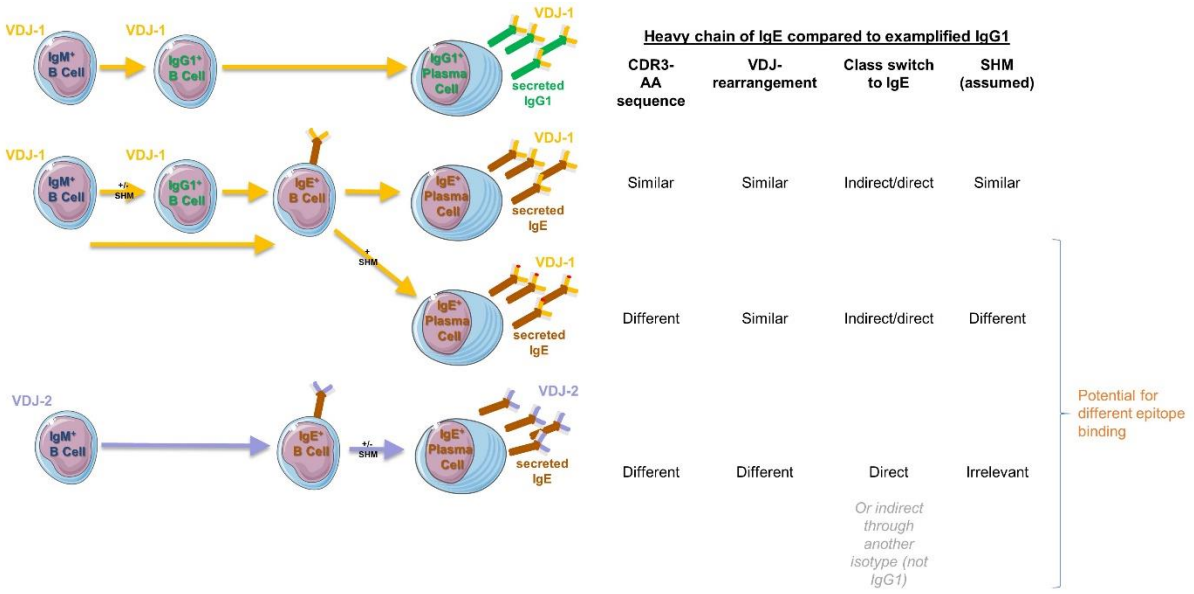

Figure 19: Differences in the CDR3-amino acid sequences of IgG1 and IgE can derive from different VDJ-gene rearrangements and somatic hypermutations
Summary of the comparative repertoire-analysis of IgG1 and IgE depicted at the cellular level. Two exemplified precursor IgM⁺ B cells with distinctly rearranged VDJ-genes (VDJ-1 yellow and VDJ-2 light blue). Class-switch to IgG1 (green) and/or IgE (brown) from these precursors as well as development from B to plasma cell is depicted as arrows. SHM was not directly analysed in this study. It can be assumed to occur differently in IgE and IgG1, because different VDJ-rearrangements only account for a part of the varying CDR3-sequences of IgE and IgG1. The light-chain variable region is depicted in grey, it was not analysed in this study and not taken into consideration.

Although the IgE repertoire contains VDJ gene combinations that are absent from the IgG1 repertoire, there are no differences in V-gene family usage between these repertoires at either the gene family or individual V gene level, as has been shown before in human and murine studies (*183*, *221*).

The low percentage of IgE-amino acid sequences that are similar to IgG1-sequences can be partially explained by the 10-40% of IgE clones (unique nt-sequences) that have a VDJ-rearrangement that is not detectable in the IgG1-repertoire. The additional unique sequences are probably generated by SHM that occurred in an IgE⁺ clone after it isotype-switched from an IgG1⁺ clone (Figure 19). This novel finding provides an additional explanation for why IgE-mediated anaphylaxis may not be blocked by IgG1.

5.4.3 Differences in the repertoire diversity of IgE and IgG1 in BM and mLN

The number of distinct detectable Ig-secreting clones provides a general idea about repertoire diversity (*181*). To better understand the relative diversity of the IgE and IgG1 repertoires, the number of clonotypes per 1000 sequences was analysed. Fewer clonotypes per 1000 analysed sequences indicates fewer unique clones as well as more proliferation of each clone, which suggests a selective pressure for the detected clonotypes.

The clonal diversity may reflect different clonal selections in BM and mLN. This can represent the local acute nature of the repertoire in mLN versus the memory nature of the BM repertoire. Although more total IgG1 transcripts are present in BM than in mLN, the number of clonotypes in BM is lower. This indicates less clonal diversity (approximately 3-fold fewer clonotypes per 1000 mRNA molecules) which indicates higher selective pressure for those IgG1-clones that end up in the BM. Intestinal dendritic cells continually capture a great variety of antigens from food and the natural gut microbiome, then migrate to the mLN where they present the processed antigen to $CD4^+$ T cells (*38*). Antigen-mediated cognate interactions between antigen-specific mLN B cells and these T cells induces clonal expansion and differentiation of these B cells (*222*). During and following this acute reaction, these B cells may die from IgG1/FcγRIIb-mediated antibody feedback inhibition (*223*) or migrate to the bone marrow as long lived plasma cells or memory B cells (*184*, *185*). However, relatively few germinal centre B cell clones receive the stimuli required to survive and develop into memory cells that migrate to the bone marrow (*224*). Death of the unselected clones in germinal centres is reflected in the lower clonal variety of BM than mLN IgG1.

In contrast to IgG1, there is both less IgE mRNA and fewer IgE clonotypes in BM than in mLN. The difference in IgE clonal diversity between mLN and bone marrow is less pronounced than for IgG1. IgE-memory is less well understood than IgG1 memory and there is a debate in the field. As compared with $IgG1^+$ B cells, antigen-activated IgE^+ B cells are more likely to develop into short-lived plasma cells than to form germinal centres (*217–219*). Furthermore, the lifespan of IgE^+ GC B cells appears to be considerably shorter than that of $IgG1^+$ GC B cells (*217*). Because GCs are the main source of memory B cells and long-lived plasma cells (*225*), most murine IgE-secreting plasma cells are thought to derive from memory B cells that had previously class-switched to IgG1 (*226*) rather than from dedicated IgE^+ memory B cells. This conclusion is supported by the observation that the IgE-memory response predominantly depends on IL-4 (*65*), the cytokine that is required for class switching to IgE. On the other hand, there is evidence that IgE^+ GC B cells do exist and can give rise to IgE^+ memory B cells (*227*) and long-lived BM plasma cells.

The results discussed in this chapter hold true for both allergen-associated as well as all analysed sequences.

5.4.4 The allergen-associated IgG1-repertoire is more diverse than the allergen-associated IgE-repertoire

In mLN, there is slightly higher relative clonal diversity, in other words, a more diverse repertoire of allergen-associated IgG1 (ca. 14 unique clonotypes per 1000 sequences) observable than there is for IgE (ca. 10 unique clonotypes per 1000 sequences). A more diverse repertoire potentially allows the recognition of a greater variety of antigens and epitopes. The lower relative repertoire of allergen-associated IgE suggests a stronger selection pressure on IgE, selecting fewer clones that are more abundant. This can be explained by the aforementioned tendency of IgE^+ B cells to become short-lived plasma cells. Fewer B cell clones class-switch into IgE^+ B cells than $IgG1^+$ ones. Those that do isotype switch proliferate and quickly develop into plasma cells that produce large amounts of RNA, while some of the activated $IgG1^+$ B cells undergo somatic hypermutation in GCs, further increasing the number and frequency of distinct clones (*217–219*).

Overall, the relative clonal diversity in the EW/EYP food allergy model seems to be less than in a study that evaluated IgG1 and IgE repertoire after helminth infection or OVA/alum-immunisation (*183*). Turqueti-Neves *et al.* showed approximately 200 unique sequences per 1000 sequences for both IgG1 and IgE in the mediastinal LN of *N. brasiliensis*-infected mice and 100 for IgE and 220 for IgG1 in OVA/alum-immunised mice. In the mLN of mice immunised in the EW/EYP food allergy model, there were ca. 14 unique clonotypes per 1000 sequences for allergen-associated IgG1 and ca. 10 unique clonotypes per 1000 sequences for IgE. The 10-fold discrepancies between this study and the study of Turqueti-Neves *et al.* may be explained by differences in the models used. In the EW/EYP food allergy mice are hyperimmunised resulting in an active immune response that continues for several weeks. *N. brasiliensis* on the other hand gets expelled after approximately 9 days. The duration of that immune response is thus much shorter than that for our EW/EYP model. The *i.p.* injection of OVA as a single antigen presumably induces a much less complex immune response that does not directly target the gut immune system.

Additional discrepancies can derive from the fact that I worked with primers for both IgE and IgG1 in a single sample during library preparation for NGS, while separate samples were used for IgE and IgG1 amplification in the Turqueti-Neves study. Using separate samples for each isotype has the advantage that more low abundant IgE-sequences can be amplified; these might be lost in our combined primer setup. However, during the sequencing itself, a sample specific bias can be introduced that is avoided with my approach. Additionally, I excluded sequences that only occurred once, because they might derive from sequencing errors.

5.4.5 Lower IgG1/IgE-ratios at the RNA-level than at the protein level

As expected, both NGS and serological analyses revealed that IgG1 (OVA-specific for antibody levels, allergen-associated for the NGS-analysis) is more abundant than IgE. However, while

antibody titres of OVA-IgG1 were 100-1000-fold higher than for OVA-IgE, NGS-analysis revealed only 10-30-fold more total IgG1 than total IgE transcripts in BM and mLN. The antibody output of an individual plasma cell that secretes IgE and one that secretes IgG1 are similar (*182*). However, the half-lives of both antibody-subclasses in serum differ greatly (*63*), which might explain the apparent discrepancy between the ratios of IgE:IgG1 mRNA and serum protein (*64*). Removal of IgE from serum can be accelerated by its binding to FcεRI or FcεRII in <6 h, serum IgE is adsorbed onto mast cells as shown by an IgE-infusion experiment in IgE-deficient mice (*65*).

Additionally, the NGS and the ELISA measure different entities: the ELISA truly measures EW-specific antibodies, with NGS measures "allergen-associated" Ig-sequences, some of which may not be EW-specific.

The comparable antibody output of IgG1- and IgE-secreting plasma cells (*182*) implies an additional conclusion: The higher number of distinct IgG1 compared to IgE sequences most likely correlates with a higher number of IgG1- than IgE-secreting cells, a conclusion that is supported by the literature (*222*, *227*).

5.4.6 The validity of the term "allergen-associated" sequences

The analysis of CDR3-sequences of IgG1 and IgE in BM and mLN was performed on total and so called "allergen-associated" sequences. My aim was to make general points about the repertoire of IgE and IgG1 as well as to analyse the IgE and IgG1 repertoires in the context of egg allergy in the EW/EYP food allergy model. In order to be able to filter for sequences that are potentially derived from allergen-specific B or plasma cells, all CDR3 amino-acid sequences (clonotypes) from naïve mice were pooled and this pool was subtracted from a pool from mice that were sensitised and challenged with EW and EYP. Sequences that are present in naïve mice correspond to immunoglobulins produced by B or plasma cells that were expanded in response to antigens and/or microbes present in the housing, food or people in contact with the mice. When all of these sequences are excluded in mice that are immunised with EW and EYP, the only clonotypes that are remaining should theoretically be allergen-specific. Although the assumption behind this simple computational approach may not be completely correct, there is considerable evidence for differences in CDR sequences between naïve and allergic mice.

Allergic mice have higher numbers of clonotypes, which may result from their exposure to relatively large quantities of additional allergens that expand more B cell clones to a level at which their CDR3-sequences become detectable. This is particularly true for IgE-switched B cells in mLN: allergic mice have approximately 10-fold higher clonotype numbers than naïve mice. This more pronounced increase in clonotype numbers in the gut draining lymph node may reflect prolonged, continuing allergen challenge of the local lymphoid tissue. Differences between naïve and allergic mice regarding IgG1 clonotypes, on the other hand, are more obvious in BM than in mLN. IgE in mice that are not helminth-infected generally reflects an

allergic response. IgG1 on the other hand can also be induced by other immune mechanisms. This is particularly the case for intestinal draining draining lymph nodes, which are constantly challenged, (e.g.; with microbial antigen derived from the natural gut microbiome), because IgG1 might be secreted in response to these non-allergen related sources. It has been shown that B cells and plasma cells migrate to the draining lymph node and proliferate there upon stimulation (*222*). The absolute number of stimulated IgG1-secreting plasma cells in the lymph node may not increase as much in response to repeated oral allergen challenges as the number of stimulated IgE-secreting plasma cells, because previous stimulation by endogenous and environmental allergens had already selectively stimulated an IgG response.

Clonotypes that are overrepresented among the sequences analysed can be interpreted as belonging to plasma cells that were most strongly clonally expanded. In an immune reaction against a particular allergen, these are the allergen-specific cells (*228*). V gene usage of highly frequent clonotypes (outliers) that are outside an interquartile range (IQR) of 3 in allergic mice differs from V gene usage in naïve mice. Thus, samples from allergic and naïve mice can be differentiated by the data obtained, at least regarding outliers. Both over-represented clonotypes (50 most abundant) as well as all clonotypes were analysed for differences in the repertoire of IgE and IgG1. Differences in CDR3 sequences and VDJ usage between IgE and IgG1 were detectable when analysing all clones and when only analysing the 50 most abundant clones. Because over-represented clones can be differentiated between allergic and naïve mice and the analysis of differences in the CDR3-regions and all clonotypes yielded similar results, it seems valid to classify the over-represented clones as “allergen-associated.”

Ideally, EW-specific B and plasma cells would have been fluorescently sorted in order to obtain a library of definitely allergen-specific IgE and IgG1 sequences. In practice, this approach is difficult. The majority of immunoglobulin-RNA that can be obtained from lymphoid tissue is derived from plasma cells because of their high content of mRNA and massive antibody secretion (*229*). Because plasma cells down-regulate surface BCR expression (*230*), demonstration of their antigen specificity requires intracellular staining with a fluorochrome-labelled antigen. Unfortunately, the permeabilisation and fixation procedures that are required for intracellular staining can decrease the quality of the RNA, although there are methods to partially prevent this (*231*).

6 OUTLOOK

In the present food allergy study, a murine model was used that induces this disease by administering a common allergenic food, hen's egg, without a non-physiological adjuvant through a physiologically relevant route. The disease features and serum allergen-specific antibodies and cytokines resemble human IgE-mediated food allergy. Investigation of additional factors that can influence disease development and severity in this model should promote a deeper understanding of the immunology and physiology of the allergic response. This model is suitable to study the interplay of factors involved in food allergy, such as relevant cell populations, local cytokine production and gut microbiome.

Allergen-specific IgG1 failed to fully block IgE-mediated anaphylaxis. One potential reason unveiled by this study is the differing CDR3-regions of IgE and IgG1 that potentially result in non-identical epitope binding. Here, antibody differences were only analysed at the RNA-level. An epitope-mapping approach could potentially validate our hypothesis at the protein level. Because it is believed that most OVA- and OVM-epitopes that are bound by IgE are sequential, sera from allergic mice can be probed against a peptide library of the relevant allergens in EW. This experiment though would only provide information about total responses. Sequencing of IgE and IgG1 heavy- and light-chains from single cell RNA would: complement our data and allow cloning and generation of monoclonal antibodies. These could be used for further epitope mapping of individual antibodies as well as for other functional analyses.

The IgG1 and IgE repertoires of allergic mice differ in the CDR3-region with respect to V(D)J-gene rearrangement and SHM. SHM has not yet been directly analysed in the present study. However, the existing NGS-data can be examined to quantify SHM in IgE and IgG1 and compare whether similar SHM occurs in both isotypes. Additionally, generation of lineage trees could provide further insight into the clonal relationship of IgE and IgG1.

7 REFERENCES

1. H. A. Sampson, Food allergy: Past, present and future. *Allergol. Int.* **65**, 363–369 (2016).
2. K. C. Bergmann, J. Heinrich, H. Niemann, Aktueller Stand zur Verbreitung von Allergien in Deutschland. *Allergo J.* **25**, 22–26 (2016).
3. S. Waserman, W. Watson, Food allergy. *Allergy Asthma. Clin. Immunol.* **7**, S7 (2011).
4. J. Wang, H. A. Sampson, Food allergy. *J. Clin. Invest.* **121**, 827–835 (2011).
5. S. H. Sicherer, Food Allergy. *Mt. Sinai J. Med. A J. Transl. Pers. Med.* **78**, 683–696 (2011).
6. Y. Ogawa, J. A. Grant, Mediators of Anaphylaxis. *Immunol. Allergy Clin. North Am.* **27**, 249–260 (2007).
7. A. Nowak-Wegrzyn, H. Szajewska, G. Lack, Food allergy and the gut. *Nat. Rev. Gastroenterol. Hepatol.* (2016), doi:10.1038/nrgastro.2016.187.
8. S. Dhami, S. Arasi, G. B. Pajno, Fernandez, A. Muraro, G. Roberts, C. Akdis, M. Alvaro-Lozano, K. Beyer, C. Bindslev-Jensen, W. Burks, G. du Toit, M. Ebisawa, P. Eigenmann, E. Knol, M. Makela, K. C. Nadeau, L. O'Mahony, N. Papadopoulos, L. K. Poulsen, C. Sackesen, H. Sampson, A. Santos, R. van Ree, F. Timmermans, A. Sheikh, Allergen immunotherapy for IgE-mediated food allergy: a systematic review and meta-analysis. *Eur. J. Allergy Clin. Immunol.* **38** (2017), doi:10.1111/ijlh.12426.
9. M. Gorelik, S. D. Narisety, A. L. Guerrerio, K. L. Chichester, C. A. Keet, A. P. Bieneman, R. G. Hamilton, R. A. Wood, J. T. Schroeder, P. A. Frischmeyer-Guerrerio, Suppression of the immunologic response to peanut during immunotherapy is often transient. *J. Allergy Clin. Immunol.* **135**, 1283–1292 (2015).
10. S. H. Sicherer, H. A. Sampson, Food allergy. *J. Allergy Clin. Immunol.* **125**, S116–S125 (2010).
11. B. I. Nwaru, L. Hickstein, S. S. Panesar, G. Roberts, A. Muraro, A. Sheikh, Prevalence of common food allergies in Europe: A systematic review and meta-analysis. *Allergy Eur. J. Allergy Clin. Immunol.* **69**, 992–1007 (2014).
12. A. H. Liu, R. Jaramillo, S. H. Sicherer, R. A. Wood, S. A. Bock, A. W. Burks, M. Massing, R. D. Cohn, D. C. Zeldin, National prevalence and risk factors for food allergy and relationship to asthma: Results from the National Health and Nutrition Examination Survey 2005-2006. *J. Allergy Clin. Immunol.* **126**, 798-806.e14 (2010).
13. M. Eggesbo, G. Botten, R. Halvorsen, P. Magnus, The prevalence of allergy to egg: a population-based study in young children. *Allergy*. **56**, 403–411 (2001).
14. T. Boyano-Martínez, C. García-Ara, J. M. Díaz-Pena, M. Martín-Esteban, Prediction of tolerance on the basis of quantification of egg white-specific IgE antibodies in children with egg allergy. *J. Allergy Clin. Immunol.* **110**, 304–309 (2002).
15. R. P. K. Ford, B. Taylor, Natural history of egg hypersensitivity. *Arch. Dis. Child.* **57**, 649–652 (1982).
16. J. H. Savage, E. C. Matsui, J. M. Skripak, R. A. Wood, The natural history of egg allergy. *J. Allergy Clin. Immunol.* **120**, 1413–1417 (2007).
17. L. P. C. Shek, L. Soderstrom, S. Ahlstedt, K. Beyer, H. A. Sampson, Determination of food specific IgE levels over time can predict the development of tolerance in cow's milk and hen's egg allergy. *J. Allergy Clin. Immunol.* **114**, 387–391 (2004).

18. H. Lemon-Mulé, H. A. Sampson, S. H. Sicherer, W. G. Shreffler, S. Noone, A. Nowak-Wegrzyn, Immunologic changes in children with egg allergy ingesting extensively heated egg. *J. Allergy Clin. Immunol.* **122** (2008), doi:10.1016/j.jaci.2008.09.007.

19. S. Sicherer, Manifestations of food allergy: Evaluation and management. *Am. Fam. Physician*. **59**, 415-424,429 (1999).

20. D. D. Metcalfe, H. A. Sampson, in *The Journal of Allergy and Clinical Immunology* (1990), vol. 86, pp. 421–442.

21. S. A. Bock, F. M. Atkins, Patterns of food hypersensitivity during sixteen years of double-blind, placebo-controlled food challenges. *J. Pediatr.* **117**, 561–567 (1990).

22. S. Allan Bock, H. A. Sampson, F. M. Atkins, R. S. Zeiger, S. Lehrer, M. Sachs, R. K. Bush, D. D. Metcafe, Double-blind, placebo-controlled food challenge (DBPCFC) as an office procedure: A manual. *J. Allergy Clin. Immunol.* **82**, 986–997 (1988).

23. R. G. Heine, N. Laske, D. J. Hill, The diagnosis and management of egg allergy. *Curr. Allergy Asthma Rep.* **6** (2006), pp. 145–152.

24. A. Pellegrini, A. J. Hülsmeier, P. Hunziker, U. Thomas, Proteolytic fragments of ovalbumin display antimicrobial activity. *Biochim. Biophys. Acta - Gen. Subj.* **1672**, 76–85 (2004).

25. Y. Mine, J. Wei Zhang, Identification and fine mapping of IgG and IgE epitopes in ovomucoid. *Biochem. Biophys. Res. Commun.* **292**, 1070–1074 (2002).

26. J. Bernhisel-Broadbent, H. M. Dintzis, R. Z. Dintzis, H. A. Sampson, Allergenicity and antigenicity of chicken egg ovomucoid (Gal d III) compared with ovalbumin (Gal d I) in children with egg allergy and in mice. *J. Allergy Clin. Immunol.* **93**, 1047–1059 (1994).

27. S. K. Cooke, H. A. Sampson, Allergenic properties of ovomucoid in man. *J. Immunol.* **159**, 2026–2032 (1997).

28. † Jennifer Kovacs-Nolan, ‡ Marshall Phillips, † and Yoshinori Mine*, Advances in the Value of Eggs and Egg Components for Human Health. *J. Agric. Food Chem.* **53**, 8421–8431 (2005).

29. P. Weber, H. Kratzin, K. Brockow, J. Ring, H. Steinhart, A. Paschke, Lysozyme in wine: A risk evaluation for consumers allergic to hen's egg. *Mol. Nutr. Food Res.* **53**, 1469–1477 (2009).

30. Y. Mine, J. W. Zhang, Comparative studies on antigenicity and allergenicity of native and denatured egg white proteins. *J. Agric. Food Chem.* **50**, 2679–2683 (2002).

31. K. M. Järvinen, K. Beyer, L. Vila, L. Bardina, M. Mishoe, H. A. Sampson, Specificity of IgE antibodies to sequential epitopes of hen's egg ovomucoid as a marker for persistence of egg allergy. *Allergy Eur. J. Allergy Clin. Immunol.* **62**, 758–765 (2007).

32. S. Quirce, F. Maranon, A. Umpierrez, M. de las Heras, E. Fernandez-Caldas, J. Sastre, Chicken serum albumin (Gal d 5 *) is a partially heat-labile inhalant and food allergen implicated in the bird-egg syndrome. *Allergy*. **56**, 754–762 (2001).

33. Z. Szépfalusi, C. Ebner, R. Pandjaitan, F. Orlicek, O. Scheiner, G. Boltz-Nitulescu, D. Kraft, H. Ebner, Egg yolk α-livetin (chicken serum albumin) is a cross-reactive allergen in the bird-egg syndrome. *J. Allergy Clin. Immunol.* **93**, 932–942 (1994).

34. C. De Silva, P. Dhanapala, T. Doran, M. L. K. Tang, C. Suphioglu, Molecular and immunological analysis of hen's egg yolk allergens with a focus on YGP42 (Gal d 6). *Mol. Immunol.* **71**, 152–160 (2016).

35. U. K. S. R. L. Samavedam, M. Khodoun, D. Wu, S. P. Hogan, F. D. Finkelman, *J. Immunol.*, in press (available at https://www.jimmunol.org/content/196/1_Supplement/123.9).

36. U. K. S. R. L. Samavedam, S. C. Morris, M. Khodoun, D. Wu, C. Potter, S. P. Hogan, F. D. Finkelman, *J. Immunol.*, in press (available at http://www.jimmunol.org/content/200/1_Supplement/104.14.abstract).

37. A. M. Mowat, W. W. Agace, Regional specialization within the intestinal immune system. *Nat Rev Immunol*. **14**, 667–685 (2014).

38. T. Worbs, U. Bode, S. Yan, M. W. Hoffmann, G. Hintzen, G. Bernhardt, R. Förster, O. Pabst, Oral tolerance originates in the intestinal immune system and relies on antigen carriage by dendritic cells. *J. Exp. Med.* **203**, 519–27 (2006).

39. H. G. Wells, T. B. Osborne, The Biological Reactions of the Vegetable Proteins. *J. Infect. Dis.* **8**, 66–1124 (1911).

40. S. Husby, J. Mestecky, Z. Moldoveanu, S. Holland, C. O. Elson, Oral tolerance in humans. T cell but not B cell tolerance after antigen feeding. *J. Immunol.* **152**, 4663–70 (1994).

41. E. Mazzini, L. Massimiliano, G. Penna, M. Rescigno, Oral Tolerance Can Be Established via Gap Junction Transfer of Fed Antigens from CX3CR1+ Macrophages to CD103+ Dendritic Cells. *Immunity*. **40**, 248–261 (2014).

42. C.-M. Sun, J. A. Hall, R. B. Blank, N. Bouladoux, M. Oukka, J. R. Mora, Y. Belkaid, Small intestine lamina propria dendritic cells promote de novo generation of Foxp3 T reg cells via retinoic acid. *J. Exp. Med.* **204**, 1775–85 (2007).

43. G. Bakdash, L. T. C. Vogelpoel, T. M. M. van Capel, M. L. Kapsenberg, E. C. de Jong, Retinoic acid primes human dendritic cells to induce gut-homing, IL-10-producing regulatory T cells. *Mucosal Immunol.* **8**, 265–78 (2015).

44. S. L. Russell, M. J. Gold, M. Hartmann, B. P. Willing, L. Thorson, M. Wlodarska, N. Gill, M. R. Blanchet, W. W. Mohn, K. M. McNagny, B. B. Finlay, Early life antibiotic-driven changes in microbiota enhance susceptibility to allergic asthma. *EMBO Rep.* **13**, 440–447 (2012).

45. H. Microorganisms, T. Environments, H. A. Krebs, P. Gurevich, M. Camacho, M. J. Bonete, H. J. Lamble, D. W. Hough, C. Biology, R. Cavicchioli, G. Fuchs, B. E. Alber, V. Brecht, H. Bothe, A. J. Pierik, B. T. Golding, R. Banerjee, J. B. Chaudhuri, M. J. Danson, S. L. Miller, B. H. A. Rehm, R. Eberhardt, A. Fouet, W. V Ng, S. L. Salzberg, L. Hood, S. Dassarma, C. Brochier, Y. Boucher, V. Vonstein, R. Overbeek, A. Osterman, S. Ueda, K. Sato, R. L. Crawford, R. S. Hanson, Induction of Colonic Regulatory T Cells by Indigenous Clostridium Species. *Science (80-.).*, 337–341 (2011).

46. J. Bollrath, F. Powrie, Feed your Tregs more fiber. *Science (80-.).* **341** (2013), pp. 463–464.

47. M. B. Geuking, J. Cahenzli, M. A. E. Lawson, D. C. K. Ng, E. Slack, S. Hapfelmeier, K. D. McCoy, A. J. Macpherson, Intestinal Bacterial Colonization Induces Mutualistic Regulatory T Cell Responses. *Immunity*. **34**, 794–806 (2011).

48. P. M. Smith, M. R. Howitt, N. Panikov, M. Michaud, C. A. Gallini, M. Bohlooly-Y, J. N. Glickman, W. S. Garrett, The microbial metabolites, short-chain fatty acids, regulate colonic T reg cell homeostasis. *Science (80-.).* **341**, 569–573 (2013).

49. R. Movérare, K. Blume, P. Lind, R. Crevel, Å. Marknell DeWitt, S. Cochrane, Human Allergen-Specific IgG Subclass Antibodies Measured Using ImmunoCAP Technology. *Int. Arch. Allergy Immunol.* **172**, 1–10 (2017).

50. M. C. Berin, Y. Zheng, M. Domaradzki, X.-M. Li, H. A. Sampson, Role of TLR4 in allergic sensitization to food proteins in mice. *Allergy*. **61**, 64–71 (2006).

51. K. Ganeshan, C. V. Neilsen, A. Hadsaitong, R. P. Schleimer, X. Luo, P. J. Bryce, Impairing oral tolerance promotes allergy and anaphylaxis: A new murine food allergy model. *J. Allergy Clin. Immunol.* **123** (2009), doi:10.1016/j.jaci.2008.10.011.

52. J. Strid, J. Hourihane, I. Kimber, R. Callard, S. Strobel, Epicutaneous exposure to peanut protein prevents oral tolerance and enhances allergic sensitization. *Clin. Exp. Allergy*. **35**, 757–766 (2005).

53. N. P. Birmingham, S. Parvataneni, H. M. A. Hassan, J. Harkema, S. Samineni, L. Navuluri, C. J. Kelly, V. Gangur, An adjuvant-free mouse model of tree nut allergy using hazelnut as a model tree nut. *Int. Arch. Allergy Immunol.* **144**, 203–210 (2007).

54. L. M. Bartnikas, M. F. Gurish, O. T. Burton, S. Leisten, E. Janssen, H. C. Oettgen, J. Beaupré, C. N. Lewis, K. F. Austen, S. Schulte, J. L. Hornick, R. S. Geha, M. K. Oyoshi, Epicutaneous sensitization results in IgE-dependent intestinal mast cell expansion and food-induced anaphylaxis. *J. Allergy Clin. Immunol.* **131** (2013), doi:10.1016/j.jaci.2012.11.032.

55. D. Dunkin, M. C. Berin, L. Mayer, Allergic sensitization can be induced via multiple physiologic routes in an adjuvant-dependent manner. *J. Allergy Clin. Immunol.* **128** (2011), doi:10.1016/j.jaci.2011.06.007.

56. V. Soumelis, P. A. Reche, H. Kanzler, W. Yuan, G. Edward, B. Homey, M. Gilliet, S. Ho, S. Antonenko, A. Lauerma, K. Smith, D. Gorman, S. Zurawski, J. Abrams, S. Menon, T. McClanahan, R. de Waal-Malefyt Rd, F. Bazan, R. A. Kastelein, Y.-J. Liu, Human epithelial cells trigger dendritic cell mediated allergic inflammation by producing TSLP. *Nat. Immunol.* **3**, 673–680 (2002).

57. R. P. Larson, M. R. Comeau, S. F. Ziegler, Cutting edge: allergen-specific CD4 T cells respond indirectly to thymic stromal lymphopoietin to promote allergic responses in the skin. *J. Immunol.* **190**, 4474–7 (2013).

58. L. C. Wu, A. A. Zarrin, The production and regulation of IgE by the immune system. *Nat. Rev. Immunol.* **14**, 247–59 (2014).

59. C. A. Carter, P. A. Frischmeyer-Guerrerio, The Genetics of Food Allergy. *Curr. Allergy Asthma Rep.* **18**, 2 (2018).

60. V. Morafo, K. Srivastava, C.-K. Huang, G. Kleiner, S.-Y. Lee, H. A. Sampson, A.-M. Li, Genetic susceptibility to food allergy is linked to differential TH2-TH1 responses in C3H/HeJ and BALB/c mice. *J. Allergy Clin. Immunol.* **111**, 1122–8 (2003).

61. N. D. Dave, L. Xiang, K. E. Rehm, G. D. Marshall, Jr., Stress and allergic diseases. *Immunol. Allergy Clin. North Am.* **31**, 55–68 (2011).

62. M. Pascal, M. Perez-Gordo, T. Caballero, M. M. Escribese, M. N. Lopez Longo, O. Luengo, L. Manso, V. Matheu, E. Seoane, M. Zamorano, M. Labrador, C. Mayorga, Microbiome and Allergic Diseases. *Front. Immunol.* **9**, 1584 (2018).

63. M. G. Lawrence, J. A. Woodfolk, A. J. Schuyler, L. C. Stillman, M. D. Chapman, T. A. E. Platts-Mills, Half-life of IgE in serum and skin: Consequences for anti-IgE therapy in patients with allergic disease. *J. Allergy Clin. Immunol.* **139**, 422-428.e4 (2017).

64. P. Vieira, K. Rajewsky, The half-lives of serum immunoglobulins in adult mice. *Eur. J. Immunol.* **18**, 313–316 (1988).

65. R. Jiménez-Saiz, D. K. Chu, T. S. Mandur, T. D. Walker, M. E. Gordon, R. Chaudhary, J.

Koenig, S. Saliba, H. J. Galipeau, A. Utley, I. L. King, K. Lee, R. Ettinger, S. Waserman, R. Kolbeck, M. Jordana, Lifelong memory responses perpetuate humoral TH2 immunity and anaphylaxis in food allergy. *J. Allergy Clin. Immunol.* **2**, 2049–2056 (2017).

66. N. Novak, C. Tepel, S. Koch, K. Brix, T. Bieber, S. Kraft, Evidence for a differential expression of the FcεRIγ chain in dendritic cells of atopic and nonatopic donors. *J. Clin. Invest.* **111**, 1047–1056 (2003).

67. B. S. Sihra, O. M. Kon, J. A. Grant, A. B. Kay, Expression of high-affinity IgE receptors (FcεRI) on peripheral blood basophils, monocytes, and eosinophils in atopic and nonatopic subjects: Relationship to total serum IgE concentrations. *J. Allergy Clin. Immunol.* **99**, 699–706 (1997).

68. A. E. Semper, K. Heron, A. C. S. Woollard, J. P. Kochan, P. S. Friedmann, M. K. Church, I. G. Reischl, Surface expression of FcεRI on Langerhans' cells of clinically uninvolved skin is associated with disease activity in atopic dermatitis, allergic asthma, and rhinitis. *J. Allergy Clin. Immunol.* **112**, 411–419 (2003).

69. D. Maurer, E. Fiebiger, B. Reininger, B. Wolff-Winiski, M. H. Jouvin, O. Kilgus, J. P. Kinet, G. Stingl, Expression of functional high affinity immunoglobulin E Receptors (FcϵRI) on Monocytes of Atopic Individuals. *J. Exp. Med.* **179**, 745–750 (1994).

70. H. C. Oettgen, O. T. Burton, in *Advances in Immunology* (Academic Press Inc., 2015), vol. 127, pp. 203–256.

71. H. Turner, J. P. Kinet, Signalling through the high-affinity IgE receptor FcεRI. *Nature*. **402** (1999), pp. 24–30.

72. I. Miyajima, D. Dombrowicz, T. R. Martin, J. V. Ravetch, J. P. Kinet, S. J. Galli, Systemic anaphylaxis in the mouse can be mediated largely through IgG1 and FcγRIII: Assessment of the cardiopulmonary changes, mast cell degranulation, and death associated with active or IgE- or IgG1-dependent passive anaphylaxis. *J. Clin. Invest.* **99**, 901–914 (1997).

73. D. Dombrowicz, V. Flamand, I. Miyajima, J. V. Ravetch, S. J. Galli, J. P. Kinet, Absence of Fc(ε)RI α chain results in upregulation of FcγRIII- dependent mast cell degranulation and anaphylaxis: Evidence of competition between Fc(ε)RI and FcγRIII for limiting amounts of FcR β and γ chains. *J. Clin. Invest.* **99**, 915–925 (1997).

74. F. D. Finkelman, Anaphylaxis: Lessons from mouse models. *J. Allergy Clin. Immunol.* **120**, 506–515 (2007).

75. R. T. Strait, S. C. Morris, M. Yang, X. W. Qu, F. D. Finkelman, Pathways of anaphylaxis in the mouse. *J. Allergy Clin. Immunol.* **109**, 658–668 (2002).

76. W. Zhao, C. L. Kepley, P. A. Morel, L. M. Okumoto, Y. Fukuoka, L. B. Schwartz, FcγRIIa, Not FcγRIIb, Is Constitutively and Functionally Expressed on Skin-Derived Human Mast Cells. *J. Immunol.* **177**, 694–701 (2006).

77. R. T. Venkatesha, E. B. Thangam, A. K. Zaidi, H. Ali, Distinct regulation of C3a-induced MCP-1/CCL2 and RANTES/CCL5 production in human mast cells by extracellular signal regulated kinase and PI3 kinase. *Mol. Immunol.* **42**, 581–587 (2005).

78. J. S. Marshall, Mast-cell responses to pathogens. *Nat. Rev. Immunol.* **4** (2004), pp. 787–799.

79. O. T. Burton, A. Epp, M. E. Fanny, S. J. Miller, A. J. Stranks, J. E. Teague, R. A. Clark, M. van de Rijn, H. C. Oettgen, Tissue-specific expression of the low-affinity IgG receptor, FcγRIIb, on human mast cells. *Front. Immunol.* **9**, 1244 (2018).

80. O. Malbec, L. Cassard, M. Albanesi, F. Jönsson, D. Mancardi, G. Chicanne, B. Payrastre, P. Dubreuil, E. Vivier, M. Daëron, Trans-inhibition of activation and proliferation signals by Fc receptors in mast cells and basophils. *Sci. Signal.* **9** (2016), doi:10.1126/scisignal.aag1401.

81. D. D. Metcalfe, R. D. Peavy, A. M. Gilfillan, Mechanisms of mast cell signaling in anaphylaxis. *J. Allergy Clin. Immunol.* **124** (2009), pp. 639–646.

82. K. Takatsu, T. Kouro, Y. Nagai, Interleukin 5 in the Link Between the Innate and Acquired Immune Response. *Adv. Immunol.* **101**, 191–236 (2009).

83. M. Barner, M. Mohrs, F. Brombacher, M. Kopf, Differences between IL-4Rα-deficient and IL-4-deficient mice reveal a role for IL-13 in the regulation of Th2 responses. *Curr. Biol.* **8**, 669–672 (1998).

84. O. T. Burton, A. R. Darling, J. S. Zhou, M. Noval-Rivas, T. G. Jones, M. F. Gurish, T. A. Chatila, H. C. Oettgen, Direct effects of IL-4 on mast cells drive their intestinal expansion and increase susceptibility to anaphylaxis in a murine model of food allergy. *Mucosal Immunol.* **6**, 740–750 (2013).

85. R. T. Strait, S. C. Morris, K. Smiley, J. F. Urban, F. D. Finkelman, IL-4 Exacerbates Anaphylaxis. *J. Immunol.* **170**, 3835–3842 (2003).

86. S. D. Boyd, S. a Joshi, High-Throughput DNA Sequencing Analysis of Antibody Repertoires. *Microbiol. Spectr.* **2**, 1–13 (2014).

87. A. F. Williams, A. N. Barclay, The immunoglobulin superfamily - Domains for cell surface recognition. *Annu. Rev. Immunol.* **6**, 381–405 (1988).

88. K. A. Smith, P. N. Nelson, P. Warren, S. J. Astley, P. G. Murray, J. Greenman, Demystified... recombinant antibodies. *J. Clin. Pathol.* **57** (2004), pp. 912–917.

89. S. Tonegawa, Somatic generation of antibody diversity. *Nature*. **302**, 575–581 (1983).

90. P. Leder, The genetics of antibody diversity. *Sci. Am.* **246**, 102–115 (1982).

91. T. Honjo, S. Packman, D. Swan, M. Nau, P. Leder, Organization of immunoglobulin genes: reiteration frequency of the mouse chain constant region gene. *Proc. Natl. Acad. Sci. U. S. A.* **71**, 3659–3663 (1974).

92. D. D. Dudley, J. Chaudhuri, C. H. Bassing, F. W. Alt, Mechanism and control of V(D)J recombination versus class switch recombination: Similarities and differences. *Adv. Immunol.* **86**, 43–112 (2005).

93. S. J. Corbett, I. M. Tomlinson, E. L. L. Sonnhammer, D. Buck, G. Winter, Sequence of the human immunoglobulin diversity (D) segment locus: A systematic analysis provides no evidence for the use of DIR segments, inverted D segments, “Minor” D segments or D-D recombination. *J. Mol. Biol.* **270**, 587–597 (1997).

94. F. Matsuda, K. Ishii, P. Bourvagnet, K. I. Kuma, H. Hayashida, T. Miyata, T. Honjo, The complete nucleotide sequence of the human immunoglobulin heavy chain variable region locus. *J. Exp. Med.* **188**, 2151–2162 (1998).

95. K. Kawasaki, S. Minoshima, E. Nakato, K. Shibuya, A. Shintani, J. L. Schmeits, J. Wang, N. Shimizu, One-megabase sequence analysis of the human immunoglobulin λ gene locus. *Genome Res.* **7**, 250–261 (1997).

96. P. M. Kirkham, H. W. Schroeder, Antibody structure and the evolution of immunoglobulin v gene segments. *Semin. Immunol.* **6**, 347–360 (1994).

97. P. H. Brodeur, R. Riblet, The immunoglobulin heavy chain variable region (Igh-V) locus in the mouse. I. One hundred Igh-V genes comprise seven families of homologous genes. *Eur. J. Immunol.* **14**, 922–930 (1984).

98. C. M. Oefner, A. Winkler, C. Hess, A. K. Lorenz, V. Holecska, M. Huxdorf, T. Schommartz, D. Petzold, J. Bitterling, A. L. Schoen, A. D. Stoehr, D. Vu Van, Y. Darcan-Nikolaisen, V. Blanchard, I. Schmudde, Y. Laumonnier, H. A. Ströver, A. N. Hegazy, S. Eiglmeier, C. T. Schoen, M. M. M. Mertes, C. Loddenkemper, M. Löhning, P. König, A. Petersen, E. O. Luger, M. Collin, J. Köhl, A. Hutloff, E. Hamelmann, M. Berger, H. Wardemann, M. Ehlers, Tolerance induction with T cell-dependent protein antigens induces regulatory sialylated IgGs. *J. Allergy Clin. Immunol.* **129**, 1647–1655 (2012).

99. K. M. Brekke, W. T. Garrard, Assembly and analysis of the mouse immunoglobulin kappa gene sequence. *Immunogenetics*. **56**, 490–505 (2004).

100. P. Sanchez, B. Nadel, P. -A Cazenave, Vλ-Jλ rearrangements are restricted within a V-J-C recombination unit in the mouse. *Eur. J. Immunol.* **21**, 907–911 (1991).

101. C. M. Johnston, A. L. Wood, D. J. Bolland, A. E. Corcoran, Complete Sequence Assembly and Characterization of the C57BL/6 Mouse Ig Heavy Chain V Region. *J. Immunol.* **176**, 4221–4234 (2006).

102. D. R. Davies, E. A. Padlan, Antibody-Antigen Complexes. *Annu. Rev. Biochem.* **59**, 439–473 (1990).

103. J. L. Xu, M. M. Davis, Diversity in the CDR3 Region of V. *Immunity*. **13**, 37–45 (2000).

104. H. P. Fell, P. W. Tucker, Immunoglobulin genes. *Immunol. Ser.* **43**, 181–202 (1989).

105. K. Akashi, M. Kondo, S. Cheshier, J. Shizuru, K. Gandy, J. Domen, R. Mebius, D. Traver, I. L. Weissman, in *Cold Spring Harbor Symposia on Quantitative Biology* (Cold Spring Harbor Laboratory Press, 1999), vol. 64, pp. 1–12.

106. T. Shimizu, C. Mundt, S. Licence, F. Melchers, I.-L. Mårtensson, VpreB1/VpreB2/λ5 Triple-Deficient Mice Show Impaired B Cell Development but Functional Allelic Exclusion of the IgH Locus. *J. Immunol.* **168**, 6286–6293 (2002).

107. D. Leslie, P. Lipsky, A. Louis Notkins, Autoantibodies as predictors of disease. *J. Clin. Invest.* **108** (2001), pp. 1417–1422.

108. N. E. Harwood, F. D. Batista, Early Events in B Cell Activation. *Annu. Rev. Immunol.* **28**, 185–210 (2010).

109. Antonio Lanzavecchia, Antigen-specfic interaction between T and B cells. *Nature*. **314**, 537–539 (1985).

110. K. (Kenneth M. . Murphy, P. Travers, M. Walport, C. Janeway, *Janeway's immunobiology* (Garland Science, London [u.a.], 8. ed., 2012).

111. J. Chaudhuri, F. W. Alt, Class-switch recombination: Interplay of transcription, DNA deamination and DNA repair. *Nat. Rev. Immunol.* **4**, 541–552 (2004).

112. J. Chaudhuri, U. Basu, A. Zarrin, C. Yan, S. Franco, T. Perlot, B. Vuong, J. Wang, R. T. Phan, A. Datta, J. Manis, F. W. Alt, Evolution of the Immunoglobulin Heavy Chain Class Switch Recombination Mechanism. *Adv. Immunol.* **94** (2007), pp. 157–214.

113. A. K. Bär, N. Phukan, J. Pinheiro, A. Simoes-Barbosa, The Interplay of Host Microbiota and Parasitic Protozoans at Mucosal Interfaces: Implications for the Outcomes of Infections and Diseases. *PLoS Negl. Trop. Dis.* **9** (2015), , doi:10.1371/journal.pntd.0004176.

114. J. Punnonen, G. Aversa, B. G. Cocks, A. N. J. Mckenziet, S. Menont, G. Zurawskit, R. De, W. Malefyt, J. E. De Vries, Interleukin 13 induces interleukin 4-independent IgG4 and IgE synthesis and CD23 expression by human B cells (B-cell differentiation/isotype switching/allergy). *Immunology*. **90**, 3730–3734 (1993).

115. G. Siebenkotten, C. Esser, M. Wabl, A. Radbruch, The murine IgG1/IgE class switch program. *Eur. J. Immunol.* **22**, 1827–34 (1992).

116. J. E. de Vries, J. Punnonen, B. G. Cocks, R. de W. Malefyt, G. Aversa, in *Research in Immunology* (1993), vol. 144, pp. 597–601.

117. S. M. Zurawski, F. Vega, B. Huyghe, G. Zurawski, Receptors for interleukin-13 and interleukin-4 are complex and share a novel component that functions in signal transduction. *EMBO J.* **12**, 2663–2670 (1993).

118. R. E. Callard, D. J. Matthews, L. Hibbert, IL-4 and IL-13 receptors: Are they one and the same? *Immunol. Today*. **17** (1996), pp. 108–110.

119. C. M. Snapper, W. E. Paul, Interferon-γ and B cell stimulatory factor-1 reciprocally regulate Ig isotype production. *Science (80-.).* **236**, 944–947 (1987).

120. F. D. Finkelman, I. M. Katona, T. R. Mosmann, R. L. Coffman, IFN-gamma regulates the isotypes of Ig secreted during in vivo humoral immune responses. *J. Immunol.* **140**, 1022–7 (1988).

121. M. Sugai, H. Gonda, T. Kusunoki, T. Katakai, Y. Yokota, A. Shimizu, Essential role of Id2 in negative regulation of IgE class switching. *Nat. Immunol.* **4**, 25–30 (2003).

122. M. B. Harris, J. Mostecki, P. B. Rothman, Repression of an interleukin-4-responsive promoter requires cooperative BCL-6 function. *J. Biol. Chem.* **280**, 13114–13121 (2005).

123. K. Yoshida, M. Matsuoka, S. Usuda, A. Mori, K. Ishizaka, H. Sakano, Immunoglobulin switch circular DNA in the mouse infected with Nippostrongylus brasiliensis: Evidence for successive class switching from μ to ε via γ1. *Proc. Natl. Acad. Sci. U. S. A.* **87**, 7829–7833 (1990).

124. F. C. Mills, G. Thyphronitis, F. D. Finkelman, E. E. Max, Ig mu-epsilon isotype switch in IL-4-treated human B lymphoblastoid cells. Evidence for a sequential switch. *J. Immunol.* **149**, 1075–85 (1992).

125. R. Mandler, F. D. Finkelman, A. D. Levine, C. M. Snapper, IL-4 induction of IgE class switching by lipopolysaccharide-activated murine B cells occurs predominantly through sequential switching. *J. Immunol.* **150**, 407–18 (1993).

126. G. Georgiou, G. C. Ippolito, J. Beausang, C. E. Busse, H. Wardemann, S. R. Quake, The promise and challenge of high-throughput sequencing of the antibody repertoire. *Nat. Biotechnol.* **32**, 158–168 (2014).

127. K. Hollowood, J. Macartney, Cell kinetics of the germinal center reaction - a stathmokinetic study. *Eur. J. Immunol.* **22**, 261–266 (1992).

128. Y. -J Liu, J. Zhang, P. J. L. Lane, E. Y. -. Chan, I. C. M. Maclennan, Sites of specific B cell activation in primary and secondary responses to T cell-dependent and T cell-independent antigens. *Eur. J. Immunol.* **21**, 2951–2962 (1991).

129. G. Kraal, R. R. Hardy, W. M. Gallatin, I. L. Weissman, E. C. Butcher, Antigen-induced changes in B cell subsets in lymph nodes: analysis by dual fluorescence flow cytofluorometry. *Eur. J. Immunol.* **16**, 829–834 (1986).

130. M. Stebegg, S. D. Kumar, A. Silva-Cayetano, V. R. Fonseca, M. A. Linterman, L. Graca,

Regulation of the germinal center response. *Front. Immunol.* **9**, 2469 (2018).

131. M. J. Shlomchik, F. Weisel, Germinal centers. *Immunol. Rev.* **247** (2012), pp. 5–10.

132. V. H. Odegard, D. G. Schatz, Targeting of somatic hypermutation. *Nat. Rev. Immunol.* **6** (2006), pp. 573–583.

133. D. R. Bentley, S. Balasubramanian, H. P. Swerdlow, G. P. Smith, J. Milton, C. G. Brown, K. P. Hall, D. J. Evers, C. L. Barnes, H. R. Bignell, J. M. Boutell, J. Bryant, R. J. Carter, R. Keira Cheetham, A. J. Cox, D. J. Ellis, M. R. Flatbush, N. A. Gormley, S. J. Humphray, L. J. Irving, M. S. Karbelashvili, S. M. Kirk, H. Li, X. Liu, K. S. Maisinger, L. J. Murray, B. Obradovic, T. Ost, M. L. Parkinson, M. R. Pratt, I. M. J. Rasolonjatovo, M. T. Reed, R. Rigatti, C. Rodighiero, M. T. Ross, A. Sabot, S. V. Sankar, A. Scally, G. P. Schroth, M. E. Smith, V. P. Smith, A. Spiridou, P. E. Torrance, S. S. Tzonev, E. H. Vermaas, K. Walter, X. Wu, L. Zhang, M. D. Alam, C. Anastasi, I. C. Aniebo, D. M. D. Bailey, I. R. Bancarz, S. Banerjee, S. G. Barbour, P. A. Baybayan, V. A. Benoit, K. F. Benson, C. Bevis, P. J. Black, A. Boodhun, J. S. Brennan, J. A. Bridgham, R. C. Brown, A. A. Brown, D. H. Buermann, A. A. Bundu, J. C. Burrows, N. P. Carter, N. Castillo, M. C. E. Catenazzi, S. Chang, R. Neil Cooley, N. R. Crake, O. O. Dada, K. D. Diakoumakos, B. Dominguez-Fernandez, D. J. Earnshaw, U. C. Egbujor, D. W. Elmore, S. S. Etchin, M. R. Ewan, M. Fedurco, L. J. Fraser, K. V. Fuentes Fajardo, W. Scott Furey, D. George, K. J. Gietzen, C. P. Goddard, G. S. Golda, P. A. Granieri, D. E. Green, D. L. Gustafson, N. F. Hansen, K. Harnish, C. D. Haudenschild, N. I. Heyer, M. M. Hims, J. T. Ho, A. M. Horgan, K. Hoschler, S. Hurwitz, D. V. Ivanov, M. Q. Johnson, T. James, T. A. Huw Jones, G. D. Kang, T. H. Kerelska, A. D. Kersey, I. Khrebtukova, A. P. Kindwall, Z. Kingsbury, P. I. Kokko-Gonzales, A. Kumar, M. A. Laurent, C. T. Lawley, S. E. Lee, X. Lee, A. K. Liao, J. A. Loch, M. Lok, S. Luo, R. M. Mammen, J. W. Martin, P. G. McCauley, P. McNitt, P. Mehta, K. W. Moon, J. W. Mullens, T. Newington, Z. Ning, B. Ling Ng, S. M. Novo, M. J. O'Neill, M. A. Osborne, A. Osnowski, O. Ostadan, L. L. Paraschos, L. Pickering, A. C. Pike, A. C. Pike, D. Chris Pinkard, D. P. Pliskin, J. Podhasky, V. J. Quijano, C. Raczy, V. H. Rae, S. R. Rawlings, A. Chiva Rodriguez, P. M. Roe, J. Rogers, M. C. Rogert Bacigalupo, N. Romanov, A. Romieu, R. K. Roth, N. J. Rourke, S. T. Ruediger, E. Rusman, R. M. Sanches-Kuiper, M. R. Schenker, J. M. Seoane, R. J. Shaw, M. K. Shiver, S. W. Short, N. L. Sizto, J. P. Sluis, M. A. Smith, J. Ernest Sohna Sohna, E. J. Spence, K. Stevens, N. Sutton, L. Szajkowski, C. L. Tregidgo, G. Turcatti, S. Vandevondele, Y. Verhovsky, S. M. Virk, S. Wakelin, G. C. Walcott, J. Wang, G. J. Worsley, J. Yan, L. Yau, M. Zuerlein, J. Rogers, J. C. Mullikin, M. E. Hurles, N. J. McCooke, J. S. West, F. L. Oaks, P. L. Lundberg, D. Klenerman, R. Durbin, A. J. Smith, Accurate whole human genome sequencing using reversible terminator chemistry. *Nature*. **456**, 53–59 (2008).

134. S. Goodwin, J. D. McPherson, W. R. McCombie, Coming of age: ten years of next-generation sequencing technologies. *Nat Rev Genet*. **17**, 333–351 (2016).

135. F. Sanger, S. Nicklen, A. . Coulson, DNA sequencing with chain-terminating. *Proc Natl Acad Sci USA*. **74**, 5463–5467 (1977).

136. J. B. Cohen, D. Givol, Allelic immunoglobulin VH genes in two mouse strains: possible germline gene recombination. *EMBO J.* **2**, 2013–2018 (1983).

137. J. Zhou, K. R. Lottenbach, S. J. Barenkamp, A. H. Lucas, D. C. Reason, Recurrent variable region gene usage and somatic mutation in the human antibody response to the capsular polysaccharide of Streptococcus pneumoniae type 23F. *Infect. Immun.* **70**, 4083–4091 (2002).

138. J. A. Weinstein, N. Jiang, R. A. White, D. S. Fisher, S. R. Quake, High-throughput sequencing of the zebrafish antibody repertoire. *Science (80-.).* **324**, 807–810 (2009).

139. E. S. Mroczek, G. C. Ippolito, T. Rogosch, K. H. Hoi, T. A. Hwangpo, M. G. Brand, Y. Zhuang, C. R. Liu, D. A. Schneider, M. Zemlin, E. E. Brown, G. Georgiou, H. W. Schroeder, Differences

in the composition of the human antibody repertoire by b cell subsets in the blood. *Front. Immunol.* **5**, 96 (2014).

140. T. Rogosch, S. Kerzel, L. Sikula, K. Gentil, M. Liebetruth, K.-P. Schlingmann, R. F. Maier, M. Zemlin, Plasma Cells and Nonplasma B Cells Express Differing IgE Repertoires in Allergic Sensitization. *J. Immunol.* **184**, 4947–4954 (2010).

141. M. P. Panjikaran, C. Orosco, B. Kwok, Y. Xia, L. Keeler, P. Petersen, G. Sims, J. Falk, C. Scott, A. Graber, B-cell enrichment for next generation sequencing (NGS): An approach to detect actionable low frequency variants in B-cell lymphomas. *J. Clin. Oncol.* **36**, e24165–e24165 (2018).

142. D. Croote, S. Darmanis, K. C. Nadeau, S. R. Quake, High-affinity allergen-specific human antibodies cloned from single IgE B cell transcriptomes. *Science (80-.).* **362**, 1306–1309 (2018).

143. H. Wardemann, S. Yurasov, A. Schaefer, J. W. Young, E. Meffre, M. C. Nussenzweig, Predominant autoantibody production by early human B cell precursors. *Science (80-.).* **301**, 1374–1377 (2003).

144. M. Aoki-Ota, A. Torkamani, T. Ota, N. Schork, D. Nemazee, Skewed Primary Igκ Repertoire and V–J Joining in C57BL/6 Mice: Implications for Recombination Accessibility and Receptor Editing. *J. Immunol.* **188**, 2305–2315 (2012).

145. K. Larimore, M. W. McCormick, H. S. Robins, P. D. Greenberg, Shaping of Human Germline IgH Repertoires Revealed by Deep Sequencing. *J. Immunol.* **189**, 3221–3230 (2012).

146. E. Scotto-Lavino, G. Du, M. A. Frohman, 5' end cDNA amplification using classic RACE. *Nat. Protoc.* **1**, 2742–2745 (2006).

147. M. A. Frohman, M. K. Dush, G. R. Martin, Rapid production of full-length cDNAs from rare transcripts: Amplification using a single gene-specific oligonucleotide primer. *Proc. Natl. Acad. Sci. U. S. A.* **85**, 8998–9002 (1988).

148. J. J. M. van Dongen, A. W. Langerak, M. Brüggemann, P. A. S. Evans, M. Hummel, F. L. Lavender, E. Delabesse, F. Davi, E. Schuuring, R. García-Sanz, J. H. J. M. van Krieken, J. Droese, D. González, C. Bastard, H. E. White, M. Spaargaren, M. González, A. Parreira, J. L. Smith, G. J. Morgan, M. Kneba, E. A. Macintyre, Design and standardization of PCR primers and protocols for detection of clonal immunoglobulin and T-cell receptor gene recombinations in suspect lymphoproliferations: Report of the BIOMED-2 concerted action BMH4-CT98-3936. *Leukemia*. **17** (2003), pp. 2257–2317.

149. Y. Liu, J. King, J. Glanville, S. D. Boyd, T. J. Looney, M. M. Davis, T. D. Pham, C. L. Dekker, J.-Y. Lee, K. M. Roskin, R. A. Hoh, Human B-cell isotype switching origins of IgE. *J. Allergy Clin. Immunol.* **137**, 579-586.e7 (2015).

150. S. D. Boyd, E. L. Marshall, J. D. Merker, J. M. Maniar, L. N. Zhang, B. Sahaf, C. D. Jones, B. B. Simen, B. Hanczaruk, K. D. Nguyen, K. C. Nadeau, M. Egholm, D. B. Miklos, J. L. Zehnder, A. Z. Fire, Measurement and clinical monitoring of human lymphocyte clonality by massively parallel V-D-J pyrosequencing. *Sci. Transl. Med.* **1**, 12ra23-12ra23 (2009).

151. X. Wu, T. Zhou, J. Zhu, B. Zhang, I. Georgiev, C. Wang, X. Chen, N. S. Longo, M. Louder, K. McKee, S. O'Dell, S. Perfetto, S. D. Schmidt, W. Shi, L. Wu, Y. Yang, Z. Y. Yang, Z. Yang, Z. Zhang, M. Bonsignori, J. A. Crump, S. H. Kapiga, N. E. Sam, B. F. Haynes, M. Simek, D. R. Burton, W. C. Koff, N. A. Doria-Rose, M. Connors, J. C. Mullikin, G. J. Nabel, M. Roederer, L. Shapiro, P. D. Kwong, J. R. Mascola, Focused evolution of HIV-1 neutralizing antibodies revealed by structures and deep sequencing. *Science (80-.).* **333**, 1593–1602 (2011).

152. J. F. Scheid, H. Mouquet, B. Ueberheide, R. Diskin, F. Klein, T. Y. K. Oliveira, J. Pietzsch, D.

Fenyo, A. Abadir, K. Velinzon, A. Hurley, S. Myung, F. Boulad, P. Poignard, D. R. Burton, F. Pereyra, D. D. Ho, B. D. Walker, M. S. Seaman, P. J. Bjorkman, B. T. Chait, M. C. Nussenzweig, Sequence and Structural Convergence of Broad and Potent HIV Antibodies That Mimic CD4 Binding. *Science (80-.).* **333**, 1633–1637 (2011).

153. A. Fähnrich, M. Krebbel, N. Decker, M. Leucker, F. D. Lange, K. Kalies, S. Möller, ClonoCalc and ClonoPlot: Immune repertoire analysis from raw files to publication figures with graphical user interface. *BMC Bioinformatics*. **18**, 1–6 (2017).

154. Z. Chen, A. M. Collins, Y. Wang, B. A. Gata, in *Immunome Research* (Immunome Res, 2010), vol. 6.

155. J. Glanville, W. Zhai, J. Berka, D. Telman, G. Huerta, G. R. Mehta, I. Ni, L. Mei, P. D. Sundar, G. M. R. Day, D. Cox, A. Rajpal, J. Pons, Precise determination of the diversity of a combinatorial antibody library gives insight into the human immunoglobulin repertoire. *Proc. Natl. Acad. Sci. U. S. A.* **106**, 20216–20221 (2009).

156. D. A. Bolotin, S. Poslavsky, I. Mitrophanov, M. Shugay, I. Z. Mamedov, E. V Putintseva, D. M. Chudakov, MiXCR: software for comprehensive adaptive immunity profiling. *Nat. Methods*. **12**, 380–381 (2015).

157. D. K. Ralph, F. A. Matsen, Consistency of VDJ Rearrangement and Substitution Parameters Enables Accurate B Cell Receptor Sequence Annotation. *PLoS Comput. Biol.* **12**, e1004409 (2016).

158. L. López-Santibáñez-Jácome, S. E. Avendaño-Vázquez, C. F. Flores-Jasso, The pipeline repertoire for Ig-Seq analysis. *Front. Immunol.* **10** (2019), p. 899.

159. B. Zhang, W. Meng, E. T. Luning Prak, U. Hershberg, Discrimination of germline V genes at different sequencing lengths and mutational burdens: A new tool for identifying and evaluating the reliability of V gene assignment. *J. Immunol. Methods*. **427**, 105–116 (2015).

160. B. Cortina-Ceballos, E. E. Godoy-Lozano, H. Sámano-Sánchez, A. Aguilar-Salgado, M. D. C. Velasco-Herrera, C. Vargas-Chávez, D. Velázquez-Ramírez, G. Romero, J. Moreno, J. Téllez-Sosa, J. Martínez-Barnetche, Reconstructing and mining the B cell repertoire with ImmunediveRsity. *MAbs*. **7**, 516–524 (2015).

161. T. Dörner, N. L. Farner, P. E. Lipsky, Ig lambda and heavy chain gene usage in early untreated systemic lupus erythematosus suggests intensive B cell stimulation. *J. Immunol.* **163**, 1027–10236 (1999).

162. O. Pritsch, X. Troussard, C. Magnac, F. R. Mauro, F. Davi, B. Payelle-Brogard, G. Dumas, M. Pulik, F. Clerget, F. Mandelli, N. Chiorazzi, H. W. Schroeder Jr, M. Leporrier, G. Dighiero, VH gene usage by family members affected with chronic lymphocytic leukaemia. *Br. J. Haematol.* **107**, 616–624 (1999).

163. I. Aguilera, J. Melero, A. Nuñez-Roldan, B. Sanchez, Molecular structure of eight human autoreactive monoclonal antibodies. *Immunology*. **102**, 273–280 (2001).

164. G. C. Ippolito, R. L. Schelonka, M. Zemlin, I. I. Ivanov, R. Kobayashi, C. Zemlin, G. L. Gartland, L. Nitschke, J. Pelkonen, K. Fujihashi, K. Rajewsky, H. W. Schroeder, Forced usage of positively charged amino acids in immunoglobulin CDR-H3 impairs B cell development and antibody production. *J. Exp. Med.* **203**, 1567–1578 (2006).

165. M. O. Hill, Diversity and Evenness: A Unifying Notation and Its Consequences. *Ecology*. **54**, 427–432 (1973).

166. R. J. M. Bashford-Rogers, A. L. Palser, B. J. Huntly, R. Rance, G. S. Vassiliou, G. A. Follows, P.

Kellam, Network properties derived from deep sequencing of human b-cell receptor repertoires delineate b-cell populations. *Genome Res.* **23**, 1874–1884 (2013).

167. A. Chao, Nonparametric Estimation of the Number of Classes in a Population. *Scand. J. Stat.* **11**, 265–270 (1984).

168. D. A. Bolotin, S. Poslavsky, I. Mitrophanov, M. Shugay, I. Z. Mamedov, E. V Putintseva, D. M. Chudakov, MiXCR: software for comprehensive adaptive immunity profiling. *Nat. Methods*. **12**, 380–381 (2015).

169. H. Heberle, V. G. Meirelles, F. R. da Silva, G. P. Telles, R. Minghim, InteractiVenn: A web-based tool for the analysis of sets through Venn diagrams. *BMC Bioinformatics*. **16**, 1–7 (2015).

170. J. J. Smit, M. Noti, L. O'Mahony, The use of animal models to discover immunological mechanisms underpinning sensitization to food allergens. *Drug Discov. Today Dis. Model.* **17–18**, 63–69 (2015).

171. C. Link, thesis, University of Lübeck (2016).

172. S. Waserman, P. Bégin, W. Watson, IgE-Mediated Food Allergy. *Allergy, Asthma Clin. Immunol.* **14**, 1–11 (2018).

173. B. P. Vickery, A. M. Scurlock, M. Kulis, P. H. Steele, J. Kamilaris, J. P. Berglund, C. Burk, A. Hiegel, S. Carlisle, L. Christie, T. T. Perry, R. D. Pesek, S. Sheikh, Y. Virkud, P. B. Smith, M. H. Shamji, S. R. Durham, S. M. Jones, A. W. Burks, Sustained unresponsiveness to peanut in subjects who have completed peanut oral immunotherapy. *J. Allergy Clin. Immunol.* **133**, 468-475.e6 (2014).

174. B. L. Wright, M. Kulis, K. A. Orgel, A. W. Burks, P. Dawson, A. K. Henning, S. M. Jones, R. A. Wood, S. H. Sicherer, R. W. Lindblad, D. Stablein, D. Y. M. Leung, B. P. Vickery, H. A. Sampson, Component-resolved analysis of IgA, IgE, and IgG4 during egg OIT identifies markers associated with sustained unresponsiveness. *Allergy Eur. J. Allergy Clin. Immunol.* **71**, 1552–1560 (2016).

175. J. M. Tamayo, K. J. Koleoglou, H. C. Oettgen, O. T. Burton, A. J. Stranks, Allergen-specific IgG antibody signaling through FcγRIIb promotes food tolerance. *J. Allergy Clin. Immunol.* **141**, 189-201.e3 (2017).

176. Z. Y. Kucuk, R. Strait, M. V. Khodoun, A. Mahler, S. Hogan, F. D. Finkelman, Induction and suppression of allergic diarrhea and systemic anaphylaxis in a murine model of food allergy. *J. Allergy Clin. Immunol.* **129**, 1343–1348 (2012).

177. S. Benedé, M. C. Berin, Mast cell heterogeneity underlies different manifestations of food allergy in mice. *PLoS One*. **13**, e0190453 (2018).

178. J. J. Ryan, Interleukin-4 and its receptor: essential mediators of the allergic response. *J. Allergy Clin. Immunol.* **99**, 1–5 (1997).

179. R. T. Strait, A. Mahler, S. Hogan, M. Khodoun, A. Shibuya, F. D. Finkelman, Ingested allergens must be absorbed systemically to induce systemic anaphylaxis. *J. Allergy Clin. Immunol.* **127**, 982-989.e1 (2011).

180. H. Renz, K. J. Allen, S. H. Sicherer, H. A. Sampson, G. Lack, K. Beyer, H. C. Oettgen, Food allergy. *Nat. Rev. Dis. Prim.* **4** (2018), doi:10.1007/978-981-10-5541-6_28.

181. U. Hershberg, E. T. Luning Prak, The analysis of clonal expansions in normal and autoimmune B cell repertoires. *Philos. Trans. R. Soc. Lond. B. Biol. Sci.* **370** (2015), doi:10.1098/rstb.2014.0239.

182. C. Werner-Favre, T. Matthes, M. Barnet, R. H. Zubler, High IgE secretion capacity of human plasma cells. *Eur. J. Immunol.* **23**, 2038–2040 (1993).

183. A. Turqueti-Neves, M. Otte, C. Schwartz, M. E. R. Schmitt, C. Lindner, O. Pabst, P. Yu, D. Voehringer, The Extracellular Domains of IgG1 and T Cell-Derived IL-4/IL-13 Are Critical for the Polyclonal Memory IgE Response In Vivo. *PLoS Biol.* **13**, 1–24 (2015).

184. F. Weisel, M. Shlomchik, Memory B Cells of Mice and Humans. *Annu. Rev. Immunol.* **35**, 255–284 (2017).

185. H.-D. Chang, K. Tokoyoda, A. Radbruch, Immunological memories of the bone marrow. *Immunol. Rev.* **283**, 86–98 (2018).

186. V. Giudicelli, D. Chaume, M.-P. Lefranc, IMGT/GENE-DB: a comprehensive database for human and mouse immunoglobulin and T cell receptor genes. *Nucleic Acids Res.* **33**, D256-61 (2005).

187. R. R. Hardy, C. E. Carmack, S. A. Shinton, J. D. Kemp, K. Hayakawa, Resolution and characterization of pro-B and pre-pro-B cell stages in normal mouse bone marrow. *J. Exp. Med.* **173**, 1213–25 (1991).

188. S. Rm. Clarke, M. Barnden, C. Kurts, F. R. Carbone, J. F. Miller, W. R. Heath, Characterization of the ovalbumin-specific TCR transgenic line OT-I: MHC elements for positive and negative selection. *Immunol. Cell Biol.* **78**, 110–117 (2000).

189. Y. Mine, M. Yang, Epitope characterization of ovalbumin in BALB/c mice using different entry routes. *Biochim. Biophys. Acta - Proteins Proteomics*. **1774**, 200–212 (2007).

190. X. M. Li, D. Serebrisky, S. Y. Lee, C. K. Huang, L. Bardina, B. H. Schofield, J. S. Stanley, A. W. Burks, G. A. Bannon, H. A. Sampson, A murine model of peanut anaphylaxis: T- and B-cell responses to a major peanut allergen mimic human responses. *J. Allergy Clin. Immunol.* **106**, 150–158 (2000).

191. U. K. Samavedam, S. C. Morris, S. P. Commins, C. Potter, C. Rau, R. A. Manz, S. P. Hogan, M. D. Kulis, M. T. Ferris, F. P.-M. de Villena, A. W. Burks, M. V. Khodoun, F. D. Finkelman, Promotion of food allergy by the unfolded protein response. *Immunity* (2020).***In revision***

192. G. Cherian, T. B. Holsonbake, M. P. Goeger, Fatty Acid Composition and Egg Components of Specialty Eggs. *Poult. Sci.* **81**, 30–33 (2002).

193. A. A. Demetriou, Jejunal mucosal injury and restitution: role of hydrolytic products of food digestion. *Am. J. Physiol. - Gastrointest. Liver Physiol.* **261**, G384–G391 (1991).

194. B. Añíbarro, M. C. García-Ara, J. A. Ojeda, Bird-egg syndrome in childhood. *J. Allergy Clin. Immunol.* **92**, 628–630 (1993).

195. A. T. Fox, P. Sasieni, G. du Toit, H. Syed, G. Lack, Household peanut consumption as a risk factor for the development of peanut allergy. *J. Allergy Clin. Immunol.* **123**, 417–423 (2009).

196. G. Lack, D. Fox, K. Northstone, J. Golding, Factors Associated with the Development of Peanut Allergy in Childhood. *N. Engl. J. Med.* **348**, 977–985 (2003).

197. S. Wavrin, H. Bernard, J.-M. Wal, K. Adel-Patient, Influence of the route of exposure and the matrix on the sensitisation potency of a major cows' milk allergen. *Clin. Transl. Allergy*. **5**, 3 (2015).

198. G. Du Toit, A. Santos, G. Roberts, A. T. Fox, P. Smith, G. Lack, The diagnosis of IgE-mediated food allergy in childhood. *Pediatr. Allergy Immunol.* **20**, 309–319 (2009).

199. T. T. Perry, E. C. Matsui, M. Kay Conover-Walker, R. A. Wood, The relationship of allergen-specific IgE levels and oral food challenge outcome. *J. Allergy Clin. Immunol.* **114**, 144–149 (2004).

200. J. M. Spergel, Nonimmunoglobulin E-mediated immune reactions to foods. *Allergy, Asthma Clin. Immunol.* **2**, 78–85 (2006).

201. R. Sidbury, W. L. Tom, J. N. Bergman, K. D. Cooper, R. A. Silverman, T. G. Berger, S. L. Chamlin, D. E. Cohen, K. M. Cordoro, D. M. Davis, S. R. Feldman, J. M. Hanifin, A. Krol, D. J. Margolis, A. S. Paller, K. Schwarzenberger, E. L. Simpson, H. C. Williams, C. A. Elmets, J. Block, C. G. Harrod, W. Smith Begolka, L. F. Eichenfield, Guidelines of care for the management of atopic dermatitis. *J. Am. Acad. Dermatol.* **71**, 1218–1233 (2014).

202. A. Dannaeus, T. Foucard, S. Ohman, S. G. O. JOHANSSON, T. Foucard, S. ÖHMAN, *Acta Paediatr. Scand.*, in press, doi:10.1111/j.1651-2227.1977.tb07803.x.

203. K. Vaali, T. J. Puumalainen, M. Lehto, H. Wolff, H. Rita, H. Alenius, T. Palosuo, Murine model of food allergy after epicutaneous sensitization: Role of mucosal mast cell protease-1. *Scand. J. Gastroenterol.* **41**, 1405–1413 (2006).

204. G. Pejler, E. Rönnberg, I. Waern, S. Wernersson, Mast cell proteases: Multifaceted regulators of inflammatory disease. *Blood*. **115**, 4981–4990 (2010).

205. J. R. McDermott, R. E. Bartram, P. A. Knight, H. R. P. Miller, D. R. Garrod, R. K. Grencis, Mast cells disrupt epithelial barrier function during enteric nematode infection. *Proc. Natl. Acad. Sci. U. S. A.* **100**, 7761–7766 (2003).

206. T. Nakano, T. Sonoda, C. Hayashi, A. Yamatodani, Y. Kanayama, T. Yamamura, H. Asai, T. Yonezawa, Y. Kitamura, S. J. Galli, Fate of bone marrow-derived cultured mast cells after intracutaneous, intraperitoneal, and intravenous transfer into genetically mast cell-deficient W/Wv mice: Evidence that cultured mast cells can give rise to both connective tissue type and mucosal mast. *J. Exp. Med.* **162**, 1025–1043 (1985).

207. S. G. A. Brown, S. F. Stone, D. M. Fatovich, S. A. Burrows, A. Holdgate, A. Celenza, A. Coulson, L. Hartnett, Y. Nagree, C. Cotterell, G. K. Isbister, Anaphylaxis: Clinical patterns, mediator release, and severity. *J. Allergy Clin. Immunol.* **132** (2013), doi:10.1016/j.jaci.2013.06.015.

208. S. J. Galli, J. R. Gordon, B. K. Wershil, Cytokine production by mast cells and basophils. *Curr. Opin. Immunol.* **3**, 865–873 (1991).

209. M. V. Khodoun, T. Orekhova, C. Potter, S. Morris, F. D. Finkelman, Basophils initiate IL-4 production during a memory T-dependent response. *J. Exp. Med.* **200**, 857–870 (2004).

210. R. T. Strait, S. C. Morris, F. D. Finkelman, IgG-blocking antibodies inhibit IgE-mediated anaphylaxis in vivo through both antigen interception and Fc gamma RIIb cross-linking. *J. Clin. Invest.* **116**, 833–41 (2006).

211. M. V. Khodoun, S. C. Morris, E. Angerman, C. Potter, R. Schuman, M. Wunderlich, J. J. Maciag, K. C. Sullivan Locker, J. C. Mulloy, A. B. Herr, F. D. Finkelman, Rapid desensitization of humanized mice with anti-human FcεRIα monoclonal antibodies. *J. Allergy Clin. Immunol.* **145**, 907-921.e3 (2020).

212. M. V. Khodoun, S. C. Morris, E. Angerman, C. Potter, R. Schuman, M. Wunderlich, J. J. Maciag, K. C. Sullivan Locker, J. C. Mulloy, A. B. Herr, F. D. Finkelman, Rapid desensitization of humanized mice with anti-human FcεRIα monoclonal antibodies. *J. Allergy Clin. Immunol.* **145**, 907-921.e3 (2020).

213. K. D. Stone, C. Prussin, D. D. Metcalfe, IgE, mast cells, basophils, and eosinophils. *J. Allergy*

Clin. Immunol. **125**, S73-80 (2010).

214. S. K. Cooke, H. A. Sampson, Allergenic properties of ovomucoid in man. *J. Immunol.* **159**, 2026–2032 (1997).

215. J. Martínez-Botas, I. Cerecedo, J. Zamora, C. Vlaicu, M. C. Dieguez, D. Gómez-Coronado, V. De Dios, S. Terrados, B. De La Hoz, Mapping of the IgE and IgG4 sequential epitopes of ovomucoid with a peptide microarray immunoassay. *Int. Arch. Allergy Immunol.* **161**, 11–20 (2013).

216. T. S. Dodev, H. Bowen, M. H. Shamji, H. J. Bax, A. J. Beavil, J. M. McDonnell, S. R. Durham, B. J. Sutton, H. J. Gould, L. K. James, Inhibition of allergen-dependent IgE activity by antibodies of the same specificity but different class. *Allergy Eur. J. Allergy Clin. Immunol.* **70**, 720–724 (2015).

217. A. Erazo, N. Kutchukhidze, M. Leung, A. P. G. Christ, J. F. Urban, M. A. Curotto de Lafaille, J. J. Lafaille, Unique Maturation Program of the IgE Response In Vivo. *Immunity*. **26**, 191–203 (2007).

218. K. Haniuda, S. Fukao, T. Kodama, H. Hasegawa, D. Kitamura, Autonomous membrane IgE signaling prevents IgE-memory formation. *Nat. Immunol.* **17**, 1109–1117 (2016).

219. Z. Yang, M. J. Robinson, X. Chen, G. A. Smith, J. Taunton, W. Liu, C. D. Allen, Regulation of B cell fate by chronic activity of the IgE B cell receptor. *Elife*. **5**, 1–31 (2016).

220. D. Hildeman, T. Jorgensen, J. Kappler, P. Marrack, Apoptosis and the homeostatic control of immune responses. *Curr. Opin. Immunol.* **19** (2007), pp. 516–521.

221. U. Andréasson, S. Flicker, M. Lindstedt, R. Valenta, L. Greiff, M. Korsgren, C. A. K. Borrebaeck, M. Ohlin, The Human IgE-encoding Transcriptome to Assess Antibody Repertoires and Repertoire Evolution. *J. Mol. Biol.* **362**, 212–227 (2006).

222. E. O. Luger, V. Fokuhl, M. Wegmann, M. Abram, K. Tillack, G. Achatz, R. A. Manz, M. Worm, A. Radbruch, H. Renz, Induction of long-lived allergen-specific plasma cells by mucosal allergen challenge. *J. Allergy Clin. Immunol.* **124**, 819-826.e4 (2009).

223. B. Heyman, Antibody Feedback Inhibition – a Biological Principle of Immune Regulation. *Transfus. Med. Hemotherapy*. **32**, 348–354 (2005).

224. D. Tarlinton, K. Good-Jacobson, Diversity among memory B cells: Origin, consequences, and utility. *Science (80-.).* **341** (2013), pp. 1205–1211.

225. B. Bergmann, O. Grimsholm, K. Thorarinsdottir, W. Ren, P. Jirholt, I. Gjertsson, I. L. Mårtensson, Memory B Cells in Mouse Models. *Scand. J. Immunol.* **78**, 149–156 (2013).

226. J. S. He, S. Subramaniam, V. Narang, K. Srinivasan, S. P. Saunders, D. Carbajo, T. Wen-Shan, N. Hidayah Hamadee, J. Lum, A. Lee, J. Chen, M. Poidinger, F. Zolezzi, J. J. Lafaille, M. A. Curotto De Lafaille, IgG1 memory B cells keep the memory of IgE responses. *Nat. Commun.* **8** (2017), doi:10.1038/s41467-017-00723-0.

227. O. Talay, D. Yan, H. D. Brightbill, E. E. M. Straney, M. Zhou, E. Ladi, W. P. Lee, J. G. Egen, C. D. Austin, M. Xu, L. C. Wu, IgE+ memory B cells and plasma cells generated through a germinal-center pathway. *Nat. Immunol.* **13**, 396–404 (2012).

228. U. Laserson, F. Vigneault, D. Gadala-Maria, G. Yaari, M. Uduman, J. A. Vander Heiden, W. Kelton, S. T. Jung, Y. Liu, J. Laserson, R. Chari, J. H. Lee, I. Bachelet, B. Hickey, E. Lieberman-Aiden, B. Hanczaruk, B. B. Simen, M. Egholm, D. Koller, G. Georgiou, S. H. Kleinstein, G. M. Church, High-resolution antibody dynamics of vaccine-induced immune responses. *Proc. Natl. Acad. Sci. U. S. A.* **111**, 4928–4933 (2014).

229. H. M. Jäck, M. Wabl, Immunoglobulin mRNA stability varies during B lymphocyte differentiation. *EMBO J.* **7**, 1041–1046 (1988).

230. T. Yoshida, H. Mei, T. Dörner, F. Hiepe, A. Radbruch, S. Fillatreau, B. F. Hoyer, Memory B and memory plasma cells. *Immunol. Rev.* **237** (2010), pp. 117–139.

231. H. Nilsson, K. M. Krawczyk, M. E. Johansson., High salt buffer improves integrity of RNA after fluorescence-activated cell sorting of intracellular labeled cells. *J. Biotechnol.* **192**, 62–65 (2014).

8 SUPPLEMENTARY FIGURES

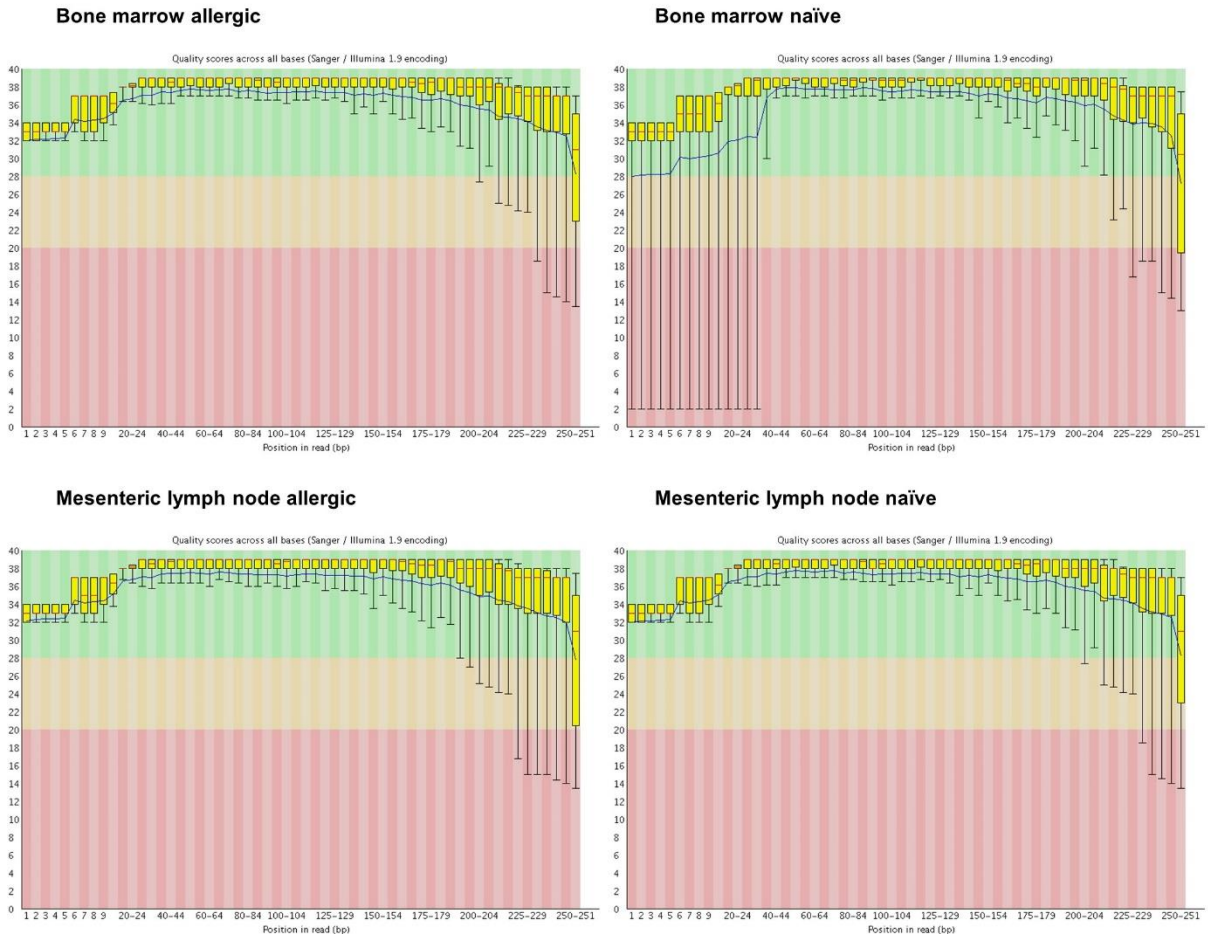

Supplementary figure 1: Quality scores of Illumina sequences
Quality scores across the bases of exemplary BM and mLN samples for naïve and allergic mice were analysed using FastQC.

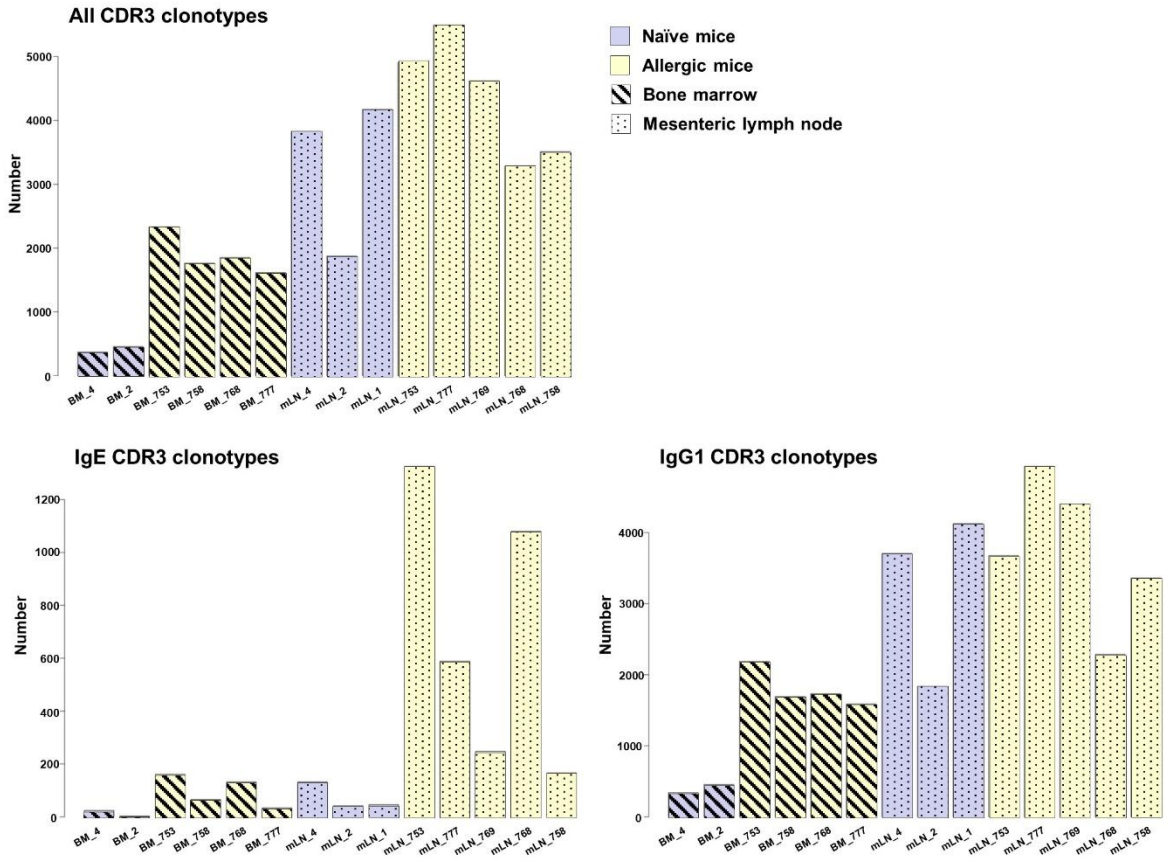

Supplementary figure 2: Numbers of clonotypes in allergic and naïve mice
All sequences of allergic and naïve mice were analysed for numbers of clonotypes using MiXCR (*156*) and shown as all CDR3 clonotypes, IgE CDR3 clonotypes and IgG1 clonotypes of individual allergic and naïve mice in BM and mLN.

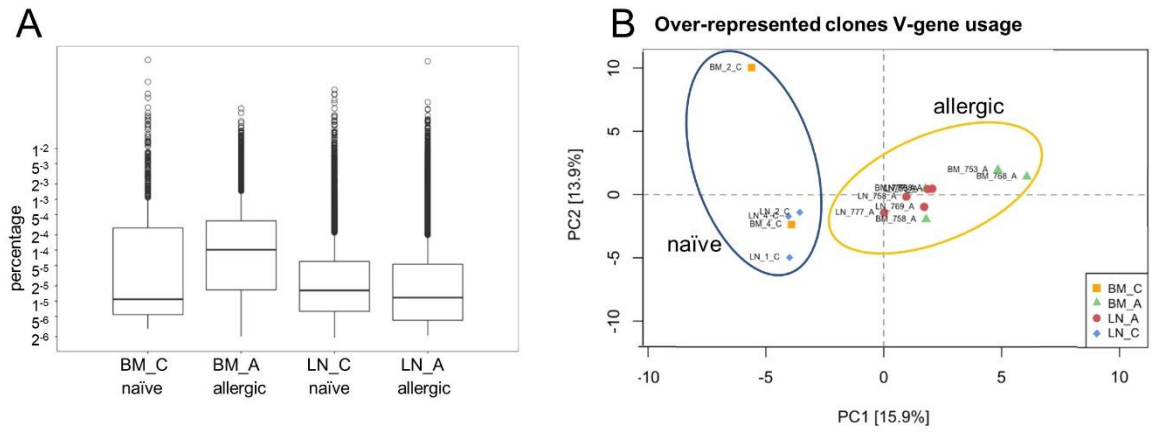

Supplementary figure 3: Allergic and naïve mice can be differentiated by the usage of different V-genes by over-represented clones
Box plot analyses were performed to compare the frequency distribution of CDR3 clonotypes. Copy numbers relative to the number of all CDR3 sequences obtained (percentage) are displayed in respective groups, naïve (control _C) and allergic (_A) BM and mLN. Extremely high-frequent clonotypes (outliers) that are outside an interquartile range (IQR) of 3 are displayed as single dots (**A**). A principle component analysis (PCA) was performed on these outliers/over-represented clonotypes (**B**). The cluster of naïve (control) and allergic samples are indicated by a circle around them.

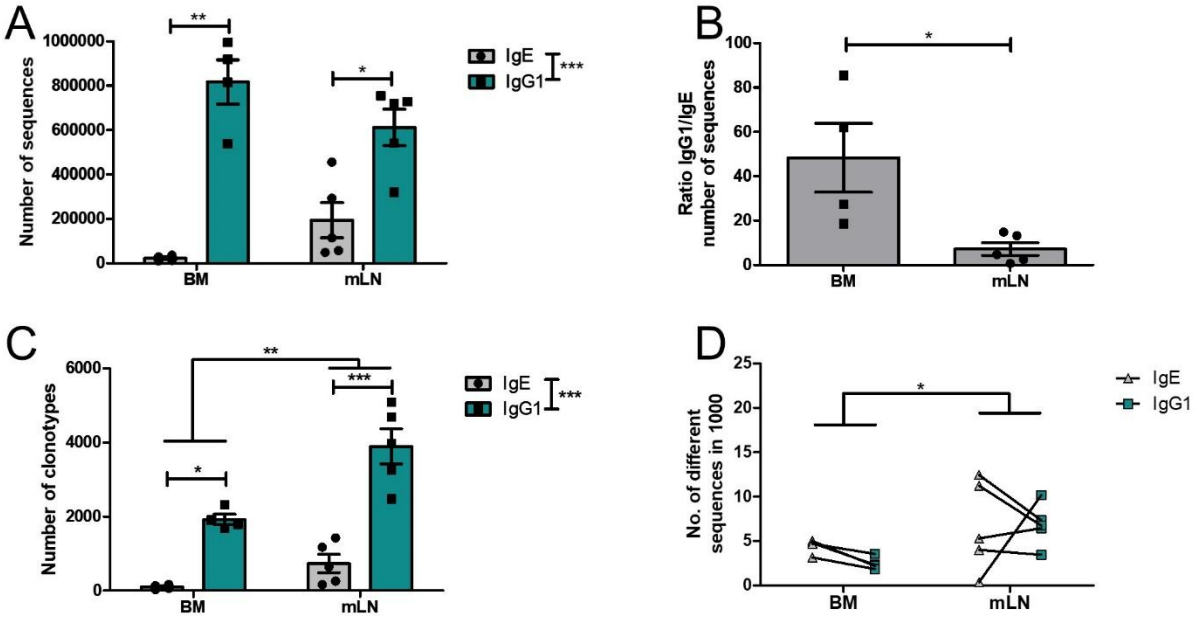

Supplementary figure 4: Differences in quantity and variety of the repertoire between BM and mLN, IgE and IgG1 in all analysed sequences

All CDR3 nucleotide sequences of allergic mice with a read count >1 were analysed. The total number of all sequences of the respective isotype (**A**) and the ratio of these sequence numbers of IgG1 and IgE (**B**) in BM and mLN are displayed. The number of clonotypes of IgE and IgG1 are shown for BM and mLN (**C**). The clonal variety (**D**) as determined by calculating the number of clonotypes (in other words unique CDR3 sequences) per 1000 sequences is displayed for IgE and IgG1 in BM and mLN. Statistics: 2-way ANOVA (row-matched) with Bonferroni post-test *: $p<0.05$, **: $p<0.01$, ***: $p<0.001$, n=4-5, mean ±SEM are displayed.

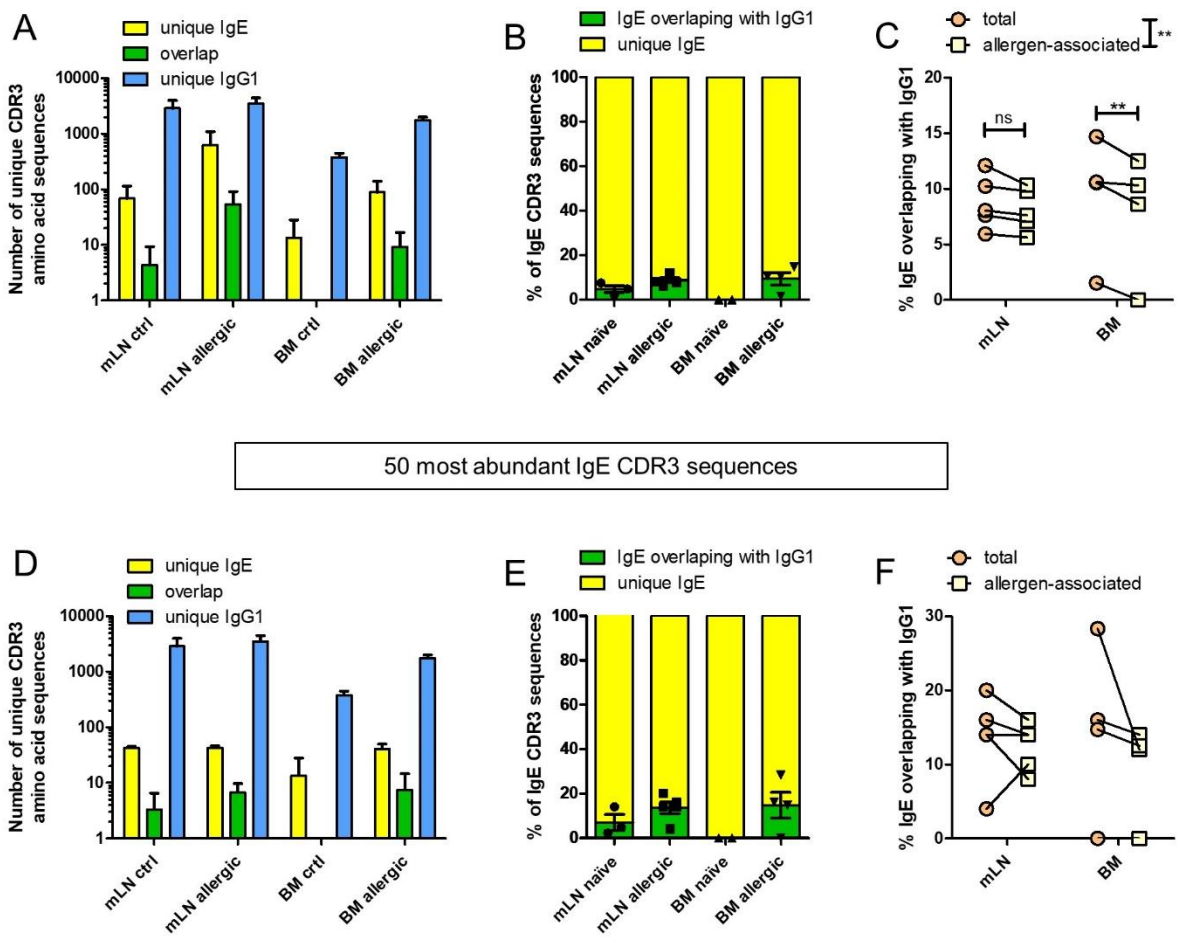

Supplementary figure 5: Most IgE CDR3 amino acid sequences are not represented in the IgG1 repertoire even when sequences from naïve and allergic mice are evaluated.

Overlaps of total IgG1 and IgE CDR3 amino acid sequences of from allergic and naïve mice with a read count >1 were calculated using InteractiVenn (*169*). The number of sequences being either uniquely present in IgE (yellow triangle), present in both IgE and IgG1 =overlap (green circle) or uniquely present in IgG1 are depicted in **A**. The corresponding percentages of IgE sequences being either unique (yellow) or also present in the IgG1 repertoire (green) are shown in **B**. Frequencies of IgE-CDR3 amino acid sequences overlapping with IgG1 were compared between total and allergen-associated sequences of allergic mice (**C;** definition see Figure 13) with a read count >1. **D**, **E** and **F** show analogous analyses to **A**, **B** and **C** for the 50 most abundant IgE sequences. Statistics: **A**, **B**, **D**, **E**: n=2-5; **C** and **F** n=4-5, 2-Way ANOVA with Bonferroni post-test; not significant (no mark/ns): p> 0.05, **: p< 0.01

LIST OF FIGURES

LIST OF TABLES

ABBREVIATIONS

5'-RACE	5'-rapid amplification of cDNA ends
A. bidest.	bi-distilled water
Ab	antibody
AD	Atopic Dermatitis
AID	activation-induced cytidine deaminase
BCA	Bicinchoninic acid
BCL	binary base call
BCR	B cell receptor
BLG	bovine β-lactoglobulin
BM	performed bone marrow
bp	base paires
ca.	circa
CCHMC	Cinicinnati Children's Hospital Medical Center
cDNA	complementary DNA
CDR	Complementarity-determining region
CDRs	complementarity-determining regions
CLP	common lymphoid progenitor
CRT	cyclic reversible termination
CSR	class-switch recombination
CT	cholera toxin
CX3CR1	CX3C-chemokine receptor 1
D	diversity
DB	dilution buffer
dC	deoxycytosine
dNTPs	desoxy-nucleoside tri-phosphates
dU	deoxyuridine
e.g.	*exempli gratia* (for example)
EoE	eosinophilic oesophagitis
EW	egg white
EYP	egg yolk plasma
FACS	fluorescent activated cell sorting
FOXP3	forkhead box P3
FR	framework region
gDNA	genomic DNA
HRP	horseradish peroxidase
i.p.	intra peritoneal
i.t.	intra tracheal
IL	interleukin
IQR	**interquartile range**

IVC	individual ventilated cages
J	joining
kDa	kilo Dalton
LN	lymph node
LTC4	leukotrienes
M cells	microfold cells
mAb	monoclonal antibody
max. ΔT	maximum temperature drop
MHCII	major histocompatibility complex class II
min	minutes
mLN	mesenteric lymph nodes
mMCP-1	Mucosal mast cell protease-1
MPPs	multipotent myeloid/lymphoid progenitors
NGS	next generation sequencing
o.g.	oral gavage
O/N	over night
OD	optical density
OFC	oral food challenge
OVA	ovalbumin
PAF	platelet-activating factor
PBMC	human peripheral mononucleated cells
PCA	principle component analysis
PCR	polymerase chain reaction
PGD2	prostaglandins
PP	polypropylene
RAGs	recombination-activating genes
RIN	RNA intregrity number
RPM	rounds per minute
RT	room temperature
s	seconds
SEB	Staphylococcal enterotoxin B
SPF	specific pathogen-free
TCR	T cell receptor
TdT	terminal deoxynucleotidyl transferase
T_{FH}	T follicular helper cell
TGF	transforming growth factor
TLR	toll-like receptor
TNFα	tumour necrose factor alpha
UPR	unfolded protein response
V	variable
WB	washing buffer

CURRICULUM VITAE

Professional Experience

10/2016 – 10/2019	**Institute for Systemic Inflammation Research**, Lübeck PhD candidate, Research fellow
03/2017 – 12/2017	**Cincinnati Children's Hospital Medical Center and University of Cincinnati,** Cincinnati, OH Research fellow
04/2013 – 06/2016	**Institute for Systemic Inflammation Research, Prof. Manz, University Hospital Schleswig-Holstein, Lübeck** Student Employee
04/2013 – 09/2015	**University Hospital Schleswig-Holstein,** Lübeck Student Employee for public relations activities
11/2007	**FAL (Forschungsanstalt für Landwirtschaftsforschung (Institute for Agricultural Research)),** Braunschweig Intern

Education

10/2016 – 10/2019	**International Research Training Group (IRTG) 1911** and **Graduate School Lübeck (GSL),** Lübeck
10/2014 – 11/2016	**University of Lübeck,** Lübeck Major: Infection Biology Degree: Master of Science Final grade: 1.4 (very good)
09/2015	**University of Lübeck, Lübeck** and the **Leibnitz Research Center,** Borstel Certification for animal research in adherence to the German Animal Protection law (Aus-, Fort- und Weiterbildung; §10 des TierSchG)

10/2011 – 10/2014 **University of Lübeck,** Lübeck
Major: Molecular Life Science
Degree: Bachelor of Science
Final grade: 2.1 (good)

08/2004 – 07/2011 **Wilhelm-Gymnasium,** Braunschweig
Abitur (A-level), final grade: 1.5 (good)

Publications

Wong, D., Winter, O., **Hartig, C.**, Siebels, S., Szyska, M., Tiburzy, B., Meng, L., Kulkarni, U., Fähnrich, A., Bommert, K., et al. (2014). Eosinophils and megakaryocytes support the early growth of murine MOPC315 myeloma cells in their bone marrow niches. *PLoS One.*

Clauder, A.-K., Kordowski, A, Bartsch, Y, Köhl, G., Lilienthal, G.-M., Nogueira de Almeida, L., Lindemann, T, Petry, J., **Rau, C.,** Gramalla-Schmitz, A., Dühring, L., Elbracht, C., Kenno, S., Tillmann, J., Wuhrer, M., Ludwig, R., Ibrahim, S., Bieber, K., Köhl, J., Ehlers, M., Manz, R. (2020). IgG Fc N-glycosylation translates MHCII haplotype into autoimmune skin disease. *J. Invest. Dermatol.* ***Accepted for publication***

Samavedam, U.K., Morris, S. C., Commins, S. P., Potter, C., Rau, C., Manz, R. A., Hogan, S. P., Kulis, M. D., Ferris, M. T., de Villena, F. P.-M., Burks, A. W., Khodoun, M. V., Finkelman, F. D. (2020). Promotion of food allergy by the unfolded protein response. *Immunity* ***In revision***